DISSERTATIONES MATHEMATICAE UNIVERSITATIS TARTUENSIS

65

DISSERTATIONES MATHEMATICAE UNIVERSITATIS TARTUENSIS
65

LARISSA ROOTS

Free vibrations of stepped cylindrical shells containing cracks

TARTU UNIVERSITY
PRESS

Faculty of Mathematics and Computer Science, University of Tartu, Tartu, Estonia

Dissertation has been accepted for the commencement of the degree of Doctor of Philosophy (PhD) in mathematics on October 20, 2010, by the Council of the Institute of Mathematics, Faculty of Mathematics and Computer Science, University of Tartu.

Supervisor:

Dr. Sci., Professor Jaan Lellep
University of Tartu
Estonia

Opponents:

Dr. rer. nat., Professor Werner H. Schmidt
Ernst-Moritz-Arndt University of Greifswald
Germany

Professor Emeritus, D. Tech. Martti Mikkola
Aalto University
Finland

Commencement will take place on December 20, 2010, at 11.00 on Liivi 2–403.

Publication of this dissertation has been granted by Estonian Target-financed project SF0180081s08 “Models of Applied Mathematics and Mechanics”.

ISSN 1024–4212
ISBN 978–9949–19–528–2 (trükis)
ISBN 978–9949–19–529–9 (PDF)

Tartu Ülikooli Kirjastus
www.tyk.ee
Tallimus nr 705

CONTENTS

INTRODUCTION AND REVIEW OF LITERATURE

Shells are probably the most efficient elements of structures available to mankind. Evidently, they should be used more in the technology than they are. They are certainly more difficult to design and fabricate than plates.

A thin shell is a three-dimensional body which is hounded by two closely spaced curved surfaces, the distance between the surfaces being small in comparison with the other dimensions. The locus of points which lie in the middle between those surfaces is called the middle surface of the shell. The distance between the surfaces measured along the normal to the middle surface is the thickness of the shell at that point. The thickness need not be constant in the formulation of a suitable theory of deformation, but constant thickness results in governing equations which are easier to solve. Shells may be regarded as generalizations of a flat plate; conversely, a flat plate is a special case of a shell having no curvature.

The bending properties of a plate depend greatly on its thickness as compared with its other dimensions. If deflections w of a plate are small in comparison with its thickness h, a very satisfactory approximate theory of bending of the plate by lateral loads can be developed by making the following assumptions, known in the literature as hypotheses of Kirchhoff-Love:

- There is no deformation in the middle surface of the plate. This surface remains neutral during bending.
- Points of the plate lying initially on a normal-to-the-middle surface of the plate remain on the normal-to-the- middle surface of the plate after bending.
- The normal stresses in the direction transverse to the plate can be disregarded.

The main suppositions of the theory of thin plates also form the basis for the usual theory of thin shells.

A general theory of bending of thin shells has been developed by Love. The first attempt to build up a theory of shells based on hypotheses of Kirchhoff, has been made by mechanic Aron [3]. However includes this work some mistakes which are noticed and corrected by the mathematician Love [46, 47].

In the classical theory of small displacements of thin shells the following assumptions were made by Love [46]:

- The thickness of the shell is small compared with the other dimensions, for example, the smallest radius of curvature of the middle surface of the shell.
- Strains and displacements are sufficiently small so that the quantities of second- and higher-order magnitude in the strain-displacement relations may be neglected in comparison with the first-order terms.
- The transverse normal stress is small compared with the other normal stress components and may be neglected.

– Normals to the undeformed middle surface remain straight and normal to the deformed middle surface and suffer no extension.

These four assumptions taken together give rise to what Love called his "first approximation" shell theory. These approximations are almost universally accepted by others in the derivation of thin shell theories. The first assumption defines what is meant by "thin shells" and sets the stage for the entire theory. Denoting the thickness of the shell by h and the smallest radius of curvature by R, then it will be convenient at various places in the subsequent derivation of shell theories to neglect higher powers of z/R or h/R in comparison with unity, where z is the third coordinate. The second assumption permits one to refer all calculations to the original configuration of the shell and ensures that the differential equations will be linear. The fourth assumption is known as the hypothesis of straight normals. The general theory of shells, taking into account the smallness their thicknesses consists of four groups of formulas, namely:

1) formulas expressing 6 components of the deformation of the middle surface, – extensions, shift, change of curvature and torsion – through the three components of the displacement vector of an arbitrary point of the surface;
2) six equations expressing the equilibrium conditions of a small element of the middle surface;
3) the four boundary conditions which must be set on the edge of the shell (if not a closed shell);
4) correlations between the forces and moments in the shell with the values that characterize the deformation of the middle surface, the two aspect ratios, shift, two changes of curvature and torsion.

So, by the end of 19 centuries the general theory of shells has been developed, in a general form, i.e. for shells of arbitrary form. But conditions for its wide application have not ripened yet. The success of the theory, in this case, is many years ahead of the needs of practical application.

Now it seems incredible that the main task of the founders of the theory of shells, was the problem of ringing bells.

In the late 19th century the famous book by Lord Rayleigh "The Theory of Sound" [60] was published. In the second volume of which there was given the approximate theory of vibration of a spherical bell. Solving this problem, Rayleigh was guided by considerations of physical nature. Thus, a question of a little practical importance, has led to the foundation for the general theory of shells today.

At the beginning of the last century the idea of thin-walled slabs from ferroconcrete was born. In the first half of the century aviation starts to develop rapidly and submarines become a terrible weapon. Optimization of structures and designs becomes a problem of great importance.

In the past century the general theory of bending of thin shells has been developed by many authors worldwide. In [35] Leissa gave an overview of the basic approximate theories of bending of the shells. The application of the gene-

ral theory of bending of cylindrical shells in even the simplest cases results in very complicated calculations. To make the theory applicable to the solution of practical problems some further simplifications in this theory are necessary.

One can mention such authors as Byrne, Flügge, Goldenveizer, Lur'ye, Novozhilov, Timoshenko [80], Reissner, Naghdi, Berry, Vlasov, Sanders, Donnell [76] and Muchtari, who have brought the essential contribution to the development of the approximate investigation of the bending of cylindrical shells. So, for example, in Lur'ye's works [77] equations of the theory of shells are deduced from the general equations of the theory of elasticity. Lurie was probably the first to write the equations of the theory of shells in the tensor form.

Novozhilov and Finkelstein's [79] showed that the error of assumptions of Kirchhoff in the theory of thin shells has the order of h/R. In the book [78] the possibility to represent the equations of the theory of shells in the complex form was used. This approach has opened new ways of transformation of the equations and new solutions are established. In Goldeinveizera's works [75] continuity conditions of deformations are formulated and the possibility of identical satisfaction of the equilibrium equations by introduction of four functions of pressure is shown.

In the theory of cylindrical shells the primary attention is paid to the calculation of closed cylindrical shells (calculation of pipes) and calculation of open cylindrical shells subjected to the internal or external pressure loading. Usually these problems are solved by the method of double or ordinary trigonometrical series. From them the great value is represented by a method of the unary series, allowing to subordinate the decision at two edges of a shell to any boundary conditions. Use of one or other methods was complicated essentially by the high order of differential equations lot of attention has been given to the simplification of initial formulas. It has appeared that the choice of this or that system of simplifications depends on the dimensions of a cylindrical shell.

In practical applications we frequently encounter problems in which a circular cylindrical shell is subjected to the action of forces distributed symmetrically with respect to the axis of the cylinder. The stress distributions in cylindrical boilers subjected to the action of the steam pressure, stresses in cylindrical containers having a vertical axis and submitted to internal liquid pressure, and stresses in circular pipers under uniform internal pressure are examples of such problems.

Axial symmetry allows to simplify considerably the basic equations of the theory of cylindrical shells. Due to symmetry, forces, deformations and displacements depend only on one co-ordinate that allows to reduce a problem to one-dimensional. But it is not easy to obtain experimentally symmetric reaction of a cylindrical shell to symmetric loading. Shells are very sensitive to their minor deviations from the given form, meaning that stresses in two shells of similar form with the same loading can differ considerably.

A very broad topic of research is the determination of the spectrum of frequencies and eigen forms of vibrations of plates and shells. It is an essential

problem in the analysis of forced vibrations and other quasi-stationary processes. Investigations of vibration of plates and shells have long history.

In 1905, Timoshenko published his first scientific article "On the phenomena of resonance in the axle". This was the first application of Rayleigh's method in engineering problems, and he also initiated the study of vibration problems in engineering.

The contemporary theory of linear vibrations of plates and shells in its form differs very little from the linear theory of statical loading of plates and shells. In fact, according to the principle of d'Alembert inertia effects can be considered as effects caused by inertial loads.

Dynamic response of thin cylindrical shells is of great technical interest to engineers. In this study the free vibration of a thin stepped cylindrical shells containing cracks is investigated.

Vibration of circular cylindrical shells is of interest of a number of different fields. However, only a handful of references available in the published literature address the effect of the thickness variations on the vibration behavior of shells. In the present work the effect of different step thickness ratios, step locations and the length to radius ratios on frequency parameters of the circular cylindrical shells is highlighted.

Thin walled beams, plates and shells are structural members which are widely used in various technical equipments. However, repeated and extreme loading causes cracks and other defects deteriorating operational parameters of structural elements. This involves the need for investigation of structures accounting for the influence of cracks on bending and vibration of structural members.

During last decades a considerable attention has been paid to the investigation of vibration and stability of elastic beams with cracks.

Rizos, Aspragathos, Dimarogonas (1990), also Liang, Hu, Choy (1991), (1992), Nandwana, Maiti (1997), Kisa, Brandon, Topcu (1998), Yang, Chen (2008), Ostachowicz, Krawczuk (1991), Bamnios, Trochides (1995) studied the behaviour of cantilever beams with cracks located at fixed positions.

Risos et al (1990); Ostachowicz, Krawczuk (1991); Kisa et al (1998) and other investigations have modelled the behaviour of a cracked beam making use the concept of a rotational spring. According to this approach the beam with a crack is treated as a structure consisting of two segments connected each other with a rotational spring. The connection is located at the same cross-section where the crack is located. This approach is based on the results of Dimarogonas (1976); Dimarogonas and Paipetis (1983) who established that the influence of a crack on the vibrational parameters of the structure can be modelled as the increase of the local flexibility. The latter can be calculated with the methods of linear elastic fracture mechanics and evaluated experimentally.

Resorting to the assumption of the strain energy concentration at the crack tip Papaeconomou and Dimarogonas (1989) developed the flexibility matrix which can be used to evaluate the influence of the crack on dynamic characteristics of the beam.

Another approach for vibrational analysis of cracked beams was suggested by Behzad, Meghdari, Ebrahimi (2005). The authors introduce a modified displacement field for the cracked beam. The additional terms are assumed to decrease exponentially with respect to the distance between current point and the crack tip.

Cawley and Adams (1979), also Adams et al (1978), have developed an experimental-theoretical method to estimate the location and dimensions of the crack making use the data about changes in the natural frequencies. The idea to employ the changes in natural frequencies as a criterion for crack detection has received considerable attention. This is because the natural frequencies can be measured experimentally and monitoring is possible from any location of the structure. Resorting to the knowledge of natural frequencies one can solve the inverse problem of determination of the crack location and its length.Narkis and Elmanah (1994, 1996) treated the problem of crack identification in the case of uncertain end conditions; Chodres (2001) developed a continuous crack flexibility model for crack identification.

In the papers by Liang, Hu, Choy (1991), and Hu, Liang (1993) an approach was developed which is similar to that of previous ones but requires the measurement of three natural frequencies of the beam. A beam with inclined surface crack or an internal crack is treated by Nandwana and Maiti (1997). In this paper vibrations of slender beams with cracks are studied whereas the model with a rotational spring is used. The magnitude of the stiffness of the spring is defined so that the rotation of the spring due to the moment at the cracked section is equal to the jump in the slope due to the extra flexibility.

Vibration and stability of hollow-sectional beams was investigated by Zheng, Fan (2003) in the case of presence of cracks in expected cross sections. An Euler-Bernoulli beam containing multiple opening cracks and subjected to the axial force is studied by Binici (2005). Both, stability and vibration problems are considered making use of the concept of additional compliance due to a crack developed by Dimarogonas (1996), also Chondros, Dimarogonas, Yao (1998). The case of inclined edge or internal cracks was studied by Nandwana and Maiti (1997) whereas segmented beams were treated by Chaudhary and Maiti (2000).

Chondros, Dimarogonas and Yao (1998) developed a theory for Euler-Bernoulli beams with single-edge or double-edge open cracks. Starting from the Hu-Washizu-Barr variational principle together with the understanding that a crack in an elastic structural element generates additional local flexibility due to the strain energy concentration in the vicinity of the crack tip the authors compile the crack disturbance function coupled with the stress intensity factor for a cracked beam specimen. The crack is modelled as a continuous flexibility corresponding to the displacement field in the vicinity of the crack determined with the help of methods of fracture mechanics. Theoretical predictions are favourably compared with experimental results.

Kisa, Brandon and Topcu (1998) developed an approach to the analysis of free vibrations of cracked Timoshenko beams. The study integrates the finite

element method and the component mode synthesis. The beam is divided into two parts with components coupled by the flexibility matrix. The latter incorporates the interaction forces which can be defined as elements of a matrix inverse to the compliance matrix. Each substructure is modelled as a Timoshenko beam and approximated by finite elements. A theoretical model for cracked Timoshenko beams was suggested by Takahaski (1999).

Yang and Chen (2008) presented a theoretical investigation of free vibrations and buckling of beams made of functionally graded materials. It is assumed that the material properties vary along the beam thickness according to the exponential law. A detailed parametric study is conducted to reveal the influence of vibrational parameters on the crack length, location and other geometrical and material parameters.

The effect of cracks on the free vibration frequencies of uniform beams with arbitrary number of cracks was investigated by Lin, Chang, Wu (2002) by the use of the transfer matrix method. Masoud, Jarrah, Al-Maamory (1999) presented theoretical and experimental results concerning an axially loaded fixed-fixed beam with cracks. Free vibrations of multistepped beams with concentrated masses are studied by Li (2001).

An alternative analytical method for evaluation of fundamental frequencies of cracked Euler- Bernoulli beams was suggested by Fernandez- Saez, Rubio and Navarro. This method is based on the approach of representing the crack in the beam through an elastic hinge whereas transverse deflection of the cracked beam is constructed by adding polynomial functions to that of the uncracked beam.

Fernandez-Saez et al introduce at each step new admissible functions which satisfy the boundary conditions and calculate with the help of Rayleigh method the fundamental frequencies. The method provides closed form expressions for natural frequencies. The results are presented for cracked beams simply supported at both ends.

In the next paper by Fernandez-Saez and Navarro (2002) the solution procedure is transformed into an eigenvalue problem for a homogeneous Fredholm integral equation with a symmetric kernel. The solution of this problem provides closed form expressions for successive lower bounds of the fundamental frequency. It is shown that the results compare favourably with those obtained by the finite element method in the cases of cantilever beams and beams with fixed-pinned edges.

Axially loaded segmented beams were considered also by De Rosa (1996) and Naguleswaran (2004). In the latter work beams with different axial forces in beam segments are studied whereas De Rosa has used an exact method to derive the frequency equation for a stepped beam with follower forces at each step. Lellep and Sakkov (2006) investigated the stability of cantilever beams with cracks.

The vibration of uniform Euler-Bernoulli beams with a single edge crack was investigated by Yokoyama, Chen (1998) making use of a modification of the distributed line-spring method which was suggested earlier by Rice and

Levy (1972) for rectangular plates with part through cracks. Rice and Levy studied the stress distribution in the neighbourhood of a crack and modelled the influence of the crack on the local behaviour of the plate with the help of a distributed spring instead of the actual crack. This concept enables to calculate the additional compliance caused by the crack and thus to evaluate approximately the energy release rate and stress intensity coefficient corresponding to the cracked plate.

As regards cylindrical shells the number of papers devoted to the determination of the stress intensity coefficient and to the vibration analysis of tubes is much smaller in comparison to that in the case of beams. Engineering estimates to the stress intensity factor for inner and outer surface cracks in pressurised cylinders were presented by Kobayashi et al (1977). Raju and Newman (1982) developed a finite element model for determination of the stress intensity factor for a cylindrical shell with semi-elliptical surface crack.

A refired theory of vibration of laminated composite cylindrical shells is developed by Chang-Tsan Sun and Whithey (1974). This study as well as the approach by Duan and Koh (2008) is confined to axisymmetric transverse vibrations. Laminated orthotropic cylindrical shells are considered by Dong (1968) whereas Soedel (1983) has presented simplified equations for orthotropic shells.

Petroski (1980) studied the behaviour of cylindrical shells with cracks using the Fourier series for determination of natural frequencies. Nikpour (1990) investigated the influence of axisymmetric cracks on the vibration parameters of orthotropic cylindrical shells. Assuming that the shell is made of a laminated composite material the author introduces a local compliance matrix as a function of the crack length and of material parameters. Simplified solutions for the case of symmetrical vibrations are obtained by Lellep et al (2009, 2010) and Lellep, Roots (2010).

In the present study is extended to free vibrations of elastic cylindrical shells. The shells under consideration have piece wise constant thickness and cracks of constant depth are located at cross sections with steps of the thickness. The main attention is focused on the axisymmetric vibrations of circular cylindrical shells with various end conditions. However, an attempt is made to develop an approximate solution of the vibration problem in the case of non-axisymmetric vibrations, as well.

1. AXISYMMETRIC VIBRATIONS OF SIMPLY SUPPORTED SHELLS WITH CRACKS

Abstract

Axisymmetric vibrations of circular cylindrical shells of piece wise constant thickness are considered. The shells are weakened with cracks emanating at the re-entrant corners of steps. The influence of circular cracks with constant depth on the vibration of the shell is prescribed with the aid of a matrix of local flexibility. The latter is related to the coefficient of the stress intensity known in the linear fracture mechanics. Numerical results are presented for the case of the shell with one and two steps.

1.1. Formulation of the problem

Let us consider small deflections of elastic axisymmetric circular cylindrical shells of length $2l$ and radius R (Fig. 1.1). We shall confine our attention to axisymmetric free vibrations of the shell caused by an initial excitation.

Assume that the ends of the shell is simply supported. Because of symmetry we will consider only right half of shell and the origin of the axis Ox be in the central cross-section of the tube. It is assumed that the thickness h of the shell is piece wise constant, e.g.

$$h(x)=h_j \tag{1.1.1}$$

for $x \in (a_j, a_{j+1})$, where $j=0,...,n$.

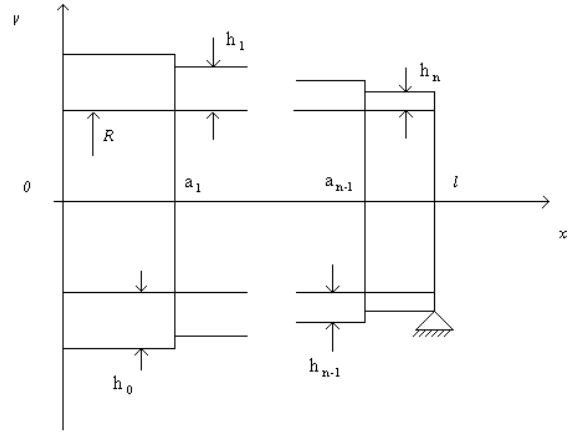

Fig. 1.1: Stepped cylindrical shell.

Here the quantities h_j $(j=0,...,\ n)$ stand for fixed constants. Similarly, a_j $(j=0,...,\ n+1)$ are given constants whereas it is reasonable to use notations $a_o=0$, $a_{n+1}=l$.

It is supposed that the cylindrical shell is long enough so that boundary conditions are not close to critical (experiments show that the condition $2l> 1{,}5R$ for this purpose should be satisfied) and at the same time it is short enough (we assume that $2l <30R$) so that it is possible not to consider a shell, as long tubular core.

It is known in the linear elastic fracture mechanics (see Anderson, 2005; Broberg, 1999; Broek, 1990) that repeated loading and stress concentration at sharp corners entails cracks. Thus it is reasonable to assume that at the re-entrant corners of steps e.g. at $x=a_j$ $(j=0,...,\ n)$ cracks of depth c_j are located. For the simplicity sake we assume that these flaws are stable circular surface cracks. In the present study like in Rizos et al. (1990), Chondros et al. (2001), Dimarogonos (1996), Kukla (2009) no attention will be paid to the crack extension during operation of the structure.

1.2. Basic equations

Thanks to hypotheses of Kirchhoff displacements at each point of a shell, also deformations are defined through displacements of the middle surface. Due to axial symmetry one can reduce the problem to an one-dimensional problem. Axial symmetry allows to simplify the basic equations of the theory of thin shells considerably.

In the case of small deflections of axisymmetric cylindrical shells the stress resultants contributing to the strain energy are membrane forces N_1 and N in the axial and hoop direction, respectively, bending moment M and shear force Q. Equilibrium conditions of a shell element have the form (see Reddy, 2007; Soedel, 2004; Ventsel and Krauthammer, 2001)

$$\begin{aligned}
&\frac{\partial N_1}{\partial x} = \rho h \frac{\partial^2 u}{\partial t^2},\\
&\frac{\partial M}{\partial x} = Q,\\
&\frac{\partial Q}{\partial x} = \frac{N}{R} - p + \rho h \frac{\partial^2 w}{\partial t^2}.
\end{aligned} \tag{1.2.1}$$

In (1.2.1) u and w stand for displacements in the axial and transverse direction whereas p is the intensity of the distributed transverse pressure**,** ρ is the material density and t stands for time. Neglecting the axial force N_1 and the axial displacement u one can present the equilibrium equations (1.2.1) as

$$\frac{\partial^2 M}{\partial x^2} - \frac{N}{R} + p - \rho h_j \frac{\partial^2 w}{\partial t^2} = 0 \tag{1.2.2}$$

for $x \in (a_j, a_{j+1})$, where j=0,...,n.

Strain components corresponding to (1.2.2) are

$$\begin{aligned} \varepsilon_1 &= \frac{\partial u}{\partial x}, \\ \varepsilon &= \frac{w}{R}, \\ \chi &= -\frac{\partial^2 w}{\partial x^2}. \end{aligned} \tag{1.2.3}$$

In the case of shells made of an isotropic elastic material generalized Hooke's law reads as (see Reddy, 2007)

$$\begin{Bmatrix} N_1 \\ N \\ M \end{Bmatrix} = \frac{Eh}{1-\nu^2} \begin{bmatrix} 1 & \nu & 0 \\ \nu & 1 & 0 \\ 0 & 0 & h^2/12 \end{bmatrix} \cdot \begin{Bmatrix} \varepsilon_1 \\ \varepsilon \\ \chi \end{Bmatrix}. \tag{1.2.4}$$

Substituting (1.2.4) with (1.2.3) in (1.2.2) yields the equation

$$\frac{\partial^4 w}{\partial x^4} + \frac{12(1-\nu^2)}{R^2 h_j^2} w = -\frac{12\rho \cdot h_j (1-\nu^2)}{E h_j^3} \frac{\partial^2 w}{\partial t^2}, \tag{1.2.5}$$

which must be satisfied for $x \in (a_j, a_{j+1})$, where j=0,...,n.

When deriving (1.2.5) it was taken into account that according to (1.2.4)

$$N_1 = \frac{Eh}{1-\nu^2}(\varepsilon_1 + \nu\varepsilon),$$

$$N = \frac{Eh}{1-\nu^2}(\nu\varepsilon_1 + \varepsilon).$$

Since N_1 =0 and ε_1=-$\nu\varepsilon$ one has

$$N = Eh\frac{w}{R} \tag{1.2.6}$$

and

$$\frac{\partial u}{\partial x} = -\nu\frac{w}{R}. \tag{1.2.7}$$

1.3. The crack disturbance function

The presence of flaws or cracks in a structural member involves considerable local flexibility. Additional local flexibility due to a crack depends on the crack geometry as well as on the geometry of the structural element and its loading. Probably the first attempt to prescribe the local flexibility of a cracked beam was undertaken by Irwin (1960) who recognized the relationship between the compliance C of the beam and stress intensity factor K. Later on, Rizos, Aspragathos, Dimarogonas (1990); Dimarogonas (1996); Chondros, Dimarogonas, Yao (1998); Kukla (2009) introduced so called massless rotating spring model which reveals the relationship between the stress intensity factor and local compliance of the beam. In the present study we attempt to extend this approach to axisymmetric vibrations of circular cylindrical shells with circular cracks of constant depth.

Let us consider the crack located at the cross section $x=a_j$ and let the segments adjacent to the crack have thicknesses h_{j-1} and h_j, respectively. According to the current approach it is assumed that the slope of deflection w' is discontinuous, e.g.

$$w'(a_j+0,t)\text{-}w'(a_j-0,t)=\theta_j, \tag{1.3.1}$$

where θ_j=0.

The quantity θ_j can be treated as an additional angle caused by the crack at $x=a_j$. If θ_j is a generalized coordinate then corresponding generalized force is $M(a_j)$ whereas

$$\theta_j = C_j M(a_j), \tag{1.3.2}$$

where C_j stands for the additional compliance of the shell at $x=a_j$. Note that the compliance C is a quantity reverse to the stiffness K_T of the shell. On the other hand,

$$\theta_j = \frac{\partial U_T}{\partial M(a_j)}, \tag{1.3.3}$$

provided U_T is the extra strain energy due to the crack. It immediately follows from (1.3.2) and (1.3.3) that

$$C_j = \frac{\partial \theta_j}{\partial M(a_j)} \tag{1.3.4}$$

or

$$C_j = \frac{\partial^2 U_T}{\partial M^2(a_j)}. \tag{1.3.5}$$

Note that equalities (1.3.2) – (1.3.5) are well known in the linear elastic fracture mechanics in the case when the generalized displacement and generalized force are u_j and P_j, respectively (see Broek (1990), Anderson (2005), Broberg (1999).

Generalized stresses, energy release rate G and the stress intensity factor K are related to each other as

$$G = \frac{M^2}{2}\frac{dC}{dA} \tag{1.3.6}$$

and

$$G = \frac{K^2}{E'}, \tag{1.3.7}$$

where A stands for the crack surface area and $E' = E$ for the plane stress state and $E' = E/(1-v^2)$ for the plane deformation state.

The stress intensity factor is defined as

$$K = \sigma\sqrt{\pi c}\ F(\frac{c}{h}) \tag{1.3.8}$$

(see Tada, Paris, 2000). Here c is the crack depth and $\sigma=6M/h^2$ whereas F stands for a function to be determined experimentally. When applying (1.3.6) – (1.3.8) for the cross section $x=a_j$ with crack depth c_j one has

$$\frac{M_j^2}{2}\frac{dC_j}{dc_j} = \frac{36M_j^2}{E'h_j^4}\pi c_j F^2(\frac{c_j}{h_j}) \tag{1.3.9}$$

provided $h_j < h_{j-1}$ and $M_j = M(a_j)$. We introduce the notation $s_j=c_j/h_j$.
Thus it follows from (1.3.9) that

$$\frac{dC_j}{ds_j} = \frac{72\pi}{E'h_j^2} s_j F^2(s_j) \tag{1.3.10}$$

and after integration one obtains

$$C_j = \frac{72\pi}{E'h_j^2}\int_0^{s_j} s_j F^2(s_j)ds_j \tag{1.3.11}$$

for the plane stress state. It is assumed herein that $C_j=0$ when $s_j=0$.

The function $F(s_j)$ in (1.3.8) – (1.3.11) is called shape function as it is different for experimental specimens of different shape. Many authors have investigated the problem of determination of the stress intensity factor for various specimens (among others Brown and Srawley, 1967; Freund and Hermann, 1976; Irwin, 1960; Tada, Paris, Irwin, 2000).

In the present study we are resorting to the data of experiments conducted by Brown and Srawley which can be approximated as (see Tada, Paris, Irwin, 2000)

$$F(s_j) = 1{,}93 - 3{,}07 s_j + 14{,}53 s_j^{\,2} - 25{,}11 s_j^{\,3} + 25{,}8 s_j^{\,4}. \tag{1.3.12}$$

Combining (1.3.11) and (1.3.12) one can obtain

$$C_j = \frac{72\pi}{E' h_j^2} f(s_j), \tag{1.3.13}$$

where

$$f(s_j) = 1{,}862 s_j^{\,2} - 3{,}95 s_j^{\,3} + 16{,}375 s_j^{\,4} - 37{,}226 s_j^{\,5} + 76{,}81 s_j^{\,6} - \\ - 126{,}9 s_j^{\,7} + 172{,}5 s_j^{\,8} - 143{,}97 s_j^{\,9} + 66{,}56 s_j^{\,10}. \tag{1.3.14}$$

The function (1.3.14) is employed also in papers by Dimarogonas (1996), Chondros, Dimarogonas, Yao (2001), Kukla (2009).

According to the concept of massless rotating spring one can equalize $K_{Tj}=1/C_j$ and thus

$$K_{Tj} = \frac{E' h_j^2}{72\pi \cdot f(s_j)}, \tag{1.3.15}$$

where

$$f(s_j) = \int_0^{s_j} \xi F^2(\xi) d\xi. \tag{1.3.16}$$

From (1.3.2) with (1.2.3), (1.2.4) one obtains

$$\theta_j = -\frac{E h_j^3}{12 K_{Tj}(1-\nu^2)} \cdot w''(a_j + ,t). \tag{1.3.17}$$

1.4. Solution of governing equations

We are looking for the general solution of the equation (1.2.5) for $x \in (a_j, a_{j+1})$ in the form

$$w(x,t) = X_j(x)T(t), \tag{1.4.1}$$

where $X_j(x)$ and $T(t)$ are functions of a single variable. Differentiating (1.4.1) with respect to x and t and substituting in (1.2.5) leads to the equation

$$X_j^{IV}(x)T(t) + \frac{12(1-\nu^2)}{R^2 h_j^2} X_j(x)T(t) = -\rho \cdot \frac{12(1-\nu^2)}{E h_j^2} X_j(x)\ddot{T}(t), \tag{1.4.2}$$

where the notation

$$X_j^{IV}(x) = \frac{d^4 X_j}{dx^4},$$
$$\ddot{T}(t) = \frac{d^2 T}{dt^2}$$

is used. Note that (1.4.2) must be satisfied for $x \in (a_j, a_{j+1})$ for $j=0,\ldots,n$.

Separating variables in (1.4.2) one easily obtains

$$\ddot{T} + \omega^2 T = 0 \tag{1.4.3}$$

and

$$X_j^{IV} - r_j^4 X_j = 0 \tag{1.4.4}$$

for $x \in (a_j, a_{j+1})$, $j=0,\ldots,n$. Here the rotation

$$r_j^4 = \omega^2 \frac{12\rho(1-\nu^2)}{E h_j^2} - \frac{12(1-\nu^2)}{R^2 h_j^2} \tag{1.4.5}$$

is introduced whereas ω stands for the frequency of free vibrations of the shell.

Equation (1.4.3) gives the solution

$$T = \alpha \sin(\omega t + \varphi_0), \tag{1.4.6}$$

α and φ_0 being arbitrary constants. Assuming that

$$w(x,0)=0,$$
$$T(0)=0$$

yields φ_0=0. Thus it follows from (1.4.6) that

$$T=\alpha\sin\omega t. \tag{1.4.7}$$

The general solution of the linear fourth order equation (1.4.4) can be presented as

$$X_j(x)=A_j\sin(r_jx)+B_j\cos(r_jx)+C_j\sinh(r_jx)+D_j\cosh(r_jx). \tag{1.4.8}$$

Note that (1.4.8) holds good for $x\in(a_j,a_{j+1})$, j=0,...,n.

We are considering the vibrations of the shell which is simply supported at both ends. Because of symmetry we will consider only right hand half of the shell and there by the origin of the axis *Ox* can be put at the central cross-section of the tube. Thus boundary requirements give following conditions. At the center of the shell due to symmetry one has

$$\begin{aligned} X_0'(0)&=0,\\ X_0'''(0)&=0. \end{aligned} \tag{1.4.9}$$

Whereas at the simply supported end $w(l,t)$=0, M(l,t)=0 and thus

$$\begin{aligned} X_n(l)&=0,\\ X_n''(l)&=0 \end{aligned} \tag{1.4.10}$$

at the simply supported right hand end .

It follows from physical considerations that the displacement $w(x,t)$ bending moment $M(x,t)$ and shear force $Q(x,t)$ must be continuous at cross sections $x=a_j$, j=0,...,n, where steps of the thickness and cracks are located.

However, the use of the rotating spring model entails discontinuities of the slope $w'(x,t)$ as it was discussed above. According to the Hooke's law the bending moment $M(x,t)$ reads

$$M(x,t)=-\frac{Eh_j^3}{12(1-\nu^2)}w''(x,t) \tag{1.4.11}$$

provided $x \in (a_j, a_{j+1})$. The last equality shows that *M(x,t)* is continuous, if $h^3 w''(x,t)$ is continuous. Similarly we can conclude that the shear force is continuous if the quantity $h^3 w'''(x,t)$ is continuous when passing the cross sections $x=a_j$.

Summarizing the results one obtains the system of intermediate conditions at $x=a_j$, $j=0,\ldots,n$ as

$$X_j(a_j+0)-X_{j-1}(a_j-0)=0,$$

$$X_j'(a_j+0)-X_{j-1}'(a_j-0)+p_j X_j''(a_j-0)=0, \qquad (1.4.12)$$

$$h_j^3 X_j''(a_j+0)-h_{j-1}^3 X_{j-1}''(a_j-0)=0,$$

$$h_j^3 X_j'''(a_j+0)-h_{j-1}^3 X_{j-1}'''(a_j-0)=0.$$

In (1.4.12) the notation

$$p_j = -\frac{Eh_j^3}{12(1-\nu^2)K_{Tj}} \qquad (1.4.13)$$

is introduced. Here and elsewhere one has to distinguish the left and right hand limits, e.g. in the case of a function $z=z_j(x)$ one has

$$Z_j(a_j \pm 0) = \lim_{x \to a_j \pm 0} Z(x).$$

1.5. Determination of eigenvalues

It follows from (1.4.5) that

$$r_j^4 h_j^2 = \frac{\omega^2 12\rho(1-\nu^2)}{E} - \frac{12(1-\nu^2)}{R^2}. \qquad (1.5.1)$$

Consequently the product $h_j r_j^2$ takes common value for each interval $x \in (a_j, a_{j+1})$, $j=0,\ldots,n$. Therefore, it is reasonable to introduce a real number k so that

$$r_j = \frac{k}{\sqrt{h_j}} \tag{1.5.2}$$

for each j=0,...,n.

From (1.5.1) with (1.5.2) one can determine the frequency of axisymmetric free vibrations of circular cylindrical shell as

$$\omega = \sqrt{\frac{E}{\rho}}\frac{1}{R}\sqrt{\frac{k^4R^2}{12(1-\nu^2)}+1}.$$

In order to specify the deflected shape of a shell generator one has to specify functions $X_j(x)$ for each j=0,...,n. So far, functions $X_j(x)$are given by (1.4.8) which involves unknown constants A_j, B_j, C_j, D_j, e.g. totally 4n+4 unknowns. These constants can be determined from boundary and intermediate conditions (1.4.9), (1.4.10) and (1.4.12). Since the number of equations in (1.4.12) is 4n the total number of available conditions is also 4n+4, as might be expected. From symmetry conditions at the point x=0 with (1.4.8) and (1.4.9) two constants are defined

$$A_0=0, \quad C_0=0. \tag{1.5.3}$$

The requirements (1.4.9) with (1.4.8) yield

$$\begin{aligned} &A_n \sin r_n l + B_n \cos r_n l + C_n \sinh r_n l + D_n \cosh r_n l = 0, \\ &-A_n \sin r_n l - B_n \cos r_n l + C_n \sinh r_n l + D_n \cosh r_n l = 0 \end{aligned} \tag{1.5.4}$$

for the simply supported right hand end of the tube.

Evidently, (1.5.4) can be converted into the system

$$\begin{aligned} &A_n \sin r_n l + B_n \cos r_n l = 0, \\ &C_n \sinh r_n l + D_n \cosh r_n l = 0. \end{aligned} \tag{1.5.5}$$

Making use of (1.4.8) one can present (1.4.12) as

$$\begin{aligned} &A_{j-1}\sin r_{j-1}a_j + B_{j-1}\cos r_{j-1}a_j + C_{j-1}\sinh r_{j-1}a_j + D_{j-1}\cosh r_{j-1}a_j - \\ &-(A_j \sin r_j a_j + B_j \cos r_j a_j + C_j \sinh r_j a_j + D_j \cosh r_j a_j) = 0, \\ &r_{j-1}(A_{j-1}\cos r_{j-1}a_j - B_{j-1}\sin r_{j-1}a_j + C_{j-1}\cosh r_{j-1}a_j + D_{j-1}\sinh r_{j-1}a_j) - \\ &r_j(A_j(\cos r_j a_j - p_j r_j \sin r_j a_j) + B_j(-\sin r_j a_j - p_j r_j \cos r_j a_j) + \\ &+ C_j(\cosh r_j a_j + p_j r_j \sinh r_j a_j) + D_j(\sinh r_j a_j + p_j r_j \cosh r_j a_j) = 0, \end{aligned} \tag{1.5.6}$$

$$h_{j-1}^3 r_{j-1}^2 (- A_{j-1} \sin r_{j-1} a_j - B_{j-1} \cos r_{j-1} a_j + C_{j-1} \sinh r_{j-1} a_j + D_{j-1} \cosh r_{j-1} a_j) -$$
$$- h_j^3 r_j^2 (- A_j \sin r_j a_j - B_j \cos r_j a_j + C_j \sinh r_j a_j + D_j \cosh r_j a_j) = 0,$$
$$h_{j-1}^3 r_{j-1}^3 (- A_{j-1} \cos r_{j-1} a_j + B_{j-1} \sin r_{j-1} a_j + C_{j-1} \cosh r_{j-1} a_j + D_{j-1} \sinh r_{j-1} a_j) -$$
$$- h_j^3 r_j^3 (- A_j \cos r_j a_j + B_j \sin r_j a_j + C_j \cosh r_j a_j + D_j \sinh r_j a_j) = 0$$

for j=0,...,n.

It is worthwhile to emphasize that equations (1.5.3), (1.5.5), (1.5.6) serve for determination of unknowns A_j, B_j, C_j, D_j (j=0,...,n). However, this is an algebraic linear homogeneous system of equations with 4n+4 equations and 4n+4 unknowns.

A non-trivial solution of this system exists if the determinant of this system vanishes.

1.6. System of recursive equations

For greater values of n the calculation of the determinant Δ is quite complicated. However, there exists another way of solution of the problem without arduous calculation of Δ.

Let us denote the vector of constants A_j, B_j, C_j, D_j by $\vec{Y}_j$, e.g.

$$\vec{\mathrm{Y}}_{\mathrm{j}} = \begin{bmatrix} A_j \\ B_j \\ C_j \\ D_j \end{bmatrix}. \tag{1.6.1}$$

The system of equations (1.5.6) can be rewritten in the form

$$\left[\mathrm{M}_{\mathrm{j-1}}\right]\vec{\mathrm{Y}}_{\mathrm{j-1}} = \left[\mathrm{N}_{\mathrm{j}}\right]\vec{\mathrm{Y}}_{\mathrm{j}} \tag{1.6.2}$$

for j=0,...,n. In (1.6.2) according to (1.5.6)

$$\left[\mathrm{N}_{\mathrm{j}}\right] = \begin{bmatrix} \sin r_j a_j & \cos r_j a_j & \sinh r_j a_j & \cosh r_j a_j \\ r_j(\cos r_j a_j - & -r_j(\sin r_j a_j + & r_j(\cosh r_j a_j + & r_j(\sinh r_j a_j + \\ -p_j r_j \sin r_j a_j) & +p_j r_j \cos r_j a_j) & +p_j r_j \sinh r_j a_j) & +p_j r_j \cosh r_j a_j) \\ -h_j^3 r_j^2 \sin r_j a_j & -h_j^3 r_j^2 \cos r_j a_j & h_j^3 r_j^2 \sinh r_j a_j & h_j^3 r_j^2 \cosh r_j a_j \\ -h_j^3 r_j^3 \cos r_j a_j & h_j^3 r_j^3 \sin r_j a_j & h_j^3 r_j^3 \cosh r_j a_j & h_j^3 r_j^3 \sinh r_j a_j \end{bmatrix} \tag{1.6.3}$$

and

$$\left[\mathrm{M}_{\mathrm{j\text{-}1}}\right]=\begin{bmatrix} \sin r_{j\text{-}1}a_j & \cos r_{j\text{-}1}a_j & \sinh r_{j\text{-}1}a_j & \cosh r_{j\text{-}1}a_j \\ r_{j\text{-}1}\cos r_{j\text{-}1}a_j & -r_{j\text{-}1}\sin r_{j\text{-}1}a_j & r_{j\text{-}1}\cosh r_{j\text{-}1}a_j & r_{j\text{-}1}\sinh r_{j\text{-}1}a_j \\ -h_{j-1}^3 r_{j-1}^2 \sin r_{j\text{-}1}a_j & -h_{j-1}^3 r_{j-1}^2 \cos r_{j\text{-}1}a_j & h_{j-1}^3 r_{j-1}^2 \sinh r_{j\text{-}1}a_j & h_{j-1}^3 r_{j-1}^2 \cosh r_{j\text{-}1}a_j \\ -h_{j-1}^3 r_{j-1}^3 \cos r_{j\text{-}1}a_j & h_{j-1}^3 r_{j-1}^3 \sin r_{j\text{-}1}a_j & h_{j-1}^3 r_{j-1}^3 \cosh r_{j\text{-}1}a_j & h_{j-1}^3 r_{j-1}^3 \sinh r_{j\text{-}1}a_j \end{bmatrix} \tag{1.6.4}$$

for each $j=0,\ldots,n$. Special care needs the case $j=0$. Now one obtains from (1.5.3) that

$$A_0=0, \qquad C_0=0.$$

Thus, then

$$\vec{\mathrm{Y}}_0=\begin{bmatrix} 0 \\ B_0 \\ 0 \\ D_0 \end{bmatrix}. \tag{1.6.5}$$

Multiplying (1.6.2) from left with $\left[\mathrm{N}_{\mathrm{j}}^{-1}\right]$ one obtains

$$\vec{\mathrm{Y}}_{\mathrm{j}}=\left[\mathrm{N}_{\mathrm{j}}^{-1}\right]\left[\mathrm{M}_{\mathrm{j-1}}\right]\vec{\mathrm{Y}}_{\mathrm{j-1}}$$

or briefly

$$\vec{\mathrm{Y}}_{\mathrm{j}}=\left[\mathrm{S}_{\mathrm{j}}\right]\vec{\mathrm{Y}}_{\mathrm{j-1}}, \tag{1.6.6}$$

where the notation

$$\left[\mathrm{S}_{\mathrm{j}}\right]=\left[\mathrm{N}_{\mathrm{j}}^{-1}\right]\left[\mathrm{M}_{\mathrm{j-1}}\right] \tag{1.6.7}$$

is used.

It immediately infers from (1.6.6) that

$$\begin{aligned}
\vec{Y}_1 &= [S_1]\vec{Y}_0, \\
\vec{Y}_2 &= [S_2]\vec{Y}_1, \\
&\text{- - - - - - -} \\
\vec{Y}_n &= [S_n]\vec{Y}_{n-1}.
\end{aligned} \tag{1.6.8}$$

When substituting $\vec{Y}_{n-1}$, $\vec{Y}_{n-2}$, …, $\vec{Y}_1$ into the last equation in (1.6.8) one obtains

$$\vec{Y}_n = [S_n][S_{n-1}]..[S_1]\vec{Y}_0 \tag{1.6.9}$$

or

$$\vec{Y}_n = [P]\vec{Y}_0 \quad , \tag{1.6.10}$$

where

$$[P] = [S_n][S_{n-1}]..[S_1] \quad . \tag{1.6.11}$$

Let us denote

$$[P] = \begin{bmatrix} p_{11} & p_{12} & p_{13} & p_{14} \\ p_{21} & p_{22} & p_{23} & p_{24} \\ p_{31} & p_{32} & p_{33} & p_{34} \\ p_{41} & p_{42} & p_{43} & p_{44} \end{bmatrix}. \tag{1.6.12}$$

When calculating elements of the matrix [P] one has to take into account that elements p_{ij} (i,j=1,2,3,4) as well as elements of matrices [S_1],…, [S_n] do not depend on unknowns B_0 and D_0.

The linear system of equations (1.5.5) can been rewritten in the matrix form as

$$\begin{vmatrix} \sin r_n l & \cos r_n l & 0 & 0 \\ 0 & 0 & \sinh r_n l & \cosh r_n l \\ 0 & 0 & 0 & 0 \\ 0 & 0 & 0 & 0 \end{vmatrix} \begin{vmatrix} A_n \\ B_n \\ C_n \\ D_n \end{vmatrix} = 0. \tag{1.6.13}$$

In order to determine these unknown constants we have to consider the system (1.6.10) together with equations (1.6.13). Now the obtained system involves two equations and two constants to be determined. Since it is a linear homogeneous system its determinant must be equal to zero. The system (1.6.10) and (1.6.13) can be rewritten as

$$\begin{vmatrix} \sin r_n l & \cos r_n l & 0 & 0 \\ 0 & 0 & \sinh r_n l & \cosh r_n l \\ 0 & 0 & 0 & 0 \\ 0 & 0 & 0 & 0 \end{vmatrix} \begin{vmatrix} p_{11} & p_{12} & p_{13} & p_{14} \\ p_{21} & p_{22} & p_{23} & p_{24} \\ p_{31} & p_{32} & p_{33} & p_{34} \\ p_{41} & p_{42} & p_{43} & p_{44} \end{vmatrix} \begin{vmatrix} 0 \\ B_0 \\ 0 \\ D_0 \end{vmatrix} = 0. \quad (1.6.14)$$

The equation (1.6.14) can be presented as a system of equations

$$(p_{12}\sin r_n l + p_{22}\cos r_n l)B_0 + (p_{14}\sin r_n l + p_{24}\cos r_n l)D_0 = 0,$$
$$(p_{32}\sinh r_n l + p_{42}\cosh r_n l)B_0 + (p_{34}\sinh r_n l + p_{44}\cosh r_n l)D_0 = 0.$$

The latter is a linear homogeneous system with respect to unknowns B_0, D_0. It has a non-trivial solution if the determinant

$$\Delta = \begin{vmatrix} p_{11}\sin r_n l p_{11} + p_{22}\cos r_n l & p_{14}\sin r_n l + p_{24}\cos r_n l \\ p_{32}\sinh r_n l + p_{42}\cosh r_n l & p_{34}\sinh r_n l + p_{44}\cosh r_n l \end{vmatrix}$$

is equal to zero.
The equality Δ=0 leads to the equation

$$\begin{aligned} &\sinh r_n l\left[(p_{12}p_{34} - p_{14}p_{32})\sin r_n l + (p_{22}p_{34} - p_{24}p_{32})\cos r_n l\right] + \\ &\cosh r_n l\left[(p_{12}p_{44} - p_{14}p_{42})\sin r_n l + (p_{22}p_{44} - p_{24}p_{42})\cos r_n l\right] = 0, \end{aligned} \quad (1.6.15)$$

where p_{ij} – components of the matrix **P**.

The equations (1.6.15) can be easily solved with the aid of existing codes with respect to the characteristic number k related to r_j by relations (1.5.2).
Let's consider a case when half of the shell consists of two parts with thickness h_0 and h_1, accordingly, and the jump is in the section $x=a$. In this case n=1 and elements of matrix [P]=[S_1]=(s_{ij}) look like

$$s_{11}(k) = (1+g_1)\sin(kl_1)\sin(kl_2) + (g_2+g_4)\cos(kl_1)\cos(kl_2) - g_3\sin(kl_1)\cos(kl_2),$$
$$s_{12}(k) = (1+g_1)\cos(kl_1)\sin(kl_2) - (g_2+g_4)\sin(kl_1)\cos(kl_2) - g_3\cos(kl_1)\cos(kl_2),$$
$$s_{13}(k) = (1-g_1)\sinh(kl_1)\sin(kl_2) + (g_2-g_4)\cosh(kl_1)\cos(kl_2) + g_3\sinh(kl_1)\cos(kl_2),$$
$$s_{14}(k) = (1-g_1)\cosh(kl_1)\sin(kl_2) + (g_2-g_4)\sinh(kl_1)\cos(kl_2) + g_3\cosh(kl_1)\cos(kl_2),$$
$$s_{21}(k) = (1+g_1)\sin(kl_1)\cos(kl_2) - (g_2+g_4)\cos(kl_1)\sin(kl_2) + g_3\sin(kl_1)\sin(kl_2),$$
$$s_{22}(k) = (1+g_1)\cos(kl_1)\cos(kl_2) + (g_2+g_4)\sin(kl_1)\sin(kl_2) + g_3\cos(kl_1)\sin(kl_2),$$
$$s_{23}(k) = (1-g_1)\sinh(kl_1)\cos(kl_2) - (g_2-g_4)\cosh(kl_1)\sin(kl_2) - g_3\sinh(kl_1)\sin(kl_2),$$

$$s_{24}(k) = (1-g_1)\cosh(kl_1)\cos(kl_2) - (g_2 - g_4)\sinh(kl_1)\sin(kl_2) - g_3\cosh(kl_1)\sin(kl_2),$$
$$s_{31}(k) = -(1-g_1)\sin(kl_1)\sinh(kl_2) + (g_2 - g_4)\cos(kl_1)\cosh(kl_2) - g_3\sin(kl_1)\cosh(kl_2),$$
$$s_{32}(k) = -(1-g_1)\cos(kl_1)\sinh(kl_2) - (g_2 - g_4)\sin(kl_1)\cosh(kl_2) - g_3\cos(kl_1)\cosh(kl_2),$$
$$s_{33}(k) = -(1+g_1)\sinh(kl_1)\sinh(kl_2) + (g_2 + g_4)\cosh(kl_1)\cosh(kl_2) + g_3\sinh(kl_1)\cosh(kl_2),$$
$$s_{34}(k) = -(1+g_1)\cosh(kl_1)\sinh(kl_2) + (g_2 + g_4)\sinh(kl_1)\cosh(kl_2) + g_3\cosh(kl_1)\cosh(kl_2),$$
$$s_{41}(k) = (1-g_1)\sin(kl_1)\cosh(kl_2) - (g_2 - g_4)\cos(kl_1)\sinh(kl_2) + g_3\sin(kl_1)\sinh(kl_2),$$
$$s_{42}(k) = (1-g_1)\cos(kl_1)\cosh(kl_2) + (g_2 - g_4)\sin(kl_1)\sinh(kl_2) + g_3\cos(kl_1)\sinh(kl_2),$$
$$s_{43}(k) = (1+g_1)\sinh(kl_1)\cosh(kl_2) - (g_2 + g_4)\cosh(kl_1)\sinh(kl_2) - g_3\sinh(kl_1)\sinh(kl_2),$$
$$s_{44}(k) = (1+g_1)\cosh(kl_1)\cosh(kl_2) - (g_2 + g_4)\sinh(kl_1)\sinh(kl_2) - g_3\cosh(kl_1)\sinh(kl_2),$$

where

$$l_1 = a/\sqrt{h_0},$$
$$l_2 = a/\sqrt{h_1},$$
$$g_1 = (h_0/h_1)^2,$$
$$g_2 = (h_1/h_0)^{1/2},$$
$$g_4 = g_1 g_2,$$
$$g_3 = 6\pi f(s_1)\sqrt{h_1}\, g_1 k,$$

h_0 and h_1 – stand for thicknesses of the shell before and after the cross-section $x=a$.

The equation for definition of characteristic number k in this case takes the form

$$\sinh kl_3\left[(s_{12}(k)s_{34}(k) - s_{14}(k)s_{32}(k))\sin kl_3 + (s_{22}(k)s_{34}(k) - s_{24}(k)s_{32}(k))\cos kl_3\right] +$$
$$\cosh kl_3\left[(s_{12}(k)s_{44}(k) - s_{14}(k)s_{42}(k))\sin kl_3 + (s_{22}(k)s_{44}(k) - s_{24}(k)s_{42}(k))\cos kl_3\right] = 0$$

or

$$\begin{aligned}
&((1-g_1)\cos kl_1\cosh kl_4 + ((g_2 - g_4)\sin kl_1 + g_3\cos kl_1)\sinh kl_4) \\
&((1-g_1)\cosh kl_1\cos kl_4 - ((g_2 - g_4)\sinh kl_1 + g_3\cosh kl_1)\sin kl_4) - \\
&-((1+g_1)\cos kl_1\cos kl_4 + ((g_2 + g_4)\sin kl_1 + g_3\cos kl_1)\sin kl_4) \\
&((1+g_1)\cosh kl_1\cosh kl_4 - ((g_2 + g_4)\sinh kl_1 + g_3\cosh kl_1)\sinh kl_4) = 0,
\end{aligned} \tag{1.6.16}$$

where

$$l_3 = l/\sqrt{h_1},$$
$$l_4 = (a-l)/\sqrt{h_1}.$$

In the case $a=l$ the equation (1.6.16) yields

$$\cos(kl_1) = 0.$$

So the influence of the crack on characteristic number k disappears when a tends to l. In the case a=0 the equation (1.6.16) gives

$$g_3 \sinh(kl_2)\cos(kl_2) + \cosh(kl_2)(-g_3 \sin(kl_2) + 2g_2 \cos(kl_2)) = 0,$$

where $g_3 = 6\pi f(s_1)\sqrt{h_1}g_1 k$.

1.7. Numerical results

For numerical calculations two samples have been chosen. These are one and two steps shells with simply supported right end and with symmetry conditions at the point x=0. Calculations were made by means of the package Mathcad.

We will use the notations for convenience: $a_i=\beta_i\ l$ and $\gamma_i=h_i/h_0$, where i is number of step.

The influence of the non-dimensional crack depth c/h on the characteristic number k in different cases is depicted in Fig. 1.2–1.10. Results of calculations are presented in Figs. 1.2–1.7 for one step shells and in Figs. 1.8–1.10 for two stepped shells.

Figs. 1.2–1.7 correspond to shells with thicknesses h_0 and h_1 having a single step of the thickness.

The parameters for the one-step shells are as following: l=0,6; h_1=0,006. It is assumed herein that the material of the shell is a homogeneous elastic material. Here and henceforth we take $h=min(h_0,\ h_1)$. Let us introduce the notations $\gamma=h_1/h_0$, $\beta=a_1/l$. In Fig. 1.2 the sensitivity of the number k (and thus the eigen frequency ω) with respect to crack length c and to size of the step $\gamma=h_1/h_0$ at a point x=0 is shown. Here the shell is of constant thickness, e.g. for case γ=1. It can be seen from Fig. 1.2 that the bigger is the crack length the smaller is the number k for all cases of γ and that the smaller is the size of the step γ the smaller is the number k. In Figs. 1.3–1.4 the dependence between the characteristic number k and the crack length c is shown for stepped shells with step coordinates a_1=0,2l and a_1=0,7l, respectively. Here different curves correspond to different values of $\gamma=h_1/h_0$. It can be from Figs. 1. 2–1.4 that in the range of small cracks the number k is almost unsensitive with respect to small changes of the crack length. However, in the range of larger cracks when c>0,6 h_1 this sensitivity is more obvious. Similar matters can be observed in Figs. 1.5–1.7, as well.

In Figs. 1.5–1.7 the number k is show for stepped shells with h_1= 0,1h_0, h_1= 0,3h_0 and h_1= 0,8h_0, respectively. Here different curves correspond to different locations of the step, e.g. to different values of $\beta=a_1/l$. It can be seen from Fig. 1.5 that the number k decreases when the crack length c increases in the case of a fixed value of β.

In Figs. 1.8–1.10 shells with two steps and two cracks are considered. In Fig. 1.8 the results corresponding to shells of constant thickness and with two cracks

are presented (in this case $\gamma_1 = \gamma_2 = 1{,}0$). In Figs. 1.9–1.10 the ratios of thicknesses are denoted by $\gamma_j = h_j/h_0$; $j = 1,2$; whereas in Figs. 1.9–1.10 the results corresponding to shells with two cracks are presented (the cases $\gamma_1 = 0{,}2$; $\gamma_2 = 0{,}5$ and the case $\gamma_1 = 0{,}5$; $\gamma_2 = 0{,}2$, respectively).

Curves S1, S2, S3, S4 in Figs. 1.8–1.10 are associated with the crack locations which are presented in Tables 1.1.

Table 1.1: Curves S1, S2, S3, S4 in Figs. 1.8–1.10.

	S1	S2	S3	S4	S4 (Fig. 1.10)
a_1	$0{,}0l$	$0{,}1l$	$0{,}3l$	$0{,}7l$	$0{,}8l$
a_2	$0{,}3l$	$0{,}4l$	$0{,}7l$	$0{,}8l$	$0{,}9l$

Thus the numerical results show that for fixed values of geometrical parameters the number k decreases when crack length c increases.

Let the one-stepped shell with a crack be simulated geometrically as a two-stepped shell with small length of the intermediate section as shown in Fig. 1.11b.

In tables 1.1 and 1.2 two models of calculation of characteristic number k are compared. The first model is the one-stepped shell with the crack whereas the second model is depicted in Fig. 1.11b. In both cases $l = 0{,}6$, $h_1 = 0{,}006$. The length of the middle sector in Fig1.11b is $\Delta = 0{,}0001$. The ratio γ of model 1 equals to γ_1 of model 2, olso $\beta = \beta_1$, $\gamma_2 = 1$. Here β stands for the coordinate of step in the case of model 1, β_1 is the coordinate of the first step in Fig. 1.11b and s is the non-dimensional depth of the crack. In table 1.2 values of k for various values of depth of a crack and co-ordinates a_1 of model 1 are presented. Table 1.3 corresponds to the model 2 cases, when $\beta = 0$, $\beta = 0{,}4$ and $\beta = 0{,}7$. From tables 1.2 and 1.3 we can see that values of characteristic number k corresponding to the different models simulating the same crack, coincide with sufficient accuracy. Results are especially close at small values of the depth of the crack.

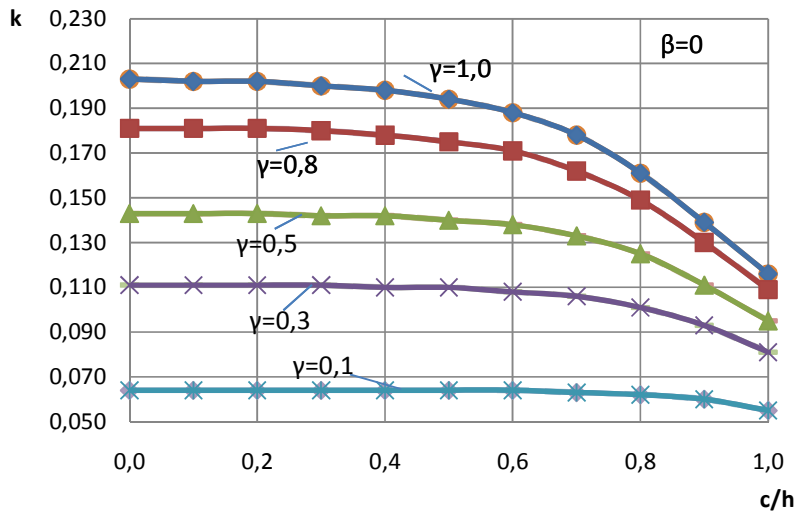

Fig. 1.2: Stepped shell with crack, the case β=0.

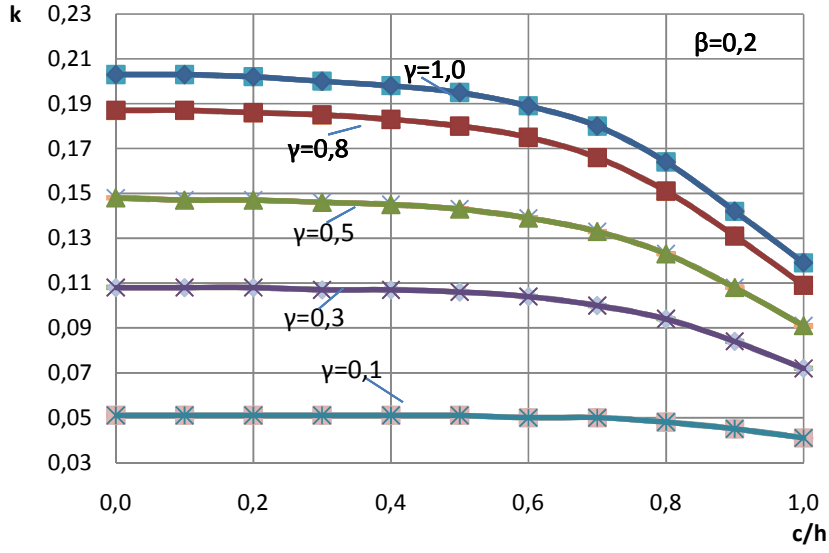

Fig. 1.3: Stepped shell with crack, the case β=0,2.

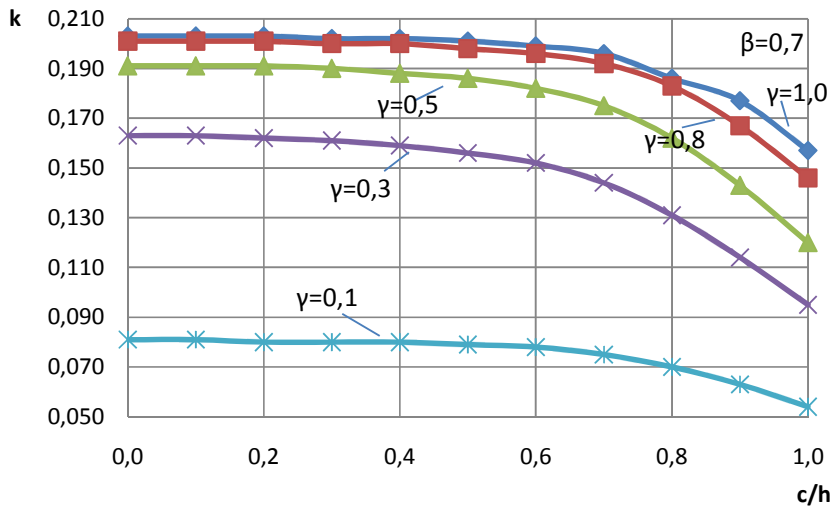

Fig. 1.4: Stepped shell with crack, the case β=0,7.

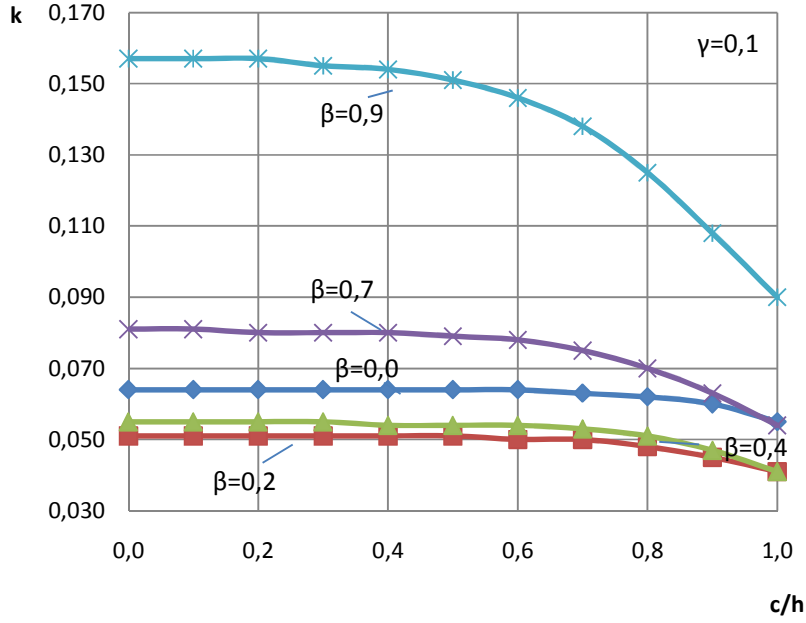

Fig. 1.5: Stepped shell with crack, the case γ=0,1.

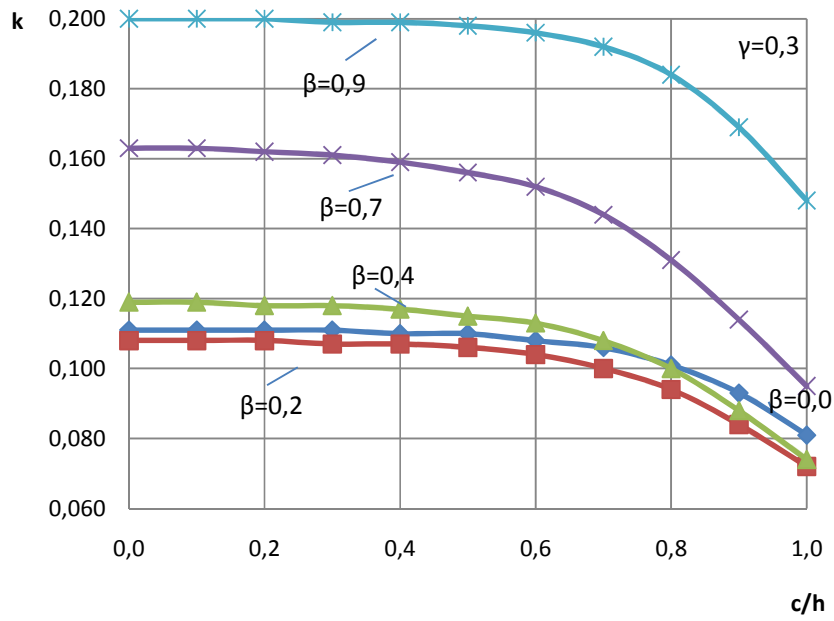

Fig. 1.6: Stepped shell with crack, the case γ=0,3.

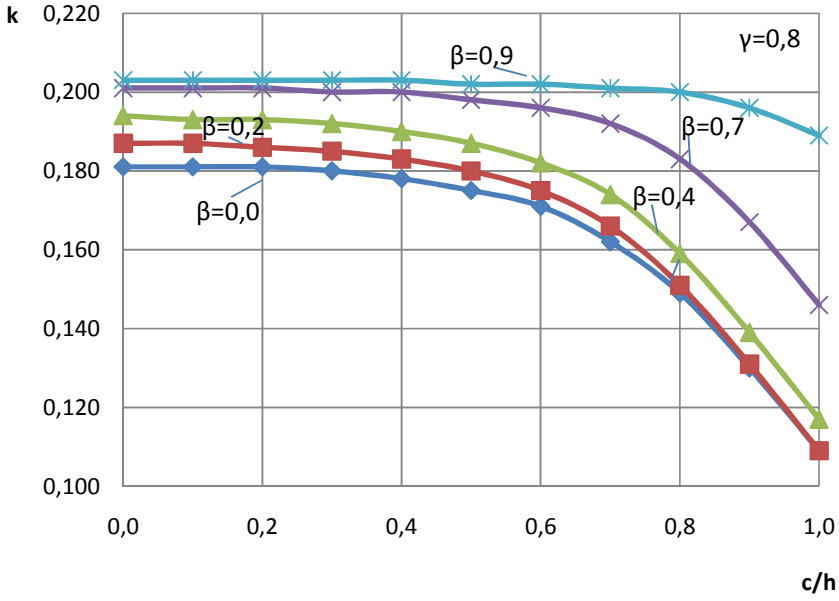

Fig. 1.7: Stepped shell with crack, the case γ=0,8.

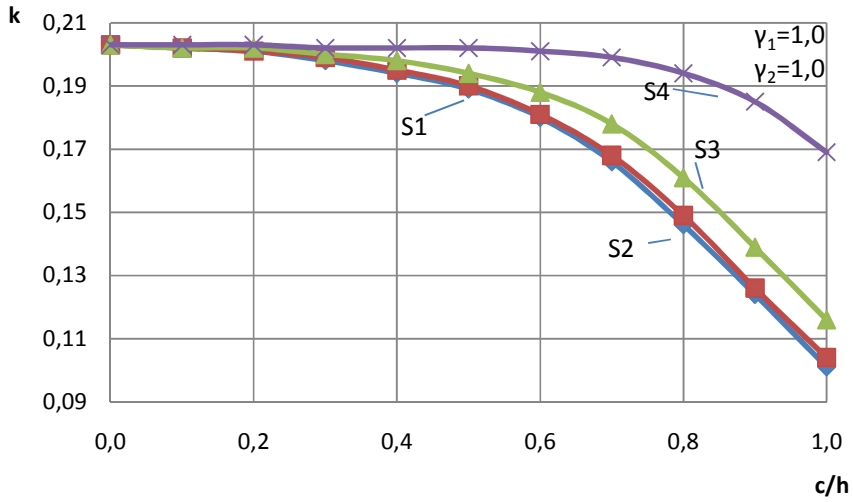

Fig. 1.8: Two-stepped cylindrical shell.

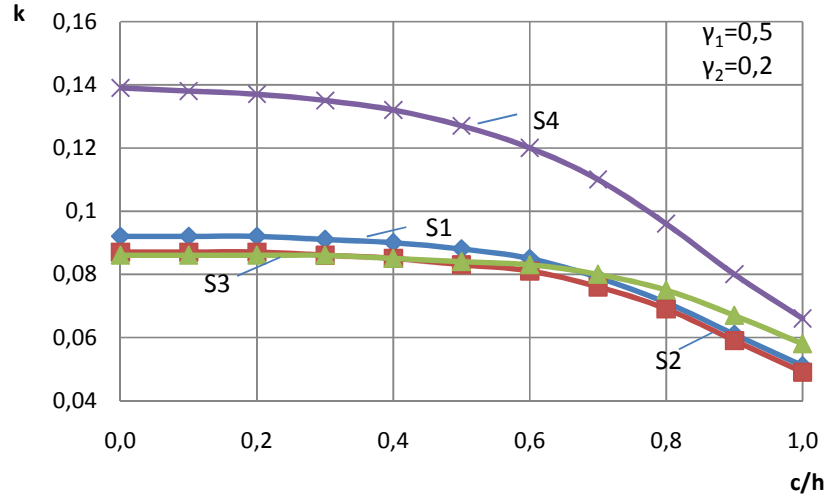

Fig. 1.9: Two-stepped cylindrical shell, the case γ_1=0,5; γ_2=0,2.

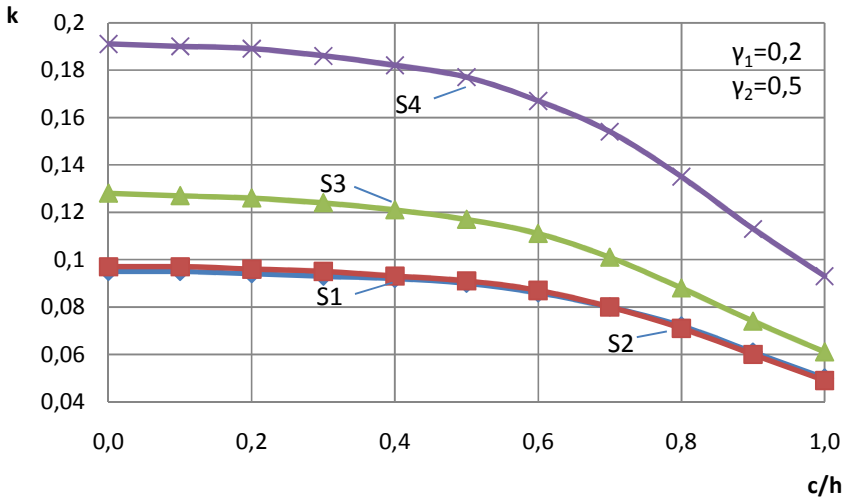

Fig. 1.10: Two-stepped cylindrical shell, the case $\gamma_1=0,2$; $\gamma_2=0,5$.

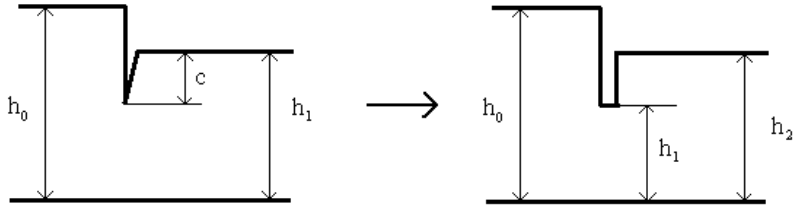

a) Crack model I b) Crack model II

Fig. 1.11: Two models of a crack in shell.

Table 1.1: Characteristic number *k* for the model I.

s	γ	1,0	0,5	0,1
	β	0,0	0,4	0,7
0,0		0,203	0,161	0,081
0,1		0,202	0,161	0,081
0,2		0,202	0,160	0,080
0,3		0,200	0,159	0,080
0,4		0,198	0,158	0,080
0,5		0,194	0,155	0,079
0,6		0,188	0,151	0,078
0,7		0,178	0,143	0,075
0,8		0,161	0,131	0,070
0,9		0,139	0,114	0,063
1,0		0,116	0,095	0,054

Table 1.2: Characteristic number *k* for model II.

s	γ_1	1,0	0,5	0,1
	β_1	0,0	0,4	0,7
0,0		0,203	0,161	0,080
0,1		0,203	0,161	0,080
0,2		0,203	0,161	0,080
0,3		0,203	0,160	0,080
0,4		0,202	0,160	0,079
0,5		0,202	0,159	0,078
0,6		0,200	0,158	0,077
0,7		0,197	0,154	0,073
0,8		0,186	0,141	0,064
0,9		0,140	0,102	0,044
1,0				

2. FREE VIBRATIONS OF CLAMPED AND CANTILEVER SHELLS WITH CRACKS

2.1. Formulation of the problem

In this chapter we will study free vibrations of one- and two-stepped circular cylindrical shells with cracks, similarly with the chapter 1 but with different boundary conditions. Let us consider small deflections of circular cylindrical shells of length l and radius R (Fig. 2.1). We shall confine our attention to axisymmetric free vibrations of the shell caused by an initial excitation. At the entrant corners of steps at $x=a_j$ cracks of depth c_j are located. The segments adjacent to the crack have thicknesses h_{j-1} and h_j.

Assume that the shell is divided into n ring segments. Here n denotes the number of total ring segments separated from the whole cylindrical shell at the locations of thickness variations. Evidently, equations (1.2.1)–(1.2.7) as well as (1.4.1)-(1.4.8) hold good in the cases of different boundary conditions. The general solution for the jth ring segment of the free vibration differential equation of shell (1.4.4) can be expressed as (1.4.8), e.g.

$$X_j(x) = A_j \sin(r_j x) + B_j \cos(r_j x) + C_j \sinh(r_j x) + D_j \cosh(r_j x). \tag{2.1.1}$$

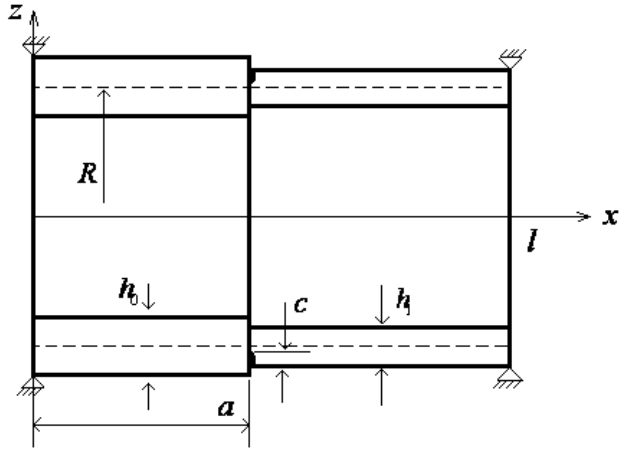

Fig. 2.1: One-stepped circular cylindrical shell with crack.

Consider first the case of the shell without defects. In this case the continuity of the deflection and generalised forces along the interface between the jth and (j+1)th ring segments leads to following continuity conditions for $X(x)$:

$$X_j(a_j+0)-X_{j-1}(a_j-0)=0,$$

$$X'_j(a_j+0)-X'_{j-1}(a_j-0)=0, \tag{2.1.2}$$

$$h_j^3X''_j(a_j+0)-h_{j-1}^3X''_{j-1}(a_j-0)=0,$$

$$h_j^3X'''_j(a_j+0)-h_{j-1}^3X'''_{j-1}(a_j-0)=0.$$

It is known that crack induces the discontinuity of the displacement field, and an extra local compliance due to the crack. In this case the continuity or discontinuity conditions can be written as (Dimarogonas 1996)

$$\begin{gathered} X_j(a_j+0)-X_{j-1}(a_j-0)=0, \\ X'_j(a_j+0)-X'_{j-1}(a_j-0)+p_jX''_j(a_j-0)=0, \\ h_j^3X''_j(a_j+0)-h_{j-1}^3X''_{j-1}(a_j-0)=0, \\ h_j^3X'''_j(a_j+0)-h_{j-1}^3X'''_{j-1}(a_j-0)=0, \end{gathered} \tag{2.1.3}$$

where

$$p_j=-\frac{Eh_j^3}{12(1-\nu^2)K_{Tj}} \tag{2.1.4}$$

2.2. Boundary conditions

We are considering the vibrations of the shell clamped at the left end and simply supported or free at the right hand end. Thus boundary requirements give for the clamped end

$$\begin{gathered} X_0(0)=0, \\ X'_0(0)=0 \end{gathered} \tag{2.2.1}$$

and for the simply supported right hand end

$$\begin{gathered} X_n(l)=0, \\ X''_n(l)=0. \end{gathered} \tag{2.2.2}$$

In the case of a free right hand end one has

$$X_n''(l) = 0, \quad X_n'''(l) = 0. \tag{2.2.3}$$

From (2.2.1) with (2.1.1) we have

$$B_0 + D_0 = 0, \quad A_0 + C_0 = 0. \tag{2.2.4}$$

For the shell simply supported at the right hand from (2.2.2) we have

$$\begin{aligned} &A_n \sin r_n l + B_n \cos r_n l + C_n \sinh r_n l + D_n \cosh r_n l = 0, \\ &- A_n \sin r_n l - B_n \cos r_n l + C_n \sinh r_n l + D_n \cosh r_n l = 0. \end{aligned} \tag{2.2.5}$$

Evidently, (2.2.5) can be converted into the system

$$\begin{aligned} &A_n \sin r_n l + B_n \cos r_n l = 0, \\ &C_n \sinh r_n l + D_n \cosh r_n l = 0. \end{aligned} \tag{2.2.6}$$

In the case of a free right hand end one has

$$\begin{aligned} &- A_n \sin r_n l - B_n \cos r_n l + C_n \sinh r_n l + D_n \cosh r_n l = 0, \\ &- A_n \cos r_n l + B_n \sin r_n l + C_n \cosh r_n l + D_n \sinh r_n l = 0. \end{aligned} \tag{2.2.7}$$

2.3. System of recursive equations

It was established above that in the present case the relations to be taken into account are the general solution (2.1.1) of equation (1.4.4), intermediate conditions (2.1.2) with cracks at $x=a_j$ (j=0,..,n) and boundary conditions at x=0 and $x=l$. However, these conditions load to an algebraic linear homogeneous system of equations with 4n+4 equations and 4n+4 unknowns. It is well known that a non-trivial solution of this system exists if the determinant of this system vanishes.

The linear system of equations for boundary conditions at $x=l$ can been rewritten in the matrix form as

$$\begin{vmatrix} a1 & b1 & c1 & d1 \\ a2 & b2 & c2 & d2 \\ 0 & 0 & 0 & 0 \\ 0 & 0 & 0 & 0 \end{vmatrix} \begin{vmatrix} A_n \\ B_n \\ C_n \\ D_n \end{vmatrix} = 0 \qquad (2.3.1)$$

From boundary conditions at x=0 one obtains that

$$C_0 = -A_0 \quad \text{and} \quad D_0 = -B_0.$$

According to boundary conditions at $x=l$ for the shell simply supported at the right hand one has

$$a1 = \sin r_n l, \quad b1 = \cos r_n l,$$

$$c2 = \sinh r_n l, \quad d2 = \cosh r_n l.$$

The system (1.6.14) for this type of shells can be put into the form

$$\begin{vmatrix} \sin r_n l & \cos r_n l & 0 & 0 \\ 0 & 0 & \sinh r_n l & \cosh r_n l \\ 0 & 0 & 0 & 0 \\ 0 & 0 & 0 & 0 \end{vmatrix} \begin{vmatrix} p_{11} & p_{12} & p_{13} & p_{14} \\ p_{21} & p_{22} & p_{23} & p_{24} \\ p_{31} & p_{32} & p_{33} & p_{34} \\ p_{41} & p_{42} & p_{43} & p_{44} \end{vmatrix} \begin{vmatrix} A_0 \\ B_0 \\ -A_0 \\ -B_0 \end{vmatrix} = 0, \qquad (2.3.2)$$

where p_{ji} is a element of the matrix **P**. In the case of one stepped shell

$$[P]=[S_1],$$

for two stepped shell

$$[P]=[S_2]\,[S_1].$$

The matrix equation (2.3.2) can be presented as a system of equations

$$A_0(\sin r_n l(p_{11}-p_{13})+\cos r_n l(p_{21}-p_{23}))+B_0(\sin r_n l(p_{12}-p_{14})+\cos r_n l(p_{22}-p_{24}))=0,$$
$$A_0(\sinh r_n l(p_{31}-p_{33})+\cosh r_n l(p_{41}-p_{43}))+B_0(\sinh r_n l(p_{32}-p_{34})+\cosh r_n l(p_{42}-p_{44}))=0.$$

This system is a linear homogeneous system with respect to unknowns A_0, B_0. It has a non-trivial solution if the determinant

$$\Delta = \begin{vmatrix} \sin r_n l(p_{11}-p_{13})+\cos r_n l(p_{21}-p_{23}) & \sin r_n l(p_{12}-p_{14})+\cos r_n l(p_{22}-p_{24}) \\ \sinh r_n l(p_{31}-p_{33})+\cosh r_n l(p_{41}-p_{43}) & \sinh r_n l(p_{32}-p_{34})+\cosh r_n l(p_{42}-p_{44}) \end{vmatrix}$$

is equal to zero.

The equality Δ=0 leads to the equation

$$(\sin r_n l(p_{11}-p_{13})+\cos r_n l(p_{21}-p_{23}))(\sinh r_n l(p_{32}-p_{34})+\cosh r_n l(p_{42}-p_{44}))- \\ -(\sin r_n l(p_{31}-p_{33})+\cos r_n l(p_{41}-p_{43}))(\sinh r_n l(p_{12}-p_{14})+\cosh r_n l(p_{22}-p_{24}))=0. \quad (2.3.3)$$

Similarly to the free right hand end, we have

$$\begin{vmatrix} -\sin r_n l & -\cos r_n l & \sinh r_n l & \cosh r_n l \\ -\cos r_n l & \sin r_n l & \cosh r_n l & \sinh r_n l \\ 0 & 0 & 0 & 0 \\ 0 & 0 & 0 & 0 \end{vmatrix} \begin{vmatrix} p_{11} & p_{12} & p_{13} & p_{14} \\ p_{21} & p_{22} & p_{23} & p_{24} \\ p_{31} & p_{32} & p_{33} & p_{34} \\ p_{41} & p_{42} & p_{43} & p_{44} \end{vmatrix} \begin{vmatrix} A_0 \\ B_0 \\ -A_0 \\ -B_0 \end{vmatrix} = 0. \quad (2.3.4)$$

The equations (2.3.2) and (2.3.4) can be easily solved with the aid of existing codes with respect to the characteristic number k related to r_j by relations (1.5.2).

2.4. Approximate evaluation of the correction function

Due to the strain energy concentration in the vicinity of the crack tip under load a crack on an elastic structural element introduces considerable local flexibility. This effect was recognized already fifty years ago and the idea of an equivalent spring, a local compliance, was used to quantify in a macroscopic way the relation between the applied load and the strain concentration around the tip of the crack (Irvin 1960). The idea of a massless spring describing the stress concentration near the crack tip was mainly implemented in methods for determining an overall factor, the stress intensity factor, describing the intensity of the stress concentration. A suitable measure for the intensity of the stress concentration is assumed to be the local compliance of a cracked body. It can be related by energy arguments to the strain energy concentration and furthermore to the stress intensity factor. This method was used for experimental determination of the stress intensity factor and a wealth of results, both analytical and experimental, were tabulated for a number of cases (Tada et al. 2000). The macroscopic influence of the local flexibility (or compliance) on the static, dynamic and stability behavior of a cracked structure was subsequently recognized.

Vibration analysis was also performed for simple structural members with a single spring model of a cracked beam member. In this way, lateral vibration of beams and plates (Dimarogonas 1996; Chondros and Dimarogonas, 1980) were

studied. Moreover, the coupling effects were recognized for bending and longitudinal motions (Dimarogonas and Paipetis 1983). Simple structures and analytical methods were used and the stiffness or compliance terms were used in the boundary conditions. For more complicated structures, applications of finite element techniques comes naturally.

According to the approach from p.1.4 it is assumed that the slope of deflection *w'* is discontinuous at the cross section $x=a$ with crack. Thus

$$w'(a+0,t)\text{-}w'(a-0,t)=\theta,$$

where $\theta\neq 0$ and

$$\theta=-C\frac{Eh^3}{12(1-\nu^2)}\cdot w''(a+,t)$$

for circular cylindrical shells. Here *C* is the local compliance of the shell at $x=a$. It should be noted that the compliance follows from the relation

$$C=\frac{u}{P},$$

Here *u* is a generalized displacement and *P* corresponding load (see Broek, 1990). Equations (1.3.6) and (1.3.7) provide a tool to determine the stress intensity factor *K* as well *G* from the compliance of a shell, either by calculation or an experiment.

For an example of approximation of stress intensity factors we will consider the vibrations of the one-stepped circular cylindrical shell simply supported at both ends. At the entrant corners of the step at $x=a$ a crack is located. The segments adjacent to the crack have thicknesses h_0 and h_1 (see Fig. 2.1). The equation for definition of characteristic number *k* in this case may be presented as

$$\begin{aligned}
&((1+g_2)(\cos r_l(l\text{-}a)/\sin r_l(l\text{-}a)+g_1\cos r_0a/\sin r_0a)-g_3) \\
&((1+g_2)(\cosh r_l(l\text{-}a)/\sinh r_l(l\text{-}a)+g_1\cosh r_0a/\sinh r_0a)+g_3)- \\
&-((1-g_2)(\cosh r_l(l\text{-}a)/\sinh r_l(l\text{-}a)+g_1\cos r_0a/\sin r_0a)-g_3) \\
&((1-g_2)(\cos r_l(l\text{-}a)/\sin r_l(l\text{-}a)+g_1\cosh r_0a/\sinh r_0a)+g_3)=0,
\end{aligned} \tag{2.4.1}$$

where

$$\begin{aligned}
g_1&=\sqrt{\gamma}, \\
g_2&=(1/\gamma)^2, \\
g_3&=6\pi f(s)g_1g_2\sqrt{h_0}k.
\end{aligned} \tag{2.4.2}$$

Here $\gamma=h_1/h_0$, and

$$r_l(l-a)=\frac{kl}{\sqrt{h_0}}\frac{1-\beta}{\sqrt{\gamma}},$$

$$r_0 a=\frac{kl}{\sqrt{h_0}}\beta,$$

$$g_3=6\pi f(s)g_1g_2\frac{kl}{\sqrt{h_0}}\frac{h_0}{l}. \qquad (2.4.3)$$

Let us note that $\beta=a/l$, and $f(s)$ is the correction function, which are depends on the crack depth.

From Eq. (2.4.1) with (2.4.2) and (2.4.3) we can determine

$$f(s)=\frac{g_3}{6\pi g_1 g_2\sqrt{h_0}k}$$

or

$$f(s)=\frac{A_3A_4-A_1A_2}{6\pi g_1 g_2\sqrt{h_0}k(A_1-A_2-(A_3-A_4))}, \qquad (2.4.4)$$

where

$$A_1=(1+g_2)(\cos r_l(l-a)/\sin r_l(l-a)+g_1\cos r_0 a/\sin r_0 a),$$

$$A_2=(1+g_2)(\cosh r_l(l-a)/\sinh r_l(l-a)+g_1\cosh r_0 a/\sinh r_0 a),$$

$$A_3=(1-g_2)(\cosh r_l(l-a)/\sinh r_l(l-a)+g_1\cos r_0 a/\sin r_0 a),$$

$$A_4=(1-g_2)(\cos r_l(l-a)/\sin r_l(l-a)+g_1\cosh r_0 a/\sinh r_0 a).$$

So between $f(s)$ and k there is an one-to-one relation.

The one-stepped shell with a crack can be simulated geometrically as a two-stepped shell as mentioned in the previous section (see Fig. 1.11)

The results of calculations in the section 1.7 showed that values of the characteristic number k calculated by different methods coincide with sufficient accuracy. So we can use the model 2 for finding a characteristic number k for fixed s, γ, β. In this way one obtains the reletionship $k=k(s, \gamma, \beta)$. Using $k=k(s, \gamma, \beta)$ from model 2 we can find by (2.4.4) $f(s) = f(k(s, \gamma, \beta))$ for model 1. Using the obtained data we can approximate correction function $f(s)$ and correction function $F(s)$ for stress intensity factor (see Fig. 2.2).

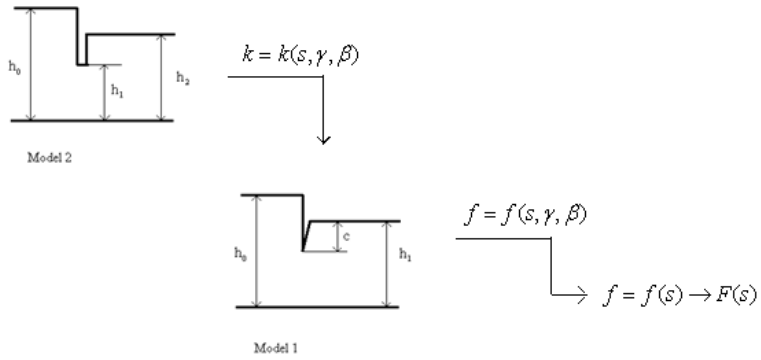

Fig. 2.2: The scheme of approximating of correction function *F(s)*.

2.5. Numerical results

Calculations have been carried out for shells with one and two steps. Special attention is paid to shells with unsymmetric end conditions.

Results of calculations are presented in Figs. 2.3–14. Figs. 2.3–10 correspond to shells with a unique step, thus with thicknesses h_0 and h_1. It is assumed herein that the material of the shell is a homogeneous elastic material. The cases of two stepped shells are considered in Figs. 2.11–14.

In calculations cylindrical shells of length l=1,2m clamped at the left hand end are considered. It has been taken h_0=0,009m.

The results of calculations regarding to shells with simply supported right hand ends are presented in Figs. 2.3–6, whereas Figs. 2.7–10 regard to cantilever cylindrical shells. In the latter case the right hand end of a tube is absolutely free.

The influence of the non-dimensional crack depth *c/h* on the characteristic number k is depicted in Fig. 2.3. Here and henceforth we take h=min(h_0, h_1). Let us introduce the notations

$\gamma=h_1/h_0$, $\beta=a_1/l$.

In Fig. 2.3 the sensitivity of the number k (and thus the eigen frequency ω) with respect to crack length c and the location of the crack $a_1=\beta l$ is shown. Here $h_0= h_1$, e.g. the shell is of constant thickness.

It can be seen from Fig. 2.3 that the number k depends on the crack length in a complicated manner. For instance, the lowest eigen frequency (the smallest number k) corresponds to the case β=0 (the crack is located at the root section) until $c< 0{,}8\ h_1$. If $c >0{,}8h_1$ in Fig. 2.3 then minimum of k is achieved when β=0,7.

In Fig. 2.7 the same situation as in Fig. 2.3 is presented in the case of a cylindrical shell clamped at the left end and absolutely free at the right hand

end. It can be seen from Fig. 2.7 that the larger the number β the higher the value k.

In Fig. 2.4 (and in Fig. 2.8) the number k is shown for stepped shells with h_1=0,3h_0. Here different curves correspond to different locations of the step, e.g. to different values of $\beta=a_1/l$. It can be seen from Fig. 2.4 (and Fig. 2.8) that the number k decreases when the crack length c increases in the case of a fixed value of β. It is interesting to note that in the range of small cracks the number k is almost unsensitive with respect to small changes of the crack length. However, in the range of larger cracks when c>0,6 h_1 this sensitivity is more obvious. Similar matters can be observed in Figs. 2.5, 2.6 (and Figs. 2.9, 2.10) in the cases β=0,2 and β=0,7, as well.

It is interesting to remark that in the case β=0,2 the highest curve corresponds to the shell of constant thickness (Fig. 2.9). If, however, β=0,7 then for smaller cracks the larger numbers of k correspond to the shell with the thickness ratio γ=0,3 (Fig. 2.10).

In Figs. 2.5, 2.6 (and Figs. 2.9, 2,10) the dependence between the characteristic number k and the crack length c is shown for stepped shells with step coordinates a_1=0,2l and a_1=0,7l, respectively. It can be seen from Fig. 2.5 (also, from Fig. 2.9) that when the step is near to the clamped end (here β=0,2) then the number k weakly depends on the crack length c. If, however, a_1=0,7l then this dependence is more remarkable, especially in the case of large cracks (Figs. 2.6, 2.10).

Similarily to previous results one can see from Figs. 2.6, 2.10 that in the case of small cracks the number k is almost unsensitive to the crack length.

In Figs. 2.11–2.14 the results corresponding to shells with two cracks are presented. Fig. 2.11 corresponds to the shell of constant thickness. Curves 1, 2, 3, 4 in Figs. 2.11–2.14 are associated with the crack locations at a_2=0,3l; a_2=0,4l; a_2=0,7l; a_2=0,9l, respectively, whereas a_1=0,1l.

In Figs. 2.12–2.15 shells with two steps are considered. In Figs. 2.12 and 2.14 the ratios of thicknesses are denoted $\gamma_j=h_j/h_0$; j=1,2.

Figs. 2.12, 2.14 correspond to the case γ_1= 0,2; γ_2= 0,5 and Fig. 2.13 is associated with γ_1= γ_2=1. The results presented in Figs. 2.11, 2.12 are obtained in the case of shells simply supported at the right hand end and these of Figs. 2.13, 2.14 correspond to shells with absolutely free right hand end. Calculations carried out showed that the number k attains smaller values for cantilever tubes in comparison to those corresponding to shells with simply supported right hand end.

The author had difficulties in finding results on axisymmetric vibration of stepped circular cylindrical shells with cracks. In [57] the first five natural frequencies of axisymmetric modes of simply supported circular cylindrical shells are reported by F. Pellicano. The parameters of the shell are shown in Table 2.1. Here the modulus of elasticity E=2,1·10^{11}N/m^2; Poisson's ratio ν=0,3; mass density ρ=7800kg/m^3; l=0,2m; R=0,2m and h=R/20. In table 2.1 first five natural frequencies of axisymmetric modes of simply supported circular cylindrical shells are reported.

Table 2.1. Comparison of natural frequencies: present theory vs. exact and finite-elements results.

Mode	Natural frequencies (Hz)		
n	Present method	Exact by F.Pellicano	F.Pellicano
1	$4{,}162 \cdot 10^3$	4140,74	4140,77
2	$4{,}794 \cdot 10^3$	4788,34	4788,66
3	$6{,}895 \cdot 10^3$	6890,30	6891,43
4	$1{,}066 \cdot 10^4$	10655,3	10657,7
5	$1{,}591 \cdot 10^4$	15900,6	15904,7

It is seen from Table 2.1 that the natural frequencies corresponding to the current analytical method are in good agreement with the natural frequencies obtained by F.Pellicano.

For approximation of the correction function *f(s)* simply supported shell was used. Numerical values of the correction function *f(s)* for different dimensionless geometric parameters *h/l* are given in Table 2.2. Graphical representation of the function *f(s)* are given in Figs. 2.15, 2.16.

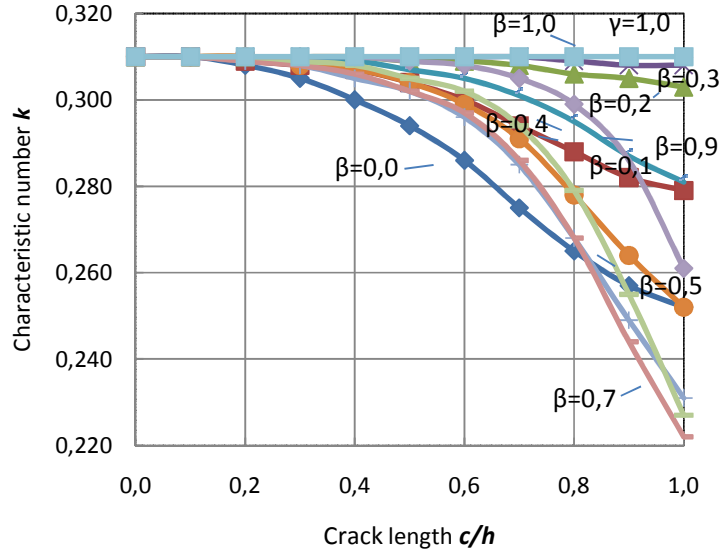

Fig. 2.3: Cylindrical shell clamped at the left hand end with simply supported right hand end, constant thickness.

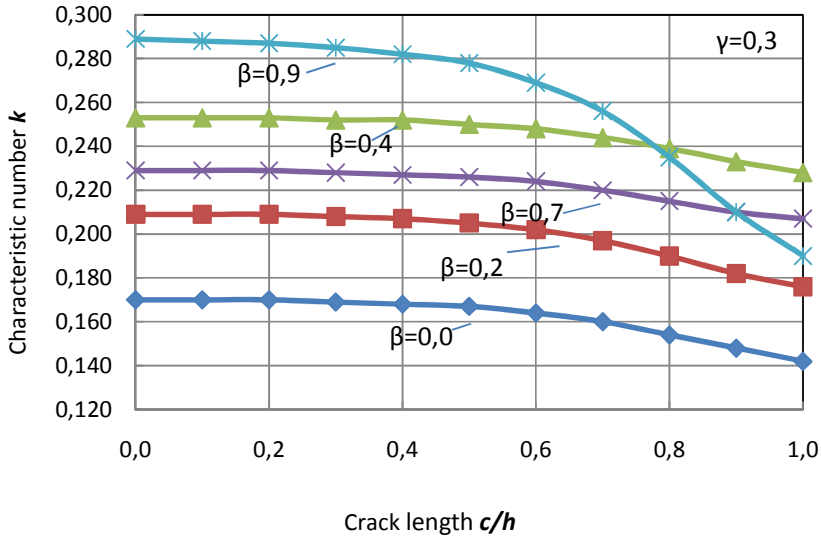

Fig. 2.4: Stepped cylindrical shell, the case γ=0,3.

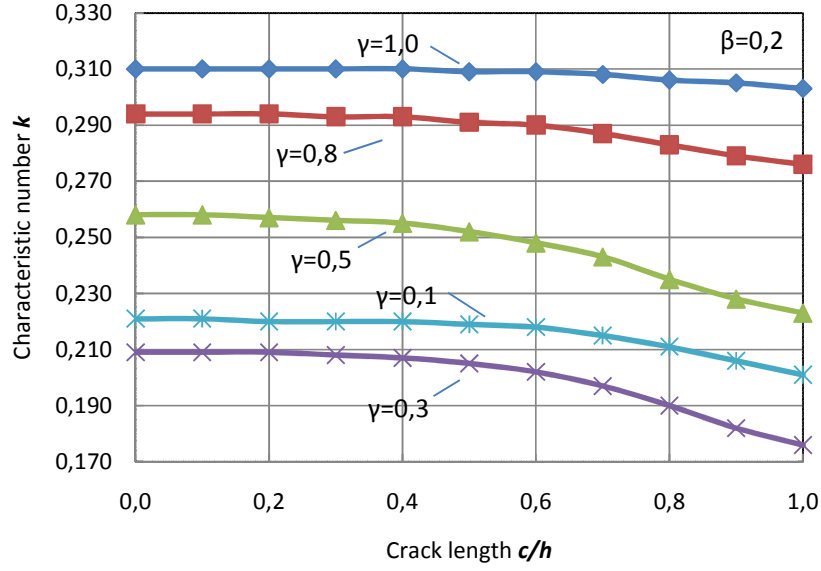

Fig. 2.5: Stepped cylindrical shell, the case β=0,2.

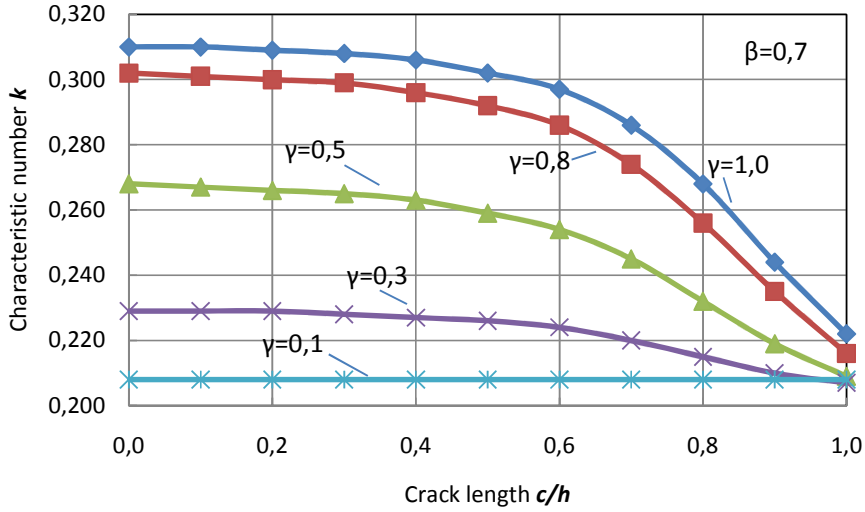

Fig. 2.6: Stepped cylindrical shell, the case β=0,7.

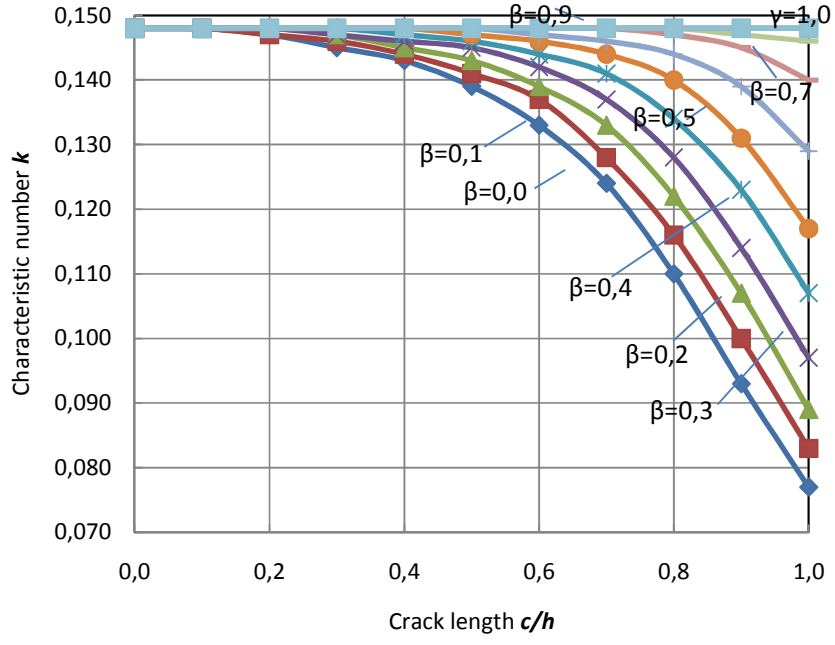

Fig. 2.7: Cantilever cylindrical shell of constant thickness.

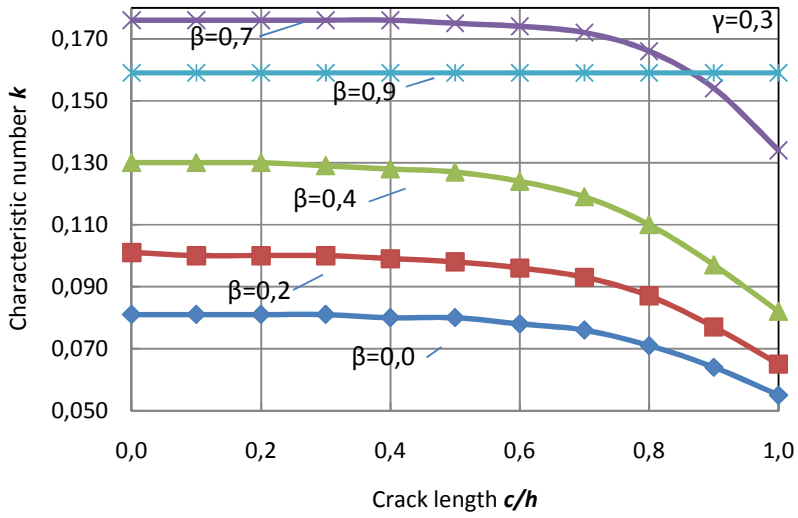

Fig. 2.8: The case γ=0,3.

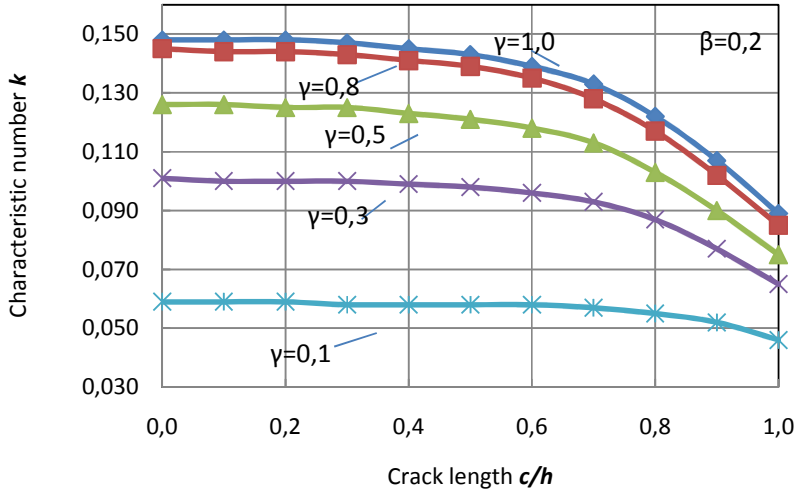

Fig. 2.9: The case β=0,2.

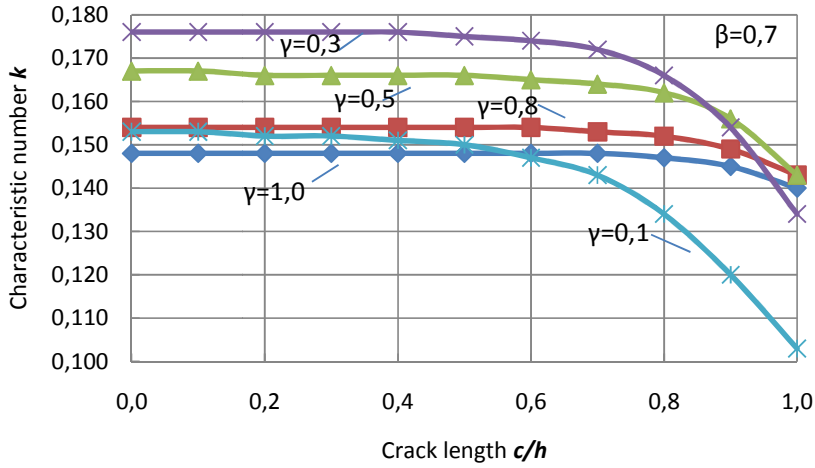

Fig. 2.10: The case β=0,7.

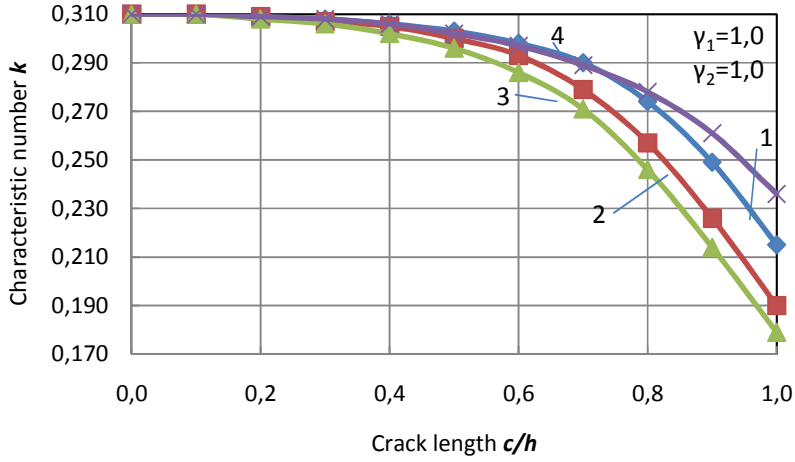

Fig. 2.11: Two stepped cylindrical shell clamped at the left hand end and simply supported at the right hand end, the case γ_1=1,0; γ_2=1,0.

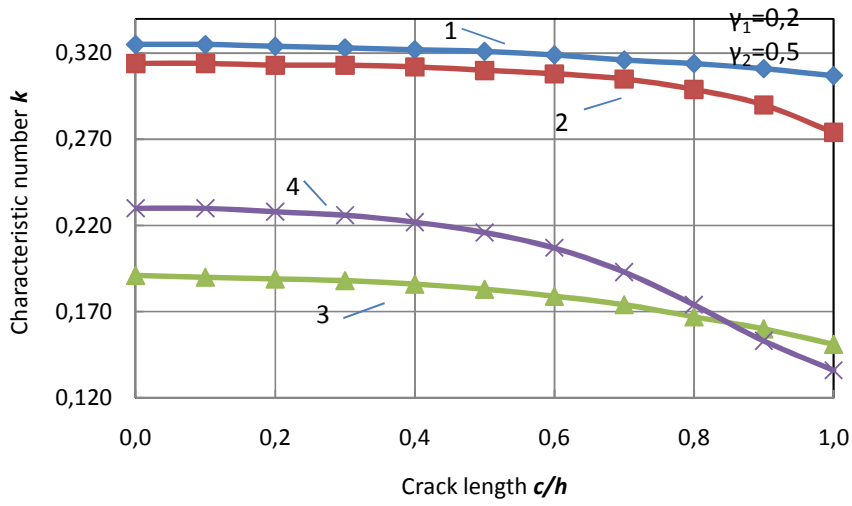

Fig. 2.12: Two stepped cylindrical shell, the case γ_1=0,2; γ_2=0,5.

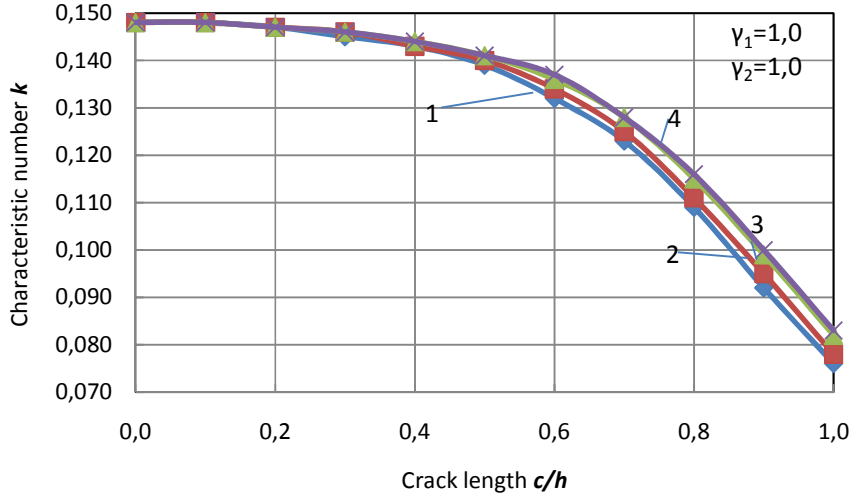

Fig. 2.13: Cantilever cylindrical shell with two steps, the case γ_1=1,0; γ_2=1,0.

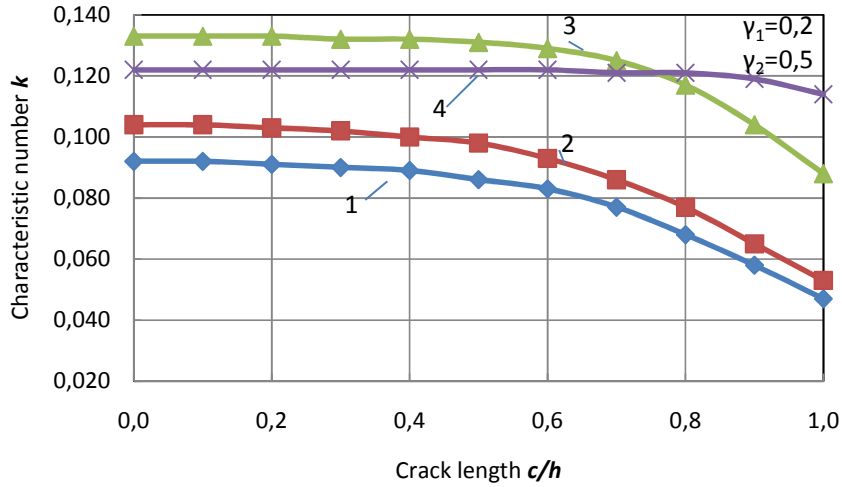

Fig. 2.14: Cantilever cylindrical shell, the case γ_1=0,2; γ_2=0,5.

Table 2.2: The approximation of correction function *f(s)*.

			s									
h/l	*γ*	*β*	0,01	0,1	0,2	0,3	0,4	0,5	0,6	0,7	0,8	0,9
0,005	1	0,1	0,000	0,004	0,012	0,025	0,051	0,102	0,220	0,553	1,929	15,621
	1	0,2	0,000	0,009	0,024	0,051	0,101	0,203	0,439	1,105	3,850	31,163
	1	0,3	0,000	0,013	0,035	0,076	0,152	0,305	0,658	1,656	5,768	46,673
	1	0,4	0,001	0,017	0,047	0,102	0,203	0,408	0,878	2,209	7,690	62,200
	1	0,5	0,002	0,022	0,060	0,128	0,254	0,511	1,101	2,768	9,629	77,823
	1	0,6	0,002	0,026	0,072	0,154	0,308	0,618	1,329	3,340	11,606	93,713
	1	0,7	0,002	0,031	0,085	0,182	0,364	0,730	1,570	3,942	13,678	110,270
	1	0,8	0,003	0,036	0,100	0,214	0,427	0,858	1,845	4,627	16,019	128,738
	1	0,9	0,003	0,044	0,122	0,261	0,520	1,045	2,250	5,648	19,534	155,714
0,0075	1	0,1	0,000	0,003	0,008	0,017	0,034	0,068	0,146	0,369	1,286	10,414
	1	0,2	0,000	0,006	0,016	0,034	0,067	0,136	0,293	0,737	2,567	20,775
	1	0,3	0,000	0,009	0,024	0,051	0,101	0,203	0,439	1,104	3,845	31,116
	1	0,4	0,001	0,011	0,032	0,068	0,135	0,272	0,585	1,473	5,127	41,466
	1	0,5	0,001	0,014	0,040	0,085	0,170	0,341	0,734	1,845	6,419	51,882
	1	0,6	0,001	0,017	0,048	0,103	0,205	0,412	0,886	2,227	7,737	62,475
	1	0,7	0,002	0,021	0,057	0,122	0,242	0,487	1,047	2,628	9,119	73,514
	1	0,8	0,002	0,024	0,067	0,143	0,285	0,572	1,230	3,085	10,679	85,825
	1	0,9	0,002	0,029	0,081	0,174	0,347	0,697	1,500	3,765	13,023	103,810

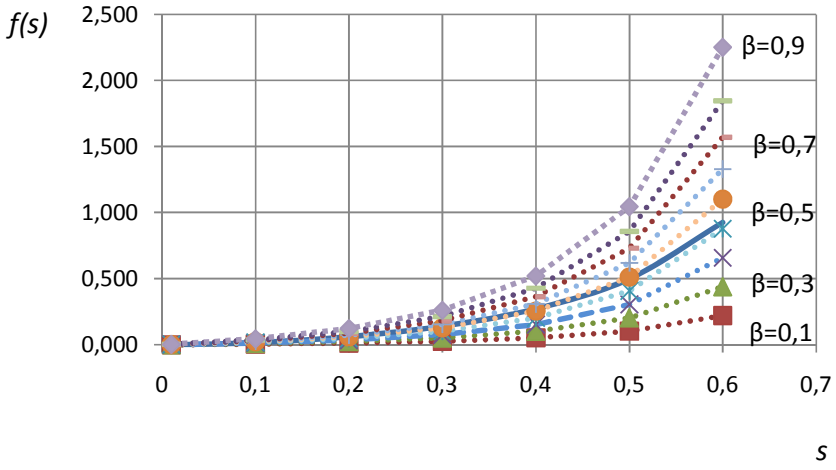

Fig. 2.15: The approximation of correction function *f(s)*, the case *h/l*=0,005.

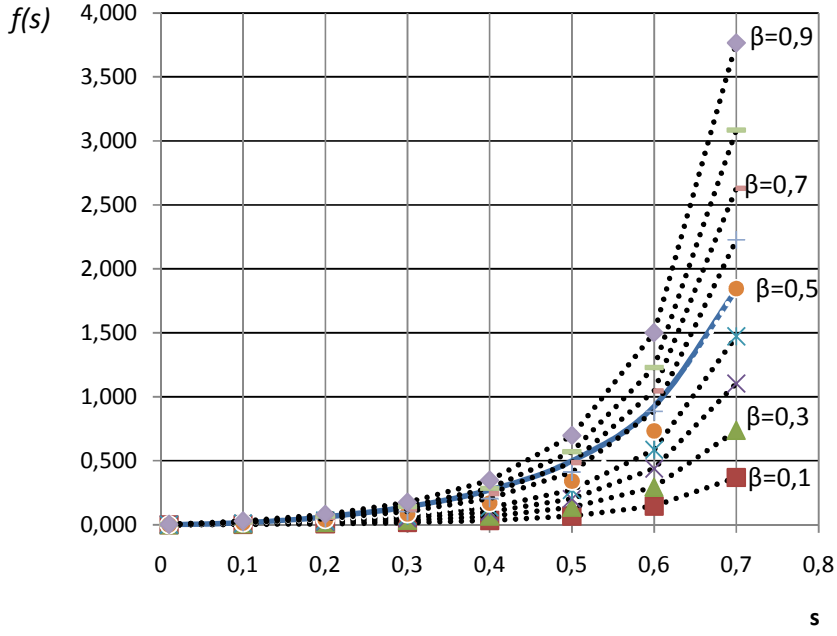

Fig. 2.16: The approximation of correction function *f(s)*, the case *h/l*=0,0075.

3. COMPOSITE AND LAYERED SHELLS

3.1. Introduction

Until the fracture takes place the large class of composites behave as elastic bodies, following the Hooke's law. Usually the facture of bodies from such material is brittle, for example, destruction of bodies from fiber-glass. Therefore for investigations of small deformations in bodies from such materials, methods of the classical theory of elasticity of an anisotropic body can be used.

Circular cylindrical shells, made of composite materials, are widely used in many fields of engineering, especially in civil, mechanical, aerospace, marine and chemical industry. Vibration of circular cylindrical shells from composite materials is of interest in a number of different fields.

The problem of the theory of elasticity of an anisotropic body is similar to that of an isotropic body. The equations of balance and the geometrical equations of the theory of elasticity do not depend on a choice of a material of a body. Only physical equations are different because laws of deformation for anisotropic and isotropic bodies are different. For investigations of laws of deformation of anisotropic materials like fiber-glasses or other composite materials there are two approaches. The first approach, so-called phenomenological, considers a composite material, as a homogeneous monolithic anisotropic material. In this case mechanical parameters of a material (limits of elasticity, durability, etc.) are considered as some integral characteristics. Exact definition of modulus of elasticity of such materials is an intricate problem. Such approach assumes direct usage of the theory of elasticity of the anisotropic continuums. The second approach – structural – assumes that a composite material is considered as an inhomogeneous reinforced continuum. In the case of this approach the mechanical characteristics of the reinforced material are defined through mechanical characteristics of initial components – matrix and fibre. For example, the rule of mixture is used widely [74], where the modulus of elasticity of composite is defined as

$$E_k = \alpha E_b V_b + E_m V_m .$$

Here E_b and E_m are moduli of elasticity of the fibre and matrix, respectively; E_k – modulus of elasticity of the composite; α – the coefficient depending on the layout of a fibre [74] (for unidirectional lay out α =1, for perpendicular α =0,5, for casual α =3/8); V_b and V_m – volumes of fibre and matrix in the composite. Both these approaches supplement each other mutually at development. As show experiments, elastic composites are anisotropic.

In this chapter we will study free axisymmetric vibration of stepped circular cylindrical shells with cracks, similarly to the previous chapters, but the material of the shell will be a composite or a layered material. The shells under

consideration have piece wise constant thickness and circular cracks of constant depth are located at cross sections with steps of the thickness.

3.2. Formulation of the problem for layered shells

Consider a layered, circular cylindrical shell with length l (see Fig. 1.1). The shell can be divided into n ring segments. The symbol n denotes the number of total ring segments separated from the rest cylindrical shell by the sections where the thickness variations take place. Every jth ring segment of shell has q layers. Each layer is isotropic with thickness h_{ij}, Young's modulus E_{ij}, Poisson's ratio v_{ij}, and mass density ρ_{ij} as show in Fig. 3.1.

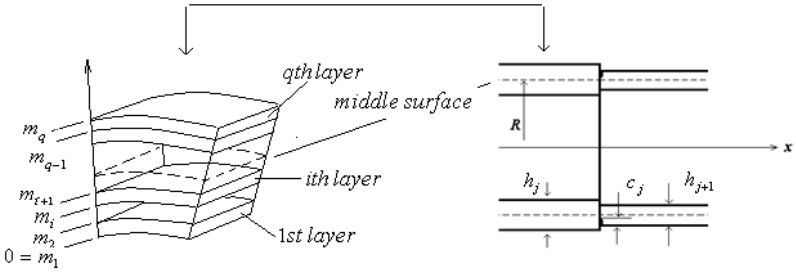

Fig. 3.1: Geometry of a layered shell.

Let's denote

$$\rho_{ij}=\rho_{1j}d_{ij}, \tag{3.2.1}$$

where d_{ij} is a constant of proportionality, d_{1j}=1and similarly Young's modulus for each layer

$$E_{ij}=E_{1j}e_{ij}, \tag{3.2.2}$$

where e_{ij} is a constant of proportionality, e_{1j}=1.
We will denote the thickness of each layer h_{ij} by

$$h_{ij}=(z_{i+1j}-z_{ij})h_{1j}, \tag{3.2.3}$$

where z_{ij} is a local coordinate of a layer with the thickness h_j and z_{1j}=0.
The mass of jth ring segment will be equal

$$\overline{m}_j = \rho_{1j} h_{1j} \sum_{i=1}^{q} d_{ij}(z_{i+1j} - z_{ij}). \tag{3.2.4}$$

For the *j*th ring segment, the free axisymmetric vibrations can be described by the equations (1.2.1) and (1.2.2)

$$\begin{aligned} \frac{\partial N_{1j}}{\partial x} &= 0, \\ \frac{\partial^2 M_j}{\partial x^2} - \frac{N_j}{R} - \rho_j h_j \frac{\partial^2 w}{\partial t^2} &= 0, \end{aligned} \tag{3.2.5}$$

Where N_{1j}, N_j and M_j stand for the membrane forces and bending moments for the current segment calculated by following formulas [76]:

$$\begin{aligned} N_{1j} &= \int_0^{h_j} \sigma_{1j} dz, \\ N_j &= \int_0^{h_j} \sigma_j dz, \\ M_j &= \int_0^{h_j} \sigma_{1j} z dz. \end{aligned} \tag{3.2.6}$$

According to the Hooke's law one has

$$\sigma_{1j} = \left[E_j/(1-\nu_j^2)\right]\left[(\varepsilon_1 + z\chi) + \nu_j \varepsilon\right],$$

$$\sigma_j = \left[E_j/(1-\nu_j^2)\right]\left[\varepsilon + \nu_j(\varepsilon_1 + z\chi)\right].$$

If for all ring segments $v_{ij}=v$ then, by using (3.2.1) – (3.2.3) and (1.2.3) the force N_j and bending moment M_j (3.2.6) can be written as

$$\begin{aligned} N_j &= b_j E_{1j} h_j \frac{w}{R}, \\ M_j &= -\frac{\mathrm{E}_{1j} h_j^{\,3}}{12(1-\nu^2)} \overline{a}_j \frac{\partial^2 w}{\partial x^2}, \end{aligned} \tag{3.2.7}$$

where

$$\overline{a}_j = \frac{4\left(\sum_{i=1}^{q} e_{ij}(z_{i+1j}^3 - z_{ij}^3)\right)\left(\sum_{i=1}^{q} e_{ij}(z_{i+1j} - z_{ij})\right) - 3\left(\sum_{i=1}^{q} e_{ij}(z_{i+1j}^2 - z_{ij}^2)\right)^2}{\sum_{i=1}^{q} e_{ij}(z_{i+1j} - z_{ij})}, \tag{3.2.8}$$

and

$$b_j = \sum_{i=1}^{q} e_{ij}(z_{i+1j} - z_{ij}). \tag{3.2.9}$$

So the equation of motion of *j*th ring segment can be described by the equation

$$\overline{D}_j \overline{a}_j \frac{\partial^4 w}{\partial x^4} + \frac{E_{1j} h_j}{R^2} b_j w = -\rho_{1j} h_j c_j \ddot{w}, \tag{3.2.10}$$

where $\overline{D}_j = E_{1j} h_j^3 / 12(1-\nu^2)$, $\nu = const$ and

$$c_j = \sum_{i=1}^{q} d_{ij}(z_{i+1j} - z_{ij}). \tag{3.2.11}$$

Evidently, it is reasonable to look for the general solution of the equation (3.2.10) in the form

$$w(x,t) = X_j(x)T(t) \tag{3.2.12}$$

It follows from (3.2.10) with (3.2.12) that

$$X_j^{IY} - r_j^4 X_j = 0 \tag{3.2.13}$$

where

$$r_j^4 = \omega^2 \cdot \frac{12\rho_{1j}(1-\nu^2)}{E_{1j} h_j^2} \frac{c_j}{\overline{a}_j} - \frac{12(1-\nu^2)}{R^2 h_j^2} \frac{b_j}{\overline{a}_j}, \tag{3.2.14}$$

The frequency of free vibrations of a layered shell will be equal

$$\omega = \sqrt{\frac{E_{1j}}{\rho_{1j}}} \frac{1}{R} \sqrt{\frac{k^4 R^2}{12(1-\nu^2)} \frac{\overline{a}_j}{c_j} + \frac{b_j}{c_j}},$$

where $r_j = k/\sqrt{h_j}$.

The general solution of the linear fourth order equation (3.2.13) can be presented as

$$X_j(x) = A_j \sin(r_j x) + B_j \cos(r_j x) + C_j \sinh(r_j x) + D_j \cosh(r_j x). \tag{3.2.15}$$

Assume that the ends of the shell are simply supported. In this case the boundary conditions at the points $x=0$ and $x=l$ are

$$w=0, \quad M=0.$$

The continuity and jump conditions at $x=a$ are

$$\begin{aligned} w(a+0)\text{-}w(a-0) &= 0, \\ w'(a+0)\text{-}w'(a\text{-}0) &= \frac{72\pi}{E'h_1^2} f(s_1)M(a\text{-}0), \\ M(a+0) &= M(a-0), \\ M'(a+0) &= M'(a-0). \end{aligned}$$

Let us consider now the case when n=2. By using equation (3.2.7) we can rewrite the equation for definition of the characteristic number k (1.6.16) as

$$\begin{aligned} &((1-g_1)\cos kl_1\cosh kl_4 + ((g_2-g_4)\sin kl_1 + g_3\cos kl_1)\sinh kl_4) \\ &((1-g_1)\cosh kl_1\cos kl_4 - ((g_2-g_4)\sinh kl_1 + g_3\cosh kl_1)\sin kl_4) - \\ &-((1+g_1)\cos kl_1\cos kl_4 + ((g_2+g_4)\sin kl_1 + g_3\cos kl_1)\sin kl_4) \\ &((1+g_1)\cosh kl_1\cosh kl_4 - ((g_2+g_4)\sinh kl_1 + g_3\cosh kl_1)\sinh kl_4) = 0, \end{aligned} \tag{3.2.16}$$

where

$$\begin{aligned} g_1 &= (h_0a_0/h_1a_1)^2, \\ g_2 &= (h_1/h_0)^{1/2}, \\ g_4 &= g_1g_2, \\ g_3 &= 6\pi f(s_1)\sqrt{h_1}\,g_1k \end{aligned}$$

and

$$l_1 = a/\sqrt{h_0}, \qquad l_4 = (l-a)/\sqrt{h_1}.$$

Here $\bar{a}_0$ and $\bar{a}_1$ –are the values of $\bar{a}_j$ for $j=0$ and $j=1$, respectively.

3.3. Determination of elastic characteristics of unidirectional fibrous composites

Composite materials have high specific durability and stiffness. Such materials allow in present-day mashines and designs to lower the weight and to raise corrosion stability. It opens essentially new possibilities in the optimum design

of structures and creation of new designs. Engineering approaches to calculation of composites allow to find approximate results, analytical approaches yield exact results only for periodic structures with enough simple geometry.

Let us consider small deflections of axisymmetric circular cylindrical shells similarly with that done in chapter 2. In this case the material of shells is a unidirectional fibrous composite (see Fig. 3.2). Let E_f and E_m be the Young's modulus of fiber material and matrix material, respectively; υ_f is the volume fraction of fibres, d is the diameter of a fibre. Let's denote the ratio of Young's moduli $E_f/E_m=f$.

In this case the basic equations of static equilibrium of the shell are of the following form [48]

$$\frac{\partial N_1}{\partial x}=0, \qquad \frac{\partial M}{\partial x}=\mathrm{Q},$$
$$\frac{\partial^2 M}{\partial x^2}-\frac{N}{R}-q=0, \tag{3.3.1}$$

where

$$N_1=\frac{E}{1-\nu^2}\int_0^h(\varepsilon_1+z\chi+\nu\varepsilon)dz, \quad (N_1=0),$$
$$N=\frac{E}{1-\nu^2}\int_0^h(\varepsilon+\nu(\varepsilon_1+z\chi)dz, \tag{3.3.2}$$
$$M=\frac{E}{1-\nu^2}\int_0^h(\varepsilon_1+z\chi+\nu\varepsilon)zdz,$$

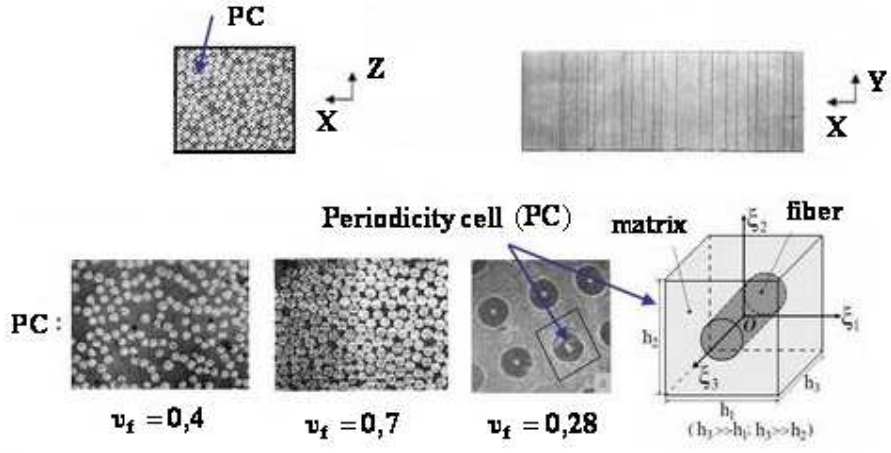

Fig. 3.2: Unidirectional fibrous composite.

In the present study the composite material reinforced with unidirectional fibers will be modeled as a multilayered body consisting of consistently stacked layers of the matrix and reinforcement materials, respectively. The number of layers is assumed to be given.

Note that relations (3.3.2) hold good, if *E=const* and *v=const.* However, *E=E(z)* and *v=v(z)* in a layered or laminate shell. In a composite structure

$$E(z)=\begin{cases} E_m, & \text{for matrix layer,} \\ E_f, & \text{for fibre layer,} \end{cases}$$

and

$$\nu(z)=\begin{cases} \nu_m, & \text{for matrix layer,} \\ \nu_f, & \text{for fibre layer,} \end{cases}$$

Thus the generalized stresses in a non-homogeneous shell should be calculated as

$$N_1=\int_0^h \frac{E(z)}{1-\nu(z)^2}(\varepsilon_1+z\chi+\nu\varepsilon)dz,$$

$$N=\int_0^h \frac{E(z)}{1-\nu(z)^2}(\varepsilon+\nu(\varepsilon_1+z\chi)dz, \qquad (3.3.3)$$

$$M=\int_0^h \frac{E(z)}{1-\nu(z)^2}(\varepsilon_1+z\chi+\nu\varepsilon)zdz.$$

Comparing (3.3.2) with (3.3.3), one can evaluate the mean values of elastic moduli as

$$Eh=E_m(fv_f+(1\text{-}v_f))h,$$

$$\frac{Eh^3}{12(1-\nu^2)}=\int_0^h \frac{E(z)}{(1-\nu(z)^2)}z^2dz-\frac{(\int_0^h \frac{E(z)}{(1-\nu(z)^2)}zdz)^2}{\int_0^h \frac{E(z)}{(1-\nu(z)^2)}dz}.$$

This results in

$$E=E_m(fv_f+(1\text{-}v_f)), \qquad (3.3.4)$$

$$\frac{E}{1-\nu^2}=4\left[(\frac{E_m}{1-\nu_m^2}-\frac{E_f}{1-\nu_f^2})\sum_{i=1}^{q}(-1)^i\frac{z_i^3}{h^3}+\frac{E_f}{1-\nu_f^2}\right]+3\frac{\left[(\frac{E_m}{1-\nu_m^2}-\frac{E_f}{1-\nu_f^2})\sum_{i=1}^{q}(-1)^i\frac{z_i^2}{h^2}+\frac{E_f}{1-\nu_f^2}\right]^2}{\frac{E_m}{1-\nu_m^2}(1-\upsilon_f)+\frac{E_f}{1-\nu_f^2}\upsilon_f},$$

where

$$E_i=\begin{cases}E_m, & \text{for matrix layer,}\\ E_f, & \text{for fibre layer}\end{cases}$$

and

$$\nu_i=\begin{cases}\nu_m, & \text{for matrix layer,}\\ \nu_f, & \text{for fibre layer.}\end{cases}$$

Note that in the present case q is an odd number.

3.4. Numerical results

For an illustration of the method presented in this chapter the simply supported shell has been considered. The shell under consideration has a uniform shell wall with Young's modulus E_m for $x\in(0,a)$ whereas it consists of two layers with Young's moduli E_m and E_s respectively, and thickness h_1 for $x\in(a,l)$, as shown in Fig. 3.3.

Geometrical parameters for the one-stepped shell are: l=0,6; h_0=0,006; h_1=γ h_0; γ=0,7. It is assumed herein that the material of the shell segment with h_0 is a homogeneous elastic material – aluminium-lithium alloy with E_m=76GPa. The shell segment with h_1 has two layers. The inner layer is made of the same material as the enother segment and the material of the top layer is a fiber-glass. In the segment with h_1, v is the volume fraction of fibres. We will consider four kinds of fiber-glasses with E_s = 20GPa, 35GPa, 50GPa, 152GPa (s= E_s/ E_m), respectively.

In this case the equation for definition of characteristic number k is

$$\begin{aligned}&((1-g_1)\cos kl_1\cosh kl_4+((g_2-g_4)\sin kl_1+g_3\cos kl_1)\sinh kl_4)\\&((1-g_1)\cosh kl_1\cos kl_4-((g_2-g_4)\sinh kl_1+g_3\cosh kl_1)\sin kl_4)-\\&-((1+g_1)\cos kl_1\cos kl_4+((g_2+g_4)\sin kl_1+g_3\cos kl_1)\sin kl_4)\\&((1+g_1)\cosh kl_1\cosh kl_4-((g_2+g_4)\sinh kl_1+g_3\cosh kl_1)\sinh kl_4)=0,\end{aligned}\qquad(3.4.1)$$

where

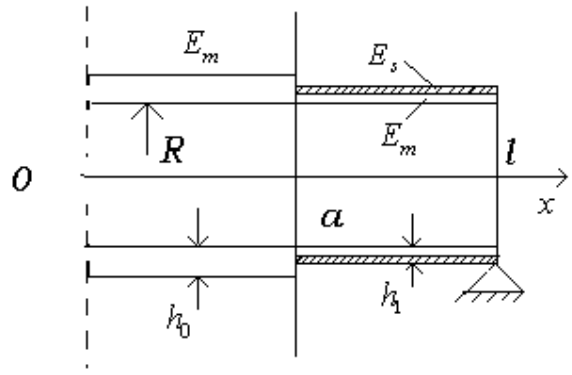

Fig. 3.3: Cylindrical shell with fiber-glass layer.

$$g_1 = (h_0/h_1(sv\ + (1-v\ ))^2,$$
$$g_2 = (h_1/h_0)^{1/2},$$
$$g_4 = g_1 g_2,$$
$$g_3 = 6\pi f(s_1)\sqrt{h_1}\, g_1 k$$

and

$$l_1 = a/\sqrt{h_0}, \qquad l_4 = (l-a)/\sqrt{h_1}.$$

The results of calculations regarding to the shell with simply supported ends are presented in Figs. 3.4–3.5. The influence of the crack *c/h* on the characteristic number *k* for the fixed values *v*=0,2; β=0,2; γ=0,7 and different values of *s* is depicted in Fig. 3.4. In Fig. 3.5 different curves corresponding to different values of *v* are presented in the case *s*=2; β=0,2; γ=0,7. Here $\beta=a_1/l$, $\gamma=h_1/h_0$, as in previous sections of the study.

Calculations carried out showed that the characteristic number *k* of the shell decreases when the crack depth increases as might be expected.

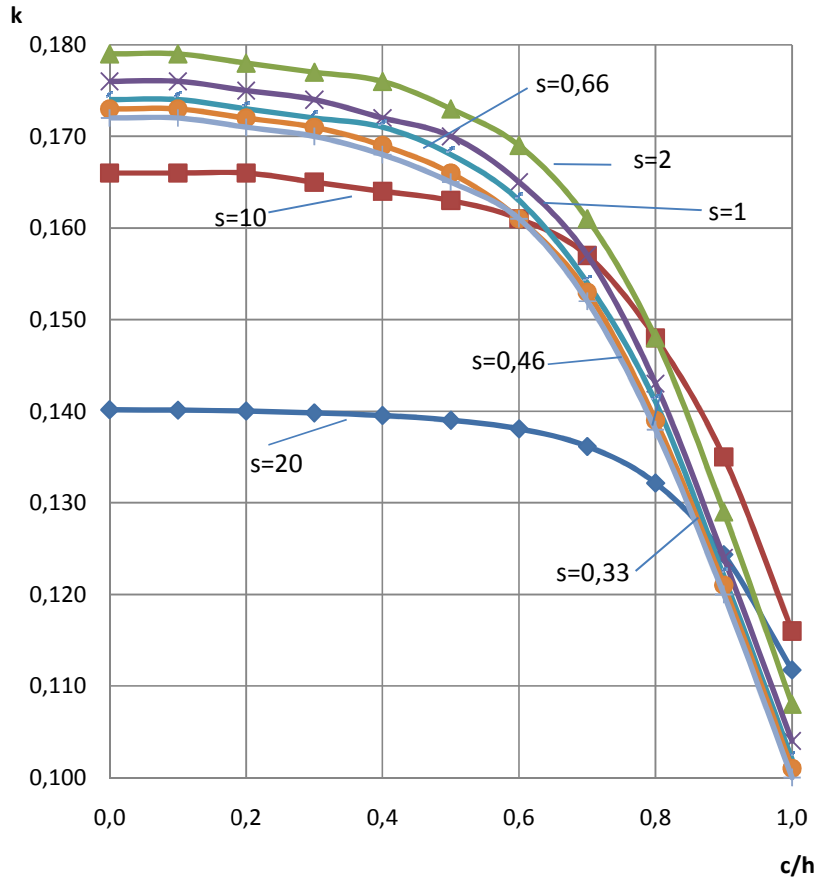

Fig. 3.4: Frequency parameter k for simply supported shells, the case ν=0,2; β=0,2; γ=0,7.

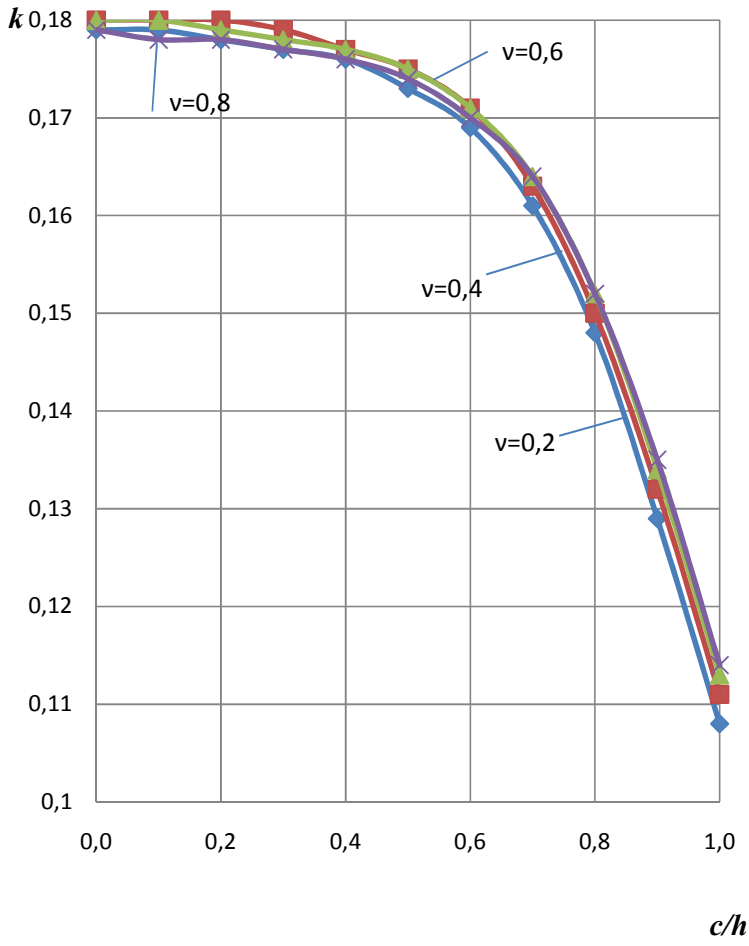

Fig. 3.5: Frequency parameters k for simply supported shells, the case s=2; β=0,2; γ=0,7.

4. NON-AXISYMMETRIC VIBRATIONS OF STEPPED CYLINDRICAL SHELLS CONTAINING CRACKS

In this chapter we will study free vibrations of stepped circular cylindrical shells with cracks, similarly to the previous chapters, but the three displacement fields are taken into account.

4.1. Summary of the basic equations

Let x, θ, z be the cylindrical coordinates for a cylindrical shell of length l, as shown in Fig. 4.1, where x and θ are surface coordinates and z is the inward normal to the reference surface. The origin of the coordinate system is located on the middle surface of the shell, and the radius of the middle surface is denoted by R.

The cylindrical coordinate system (x, θ, z) is considered in order to take advantage from the axial symmetry of the structure, the origin of the reference system is located at the centre of left end of the shell.The shell thickness is $h(x)=h_j$ for $x\in(a_j,a_{j+1})$, where $j=0,...,n$. Here the quantities h_j ($j=0,...,n$) stand for fixed constants. Similarly, a_j ($j=0,...,n+1$) are given constants whereas it is reasonable to use notations $a_o=0$, $a_{n+1}=l$.

In Fig. 4.1 three displacement fields are represented: axial $u(x, \theta, t)$, circumferential $v(x, \theta, t)$, and radial $w(x, \theta, t)$, where t is time.

Assume that the ends of the shell are simply supported.

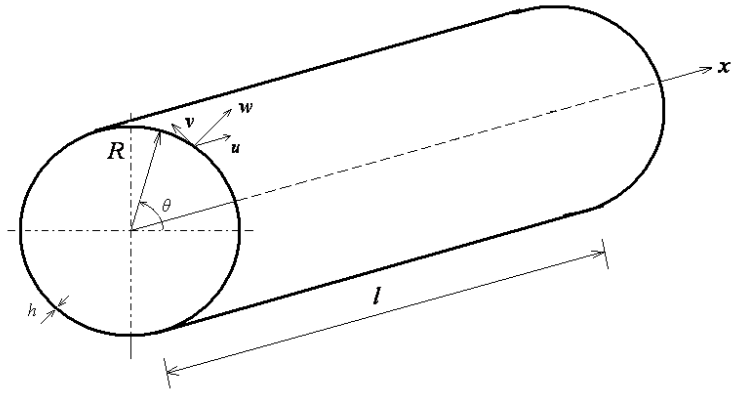

Fig. 4.1: Circular cylindrical shell: coordinate system and dimensions.

The equations of motion obtained by Donnell, Mushtari, and Vlasov will be used [65]. This system neglects neither bending nor membrane effects. It applies to shells that are loaded normal to their surface and concentrates on transverse deflection behavior. The approach was developed, apparently independently, by Donnell (1982) and Mushtari (1938). Donnell derived it for the circular cylindrical shell. The approach was generalized for any geometry by Vlasov (1951).

A system of displacement equilibrium equations, based on Donnell's approximations, is used to investigate the vibrational characteristics of a cylindrical shell [80]

$$\frac{\partial^2 u_j}{\partial x^2}+\frac{1-\nu}{2R^2}\frac{\partial^2 u_j}{\partial \theta^2}+\frac{1+\nu}{2R}\frac{\partial^2 v_j}{\partial x\partial \theta}-\frac{\nu}{R}\frac{\partial w_j}{\partial x}=0, \tag{4.1.1}$$

$$\frac{1+\nu}{2}\frac{\partial^2 u_j}{\partial x\partial \theta}+R\frac{1-\nu}{2}\frac{\partial^2 v_j}{\partial x^2}+\frac{1}{R}\frac{\partial^2 v_j}{\partial \theta^2}-\frac{1}{R}\frac{\partial w_j}{\partial \theta}=0, \tag{4.1.2}$$

$$\nu\frac{\partial u_j}{\partial x}+\frac{1}{R}\frac{\partial v_j}{\partial \theta}-\frac{w}{R}-\frac{h_j^{\,2}}{12}\left(R\frac{\partial^4 w_j}{\partial x^4}+\frac{2}{R}\frac{\partial^4 w_j}{\partial x^2\partial \theta^2}+\frac{1}{R^3}\frac{\partial^4 w_j}{\partial \theta^4}\right)=\frac{R\rho(1-\nu^2)}{E}\frac{\partial^2 w_j}{\partial t^2}. \tag{4.1.3}$$

In (4.1.1)-(4.13) $u_j(x,\theta,t)$, $v_j(x,\theta,t)$ and $w_j(x,\theta,t)$ are the displacements of the jth ring segment in the x, θ, and radial directions, ρ is the mass density of the shell, E is the Young's modulus and ν is the Poisson's ratio.

In accordance with the simplifications leading to equations (4.1.1–3), the effect of the displacements u_j and v_j on the bending and twisting moments must be considered as negligible. Thus, with the notation

$$D_j=\frac{Eh_j^{\,3}}{12(1-\nu^2)}, \tag{4.1.4}$$

the following expressions are obtained for the bending moment $(M_x)_j$, shear force $(Q_x)_j$ and membrane force $(N_x)_j$:

$$\begin{aligned}(M_x)_j&=-D_j\left(\frac{\partial^2 w_j}{\partial x^2}+\frac{\nu}{R^2}\frac{\partial^2 w_j}{\partial \theta^2}\right),\\ (Q_x)_j&=-D_j\frac{\partial}{\partial x}\left(\frac{\partial^2 w_j}{\partial x^2}+\frac{1}{R^2}\frac{\partial^2 w_j}{\partial \theta^2}\right),\\ (N_x)_j&=\frac{Eh_j}{1-\nu^2}\left(\frac{\partial u_j}{\partial x}+\frac{\nu}{R}\left(\frac{\partial v_j}{\partial \theta}-w_j\right)\right).\end{aligned} \tag{4.1.5}$$

Donnell has received from the system of the equations (4.1.1–3) by using special function φ a following equation for w_j [76]

$$\frac{Eh_j^{\,3}}{12(1-\nu^2)}\nabla^8 w_j + \frac{Eh_j}{R^2}\frac{\partial^4 w_j}{\partial x^4} = \nabla^4 p_j, \tag{4.1.6}$$

where $p_j = -\rho h_j \dfrac{\partial^2 w_j}{\partial t^2}$ and $\nabla^8 = (\nabla^2)^4$, $\nabla^4 = (\nabla^2)^2$,

where $\nabla^2 = \dfrac{\partial^2}{\partial x^2} + \dfrac{1}{R^2}\dfrac{\partial^2}{\partial \theta^2}$.

Later the equation (4.1.6) has been specified by Donnell [76] as

$$\frac{Eh_j^{\,3}}{12(1-\nu^2)}(\nabla^8 w_j + \frac{1}{R^2}\nabla^2(5\frac{1}{R^2}\frac{\partial^4 w_j}{\partial^2 x \partial^2 \theta} + 2\frac{1}{R^4}\frac{\partial^4 w_j}{\partial \theta^4}) + \frac{1}{R^4}(3\frac{1}{R^2}\frac{\partial^4 w_j}{\partial^2 x \partial^2 \theta} + \\ + \frac{1}{R^4}\frac{\partial^4 w_j}{\partial \theta^4})) + \frac{Eh_j}{R^2}\frac{\partial^4 w_j}{\partial x^4} = \nabla^4 p_j. \tag{4.1.7}$$

We substitute

$$w_j(x,\theta,t) = e^{r_j x}\cos p\theta \sin \omega t,$$

where p – number of waves in a circumferential direction;

ω – the circular natural frequency.

This gives with (4.1.6) the characteristic equation

$$\frac{Eh_j^{\,3}}{12(1-\nu^2)}(r_j^{\,2} - \frac{p^2}{R^2})^4 + \frac{Eh_j}{R^2}r_j^{\,4} - \rho h_j \omega^2 (r_j^{\,2} - \frac{p^2}{R^2})^2 = 0. \tag{4.1.8}$$

Let's denote

$$r_j^{\,2} - \frac{p^2}{R^2} = \pm\frac{k}{h_j}, \tag{4.1.9}$$

then the equation (4.1.8) can be rewriten as

$$\frac{Eh_j^{\,3}}{12(1-\nu^2)}\frac{k^4}{h_j^4} + \frac{Eh_j}{R^2}(\pm\frac{k}{h_j} + \frac{p^2}{R^2})^2 - \rho h_j \omega^2 \frac{k^2}{h_j^2} = 0 \tag{4.1.10}$$

or

$$k_j^{\,4} + a k_j^{\,2} + b_j k_j + c_j = 0,$$

where

$$a = 12(1-\nu^2)(\frac{1}{R^2} - \omega^2\frac{\rho}{E}), \quad b_j = \pm 24(1-\nu^2)h_j\frac{p^2}{R^4}, \quad c_j = 12(1-\nu^2)h_j^{\,2}\frac{p^4}{R^4}.$$

This equation has four different solutions k_{ij} which meet the equalities

$$k_{1,2j} = \frac{z_{1j}}{2} \pm \sqrt{\left(\frac{z_{1j}}{2}\right)^2 - z_{2j}},$$

$$k_{3,4j} = -\frac{z_{1j}}{2} \pm \sqrt{\left(\frac{z_{1j}}{2}\right)^2 - \frac{c_j}{z_{2j}}},$$

where

$$z_{1j}^2 = x_j,$$

$$z_{2j} = \frac{1}{2}(z_{1j}{}^2 + a + \frac{b_j}{z_{1j}}),$$

Here x_j is the solution of the equation

$$x_j{}^3 + 2ax_j{}^2 + (a^2 - 4c_j)x_j - b_j{}^2 = 0.$$

It immediately follows from (4.1.9) that

$$r_{1j} = \pm i\sqrt{\frac{k}{h_j} - \frac{p^2}{R^2}}, \qquad r_{2j} = \pm\sqrt{\frac{k}{h_j} + \frac{p^2}{R^2}},$$

or

$$r_{1j} = \pm i\frac{1}{R}\sqrt{\frac{a\,R}{h_j} - p^2}, \qquad r_{2j} = \frac{1}{R}\sqrt{\frac{a\,R}{h_j} + p^2}, \tag{4.1.11}$$

where $a=kR$, i^2=-1.

The value of k can be a real or a complex number $\alpha+i\beta$. Roots in the form of (4.1.11) are two real and two complex roots. In this case we can present a solution of (4.1.7) in the form

$$w_j(x,\theta,t) = (A_{1j}\sin r_{1j}x + A_{2j}\cos r_{1j}x + A_{3j}\sinh r_{2j}x + A_{4j}\cosh r_{2j}x)\cos p\theta\sin\omega t, \tag{4.1.12}$$

where A_{1j}, A_{2j}, A_{3j}, A_{4j} are unknown constants.

The solution (4.1.12) has to meet appropriate boundary conditions at both ends with the four continuity conditions (with or without crack). The determinant of the resulting 4×4 matrix will give the roots $\lambda_m=a_m/\beta$, where $\beta=h/R$. It can be easily shown that the equation for determination of quantities λ_m is

$$\lambda_m{}^4 + 12(1-\nu^2)\beta^{-2}\left(\lambda_m - p^2\right) = \omega_{mp}{}^2 R^2 \frac{\rho\left(1-\nu^2\right)}{E} 12\beta^{-2}\lambda_m{}^2, \tag{4.1.13}$$

This results in

$$\omega_{mp} = \sqrt{\frac{E}{\rho 12\left(1-\nu^2\right)}}\frac{\beta}{R}\sqrt{\lambda_m{}^2 + 12(1-\nu^2)\beta^{-2}\frac{\left(\lambda_m - p^2\right)^2}{\lambda_m{}^2}}. \tag{4.1.14}$$

The natural frequencies are obtained from equation (4.1.7) as

$$\omega_{mp} = \sqrt{\frac{E}{\rho 12\left(1-\nu^2\right)}}\frac{\beta}{R}\sqrt{\lambda_m{}^2 - \frac{5(\lambda_m - p^2)p^2 + 2p^2}{\lambda_m} + \frac{3(\lambda_m - p^2)p^2 + p^4}{\lambda_m{}^2} + 12(1-\nu^2)\beta^{-2}\frac{\left(\lambda_m - p^2\right)^2}{\lambda_m{}^2}}. \tag{4.1.15}$$

Let the vibration frequency ω be expressed in terms of a non-dimensional frequency parameter

$$\Omega = \omega R\sqrt{\frac{\rho\left(1-\nu^2\right)}{E}}.$$

Accounting for this notation the equation (4.1.14) can be written as

$$\Omega_{mp} = \frac{\beta}{\sqrt{12}}\sqrt{\lambda_m{}^2 + 12(1-\nu^2)\beta^{-2}\frac{\left(\lambda_m - p^2\right)^2}{\lambda_m{}^2}} \tag{4.1.16}$$

From equation (4.1.15) one obtains

$$\Omega_{nm} = \frac{\beta}{\sqrt{12}}\sqrt{\lambda_m{}^2 - \frac{5(\lambda_m - p^2)p^2 + 2p^2}{\lambda_m} + \frac{3(\lambda_m - p^2)p^2 + p^4}{\lambda_m{}^2} + 12(1-\nu^2)\beta^{-2}\frac{\left(\lambda_m - p^2\right)^2}{\lambda_m{}^2}}. \tag{4.1.17}$$

4.2. Continuity condition and local flexibility

Let us study a cylindrical shell with a step at the section $x=a$. Assume that there exists a circumferential surface crack with uniform depth c in the cylindrical shell.

Let the segments adjacent to the crack have thicknesses h_0 and h_1, respectively (Fig. 4.2).

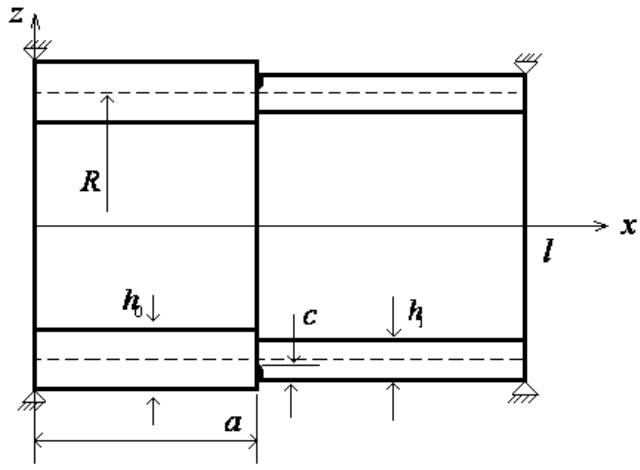

Fig. 4.2: One-step circular cylindrical shell with crack.

For the simplicity sake we assume that these flaws are stable circular surface cracks. In this study it is assumed that the surface crack is always open. One can isolate a longitudinal element of unit width from the shell, as shown in Fig. 4.3.

The surface crack in the shell can be modeled as a distributed line spring [73]. The presence of the crack in the shell will cause the local flexibility. The flexibility of the spring is a function of the local dimensions and the elastic properties of the cracked region. If the local stress-strain state in the shell will result in the discontinuity of the generalized displacement at the both sides of crack's section, then the deformation at the cracked region can be described according to the local compliance [8]

$$\delta_i^{+} - \delta_i^{-} = C_{ij} P_i, \tag{4.2.1}$$

where δ_i^{+} and δ_i^{-} are the generalized displacements at the left and the right side of the cracked section of the shell, respectively.

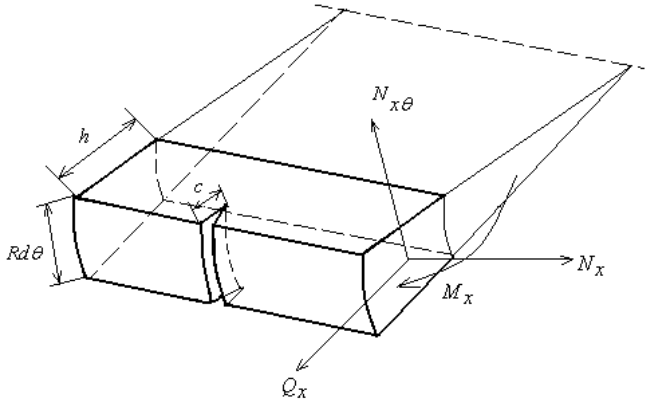

Fig. 4.3: Geometry of an element of cracked shell.

C_{ij} and P_i denote the local compliance and the generalized force, respectively. Let us denote the elements of the vector of generalized displacements by $\vec{U} = (u, \frac{\partial w}{\partial x}, w, v)$ thus U_1=u, $U_2 = \frac{\partial w}{\partial x}$, U_3=w, U_4=v.Using this notation one can present the generalized displacement U_i as a function of the strain energy release rate J as (Anderson, 2005; Dimarogonas, 1989)

$$U_i = \frac{\partial}{\partial P_i} \int_0^c J dc. \tag{4.2.2}$$

Therefore, the compliance can be expressed as

$$C_{ij} = \frac{\partial U_i}{\partial P_j} = \frac{\partial^2}{\partial P_i \partial P_j} \int_0^c J dc. \tag{4.2.3}$$

The crack in a solid can be stressed in three different modes, as illustrated in Fig. 4.4.

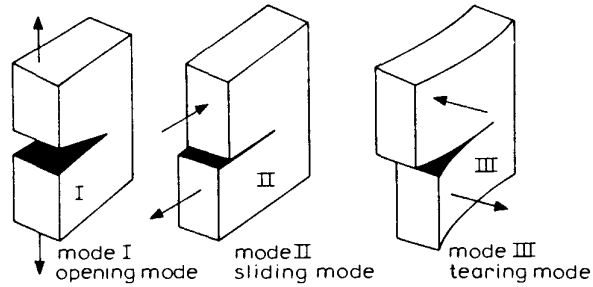

Fig. 4.4: The three modes of cracking.

The crack mode I is called the case of cracking when the crack opening is caused by normal stresses. The displacements of the crack surfaces are perpendicular to the plane of the crack. In-plane shear results in mode II or "sliding mode": the displacement of the crack surfaces is in the plane of the crack and perpendicular to the leading edge of the crack. The "tearing mode" or mode III is caused by out-of-plane shear. Crack surface displacements are in the plane of the crack and parallel to the leading edge of the crack. The superposition of the three modes describes the general case of cracking.
In addition, expressions for the strain energy release ratio can be directly expressed as function of the stress intensity factor [65]

$$J = \frac{1}{E'}\left[\left(\sum_{n=1}^{4} K_{\mathrm{I}n}\right)^2 + \left(\sum_{n=1}^{4} K_{\mathrm{II}n}\right)^2 + g\left(\sum_{n=1}^{4} K_{\mathrm{III}n}\right)^2\right],$$

where $K_{\mathrm{I}n}$, $K_{\mathrm{II}n}$, $K_{\mathrm{III}n}$ are the stress intensity factor for modes of I, II and III, respectively, $E' = E$ for plane stress, $E' = E/(1-\nu^2)$ for plane strain, $g = 1+\nu$.

The stress intensity factors of different modes can be tabulated as shown in Table 4.1 [66].

Table 4.1: Stress intensity factor [66].

	N_x	M_x	Q_x	$N_{x\theta}$
$K_{\mathrm{I}n}$	$F_1 N_x\sqrt{\pi c}/h$	$F_2 M_x\sqrt{\pi c}/h^2$	0	0
$K_{\mathrm{II}n}$	0	0	$1{,}5F_3 Q_x(1-0{,}5\ \bar{a}^2)\sqrt{\pi c}/h$	0
$K_{\mathrm{III}n}$	0	0	0	$F_4 N_{x\theta}\sqrt{\pi c}/h$

In the Table 4.1 F_n are the correction functions, which are dimensionless functions of the crack depth ratio. It was shown in [66] that in the case when the compliance matrix is a 4×4 matrix one has

$$\text{TI}F_1 = F_4[0{,}752 + 1{,}287\alpha + 0{,}37(1 - \sin\alpha)^3]/\cos\alpha\,,$$

$$F_2 = F_4[0{,}923 + 0{,}199(1 - \sin\alpha)^4]/\cos\alpha\,,$$

$$F_3 = (1{,}122 - 0{,}561\,\bar{a} + 0{,}085\,\bar{a}^2 + 0{,}18\,\bar{a}^3)/\sqrt{1-\bar{c}}\,, \tag{4.2.3}$$

$$F_4 = \sqrt{\tan\alpha/\alpha},$$

$$\bar{c} = c/h,\ \alpha = \pi\bar{c}/2.$$

By substituting the stress intensity factors tabulated in Table 4.1 into Eq. (4.2.3) and differentiating twice with respect to P_i and P_j, one can obtain the local compliances pertinent to different internal forces.

When $P_j = P_i = N_x$, the tensile component of the compliance matrix with respect to N_x can be obtained as

$$C_{11} = 2\pi / E' \int_0^c F_1^2 c / h^2 dc. \tag{4.2.4}$$

Similarly, the compliance with respect to M_x is

$$C_{22} = 72\pi / E' \int_0^c F_2^2 c / h^4 dc. \tag{4.2.5}$$

For Q_x and $N_{x\theta}$, one can get

$$C_{33} = 4{,}5\pi / E' \int_0^c F_3^2 (1 - 0{,}5\bar{a}^2)^2 c / h^2 dc, \tag{4.2.6}$$

$$C_{44} = 2\pi g / E' \int_0^c F_4^2 c / h^2 dc. \tag{4.2.7}$$

Considering the coupling of longitudinal, bending and transverse shear displacement, for $P_j \neq P_i$, we have

$$C_{12} = 12\pi / E' \int_0^c F_1 \, F_2 \, c / h^3 dc,$$
$$C_{21} = C_{12},\ C_{13} = C_{14} = C_{23} = C_{24} = C_{34} = 0, \qquad (4.2.8)$$
$$C_{31} = C_{13},\ C_{41} = C_{14},\ C_{32} = C_{23},\ C_{42} = C_{24},\ C_{43} = C_{34}.$$

Thus, the local compliance matrix can be obtained, which is a 4×4-dimensional matrix. If the diagonal elements C_{ii} of the local compliance matrix with different crack depth are plotted together, it can be seen from this figure that the local compliances increase with increasing crack relative depth *a/h*. In addition, the compliance C_{22} with respect to bending moment M_x is much larger than any others. It means that the local compliance with respect to bending moment in the shell is dominant in the local compliance matrix, which is consistent with the results obtained by Gounaris and Dimarogonas [26] in the cracked beam structures.

At the cross-section $x=a_j$ of the shell, the continuity of axial force, angular bending moment, total shear force, and resultant membrane force should be satisfied, so

$$\begin{aligned} (N_x)_j &= (N_x)_{j+1}, \\ (M_x)_j &= (M_x)_{j+1}, \\ (T_x)_j &= (T_x)_{j+1}, \\ (S_x)_j &= (S_x)_{j+1}, \end{aligned} \qquad (4.2.9)$$

where subscripts j and $j+1$ represent the right side and left side of the cross-section, respectively.

The total shear force $(T_x)_j$ is

$$(T_x)_j = (Q_x)_j - \frac{\partial (M_{x\theta})_j}{R\partial\theta}, \qquad (4.2.10)$$

and the resultant membrane force $(S_x)_j$ becomes

$$(S_x)_j = (N_{x\theta})_j + \frac{(M_{x\theta})_j}{R}, \qquad (4.2.11)$$

where

$$(M_{x\theta})_j = \frac{D_j(1-\nu)}{R}\frac{\partial^2 w_j}{\partial x \partial\theta}, \qquad (N_{x\theta})_j = \frac{Eh_j}{2(1+\nu)}\left(\frac{\partial u_j}{R\partial\theta} + \frac{\partial v_j}{\partial x}\right). \qquad (4.2.12)$$

The axial, tangential, radial and angular displacements are continuous, respectively, at the cross-section of $x=a_j$ with step but without crack, so

$$u_j = u_{j+1},\ v_j = v_{j+1},\ w_j = w_{j+1},\ \ \partial w_j / \partial x = \partial w_{j+1} / \partial x. \tag{4.2.13}$$

The crack induces the discontinuity of the displacement at $x=a$, and the local compliance matrix is deduced above. So the discontinuity of displacements or the different of their values at both sides of the crack can be written as

$$\begin{bmatrix} u_j - u_{j+1} \\ \partial w_j / \partial x - \partial w_{j+1} / \partial x \\ w_j - w_{j+1} \\ v_j - v_{j+1} \end{bmatrix} = [C] \begin{bmatrix} N_x \\ M_x \\ Q_x \\ N_{x\theta} \end{bmatrix}. \tag{4.2.14}$$

In the current case we have a crack of mode I (opening mode). Assume that the compliance C_{22} with respect to bending moment is much larger than the elements C_{11}, C_{12}, C_{33}, C_{44} of the compliance matrix and thus the local compliance with respect to bending moment is dominating element in the local compliance matrix. Therefore from (4.2.14) by use Table 4.1 we can find for the deffection

$$\begin{aligned} &\partial w_j / \partial x - \partial w_{j+1} / \partial x = (C_{22})_{j+1} (M_x)_{j+1}, \\ &w_j - w_{j+1} = 0. \end{aligned} \tag{4.2.15}$$

The stress correction function F_2 gives by (4.2.3) and the function $F_1(s)$ (1.3.13) are compared in Fig. 4.5. As we can see from Fig. 4.5 functions $F_2(s)$ and $F_1(s)$ are quite close. Thus in the following we shall use the function defined by (1.3.13) and take

$$(C_{22})_{j+1} = \frac{72\pi}{E' h_{j+1}^{\ 2}} f(s_{j+1}), \tag{4.2.16}$$

where

$$\begin{aligned} f(s) = 1{,}862 s^2 - 3{,}95 s^3 + 16{,}375 s^4 - 37{,}226 s^5 + 76{,}81 s^6 - \\ + 126{,}9 s^7 + 172{,}5 s^8 - 143{,}97 s^9 + 66{,}56 s^{10}. \end{aligned}$$

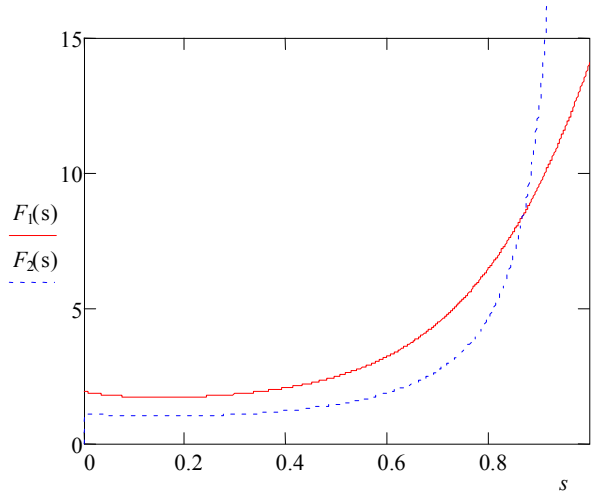

Fig. 4.5: Functions $F_1(s)$ and $F_2(s)$ for C_{22}.

The continuity and jump conditions at $x=a$ are

$$w(a+0,\theta,t)\text{-}w(a-0,\theta,t)=0, \tag{4.2.17}$$

$$\frac{\partial w}{\partial x}(a+0,\theta,t)\text{-}\frac{\partial w}{\partial x}(a-0,\theta,t)=\frac{72\pi}{E'h_1^2}f(s_1)M_x(a-0), \tag{4.2.18}$$

$$M_x(a+0,\theta,t)-M_x(a-0,\theta,t)=0, \tag{4.2.19}$$

$$T_x(a+0,\theta,t)-T_x(a-0,\theta,t)=0, \tag{4.2.20}$$

Taking equations (4.1.5), (4.2.10), (4.2.12) into account one can write

$$w_1(a,\theta,t)=w_0(a,\theta,t),$$
$$\frac{\partial w_1}{\partial x}(a,\theta,t)=\frac{\partial w_0}{\partial x}(a,\theta,t)-\frac{72\pi}{E'h_1^2}f(s_1)D_0\left(\frac{\partial^2 w_0(a,\theta,t)}{\partial x^2}+\frac{\nu}{R^2}\frac{\partial^2 w_0(a,\theta,t)}{\partial\theta^2}\right), \tag{4.2.21}$$

$$D_1\left(\frac{\partial^2 w_1(a,\theta,t)}{\partial x^2}+\frac{\nu}{R^2}\frac{\partial^2 w_1(a,\theta,t)}{\partial \theta^2}\right)=D_0\left(\frac{\partial^2 w_0(a,\theta,t)}{\partial x^2}+\frac{\nu}{R^2}\frac{\partial^2 w_0(a,\theta,t)}{\partial \theta^2}\right),$$

$$D_1\frac{\partial}{\partial x}\left(\frac{\partial^2 w_1(a,\theta,t)}{\partial x^2}+\frac{\nu}{R^2}\frac{\partial^2 w_1(a,\theta,t)}{\partial \theta^2}\right)=D_0\frac{\partial}{\partial x}\left(\frac{\partial^2 w_0(a,\theta,t)}{\partial x^2}+\frac{\nu}{R^2}\frac{\partial^2 w_0(a,\theta,t)}{\partial \theta^2}\right),$$

where w_0, D_0 and w_1, D_1 stand for the quantities w and D in the segments with thickness h_0 and h_1, respectively.

4.3. Boundary conditions

Let us consider the case of a cylindrical shell simply supported at the ends. Such a hinged edge is not able to transmit a moment M_x, needed to enforce the condition $\frac{\partial w}{\partial x}=0$. Assuming also that there is no edge resistance in the direction x, we arrive at the boundary conditions

$$v=0, \qquad N_x=0 \tag{4.3.1}$$

and

$$w=0, \qquad M_x=0 \tag{4.3.2}$$

at both ends.
From conditions (4.3.2) and (4.1.12) it follows that at the point x=0:

$$A_{20}=A_{40}=0 \tag{4.3.3}$$

and at the point $x=l$:

$$\begin{aligned} &A_{1n}\sin r_1 l+A_{2n}\cos r_1 l=0,\\ &A_{3n}\sinh r_2 l+A_{4n}\cosh r_2 l=0. \end{aligned} \tag{4.3.4}$$

4.4. System of recursive equations

For a circular cylindrical shell of constant thickness with simply supported ends from boundary conditions (4.3.3)–(4.3.4) and from the general solution w_j in the form (4.1.8) we have

$$\sin r_1 l=0.$$

This results in

$$r_1 l=\pi m; \qquad (m=0,1,\ldots)$$

$$\lambda_{mp} = (\pi m \frac{R}{l})^2 + p^2. \tag{4.4.1}$$

The natural frequencies are then obtained from equations (4.1.12) as

$$\omega_{mp} = \sqrt{\frac{E}{\rho 12(1-\nu^2)}} \frac{\beta}{R} \sqrt{((\pi m \frac{R}{l})^2 + p^2)^2 + 12(1-\nu^2)\beta^{-2} \frac{\left(\pi m \frac{R}{l}\right)^4}{((\pi m \frac{R}{l})^2 + p^2)^2}}. \tag{4.4.2}$$

For this case the specified formula for natural frequencies is

$$\omega_{mp} = \sqrt{\frac{E}{\rho 12(1-\nu^2)}} \frac{\beta}{R} \times$$
$$\times \sqrt{((\pi m \frac{R}{l})^2 + p^2)^2 - \frac{5(\pi m \frac{R}{l})^2 p^2 + 2p^2}{(\pi m \frac{R}{l})^2 + p^2} + \frac{3(\pi m \frac{R}{l})^2 p^2 + p^4}{((\pi m \frac{R}{l})^2 + p^2)^2} + \frac{12(1-\nu^2)}{\beta^2} \frac{\left(\pi m \frac{R}{l}\right)^4}{((\pi m \frac{R}{l})^2 + p^2)^2}}. \tag{4.4.3}$$

In the case of the shell with unique step boundary conditions (4.3.3)-(4.3.4) and continuity conditions for w at $x=a$

$$w_1(a,\theta,t) - w_0(a,\theta,t) = 0,$$

$$\frac{\partial w_1}{\partial x}(a,\theta,t) - \frac{\partial w_0}{\partial x}(a,\theta,t) = 0,$$

$$D_1(\frac{\partial^2 w_1(a,\theta,t)}{\partial x^2} + \frac{\nu}{R^2}\frac{\partial^2 w_1(a,\theta,t)}{\partial \theta^2}) = D_0(\frac{\partial^2 w_0(a,\theta,t)}{\partial x^2} + \frac{\nu}{R^2}\frac{\partial^2 w_0(a,\theta,t)}{\partial \theta^2}),$$

$$D_1 \frac{\partial}{\partial x}(\frac{\partial^2 w_1(a,\theta,t)}{\partial x^2} + \frac{\nu}{R^2}\frac{\partial^2 w_1(a,\theta,t)}{\partial \theta^2}) = D_0 \frac{\partial}{\partial x}(\frac{\partial^2 w_0(a,\theta,t)}{\partial x^2} + \frac{\nu}{R^2}\frac{\partial^2 w_0(a,\theta,t)}{\partial \theta^2})$$

Thus we have the characteristic equation

$$\left[(b_2 + \frac{c}{\gamma^3})\sinh r_{10}a \cosh r_{1l}(l-a) + \frac{r_{10}}{r_{1l}}(b_1 + \frac{d}{\gamma^3})\cosh r_{10}a \sinh r_{1l}(l-a)\right] \times$$
$$\times \left[(b_1 + \frac{d}{\gamma^3})\sin r_{20}a \cos r_{2l}(l-a) + \frac{r_{10}}{r_{2l}}(b_2 + \frac{c}{\gamma^3})\cos r_{20}a \sin r_{2l}(l-a)\right] -$$

$$-\left[(b_2-\frac{d}{\gamma^3})\sin r_{20}a\cosh r_{1l}(l-a)+\frac{r_{20}}{r_{1l}}(b_1-\frac{c}{\gamma^3})\cos r_{20}a\sinh r_{1l}(l-a)\right]\times$$

$$\times\left[(b_1-\frac{c}{\gamma^3})\sinh r_{10}a\cos r_{2l}(l-a)+\frac{r_{10}}{r_{2l}}(b_2-\frac{d}{\gamma^3})\cosh r_{10}a\sin r_{2l}(l-a)\right]=0,$$

where

$$r_{10}=\frac{1}{R}\sqrt{x+p^2},\qquad r_{20}=\frac{1}{R}\sqrt{x-p^2},$$

$$r_{1l}=\frac{1}{R}\sqrt{\frac{x}{\gamma}+p^2},\qquad r_{2l}=\frac{1}{R}\sqrt{\frac{x}{\gamma}-p^2},$$

$$b_1=\frac{1}{R^2}(\frac{x}{\gamma}+(1-\nu^2)p^2),\qquad b_2=\frac{1}{R^2}(\frac{x}{\gamma}-(1-\nu^2)p^2),$$

$$c=\frac{1}{R^2}(x+(1-\nu^2)p^2),\qquad d=\frac{1}{R^2}(x-(1-\nu^2)p^2),$$

where $\gamma=h_1/h_0$, $x=kR/h_0$.

In the case n=1 from boundary conditions (4.3.3)-(4.3.4) and continuity conditions for w at $x=a$ (4.2.21) we obtain characteristic equation

$$\left[(b_2+\frac{c}{\gamma^3})\sinh r_{10}a\cosh r_{1l}(l-a)+\frac{r_{10}}{r_{1l}}(b_1+\frac{d}{\gamma^3})\cosh r_{10}a\sinh r_{1l}(l-a)+\right.$$

$$\left.+cb_1\frac{p}{r_{1l}}\sinh r_{10}a\sinh r_{1l}(l-a)\right]\times$$

$$\times\left[(b_1+\frac{d}{\gamma^3})\sin r_{20}a\cos r_{2l}(l-a)+\frac{r_{10}}{r_{2l}}(b_2+\frac{c}{\gamma^3})\cos r_{20}a\sin r_{2l}(l-a)-\right.$$

$$\left.-b_2c\frac{p}{r_{2l}}\sin r_{20}a\sin r_{2l}(l-a)\right]-$$

$$-\left[(b_2-\frac{d}{\gamma^3})\sin r_{20}a\cosh r_{1l}(l-a)+\frac{r_{20}}{r_{1l}}(b_1-\frac{c}{\gamma^3})\cos r_{20}a\sinh r_{1l}(l-a)+\right.$$

$$\left.+b_1d\frac{p}{r_{1l}}\sin r_{20}a\cosh r_{1l}(l-a)\right]\times$$

$$\times\left[(b_1-\frac{c}{\gamma^3})\sinh r_{10}a\cos r_{2l}(l-a)+\frac{r_{10}}{r_{2l}}(b_2-\frac{d}{\gamma^3})\cosh r_{10}a\sin r_{2l}(l-a)+\right.$$

$$+ b_2 c \frac{p}{r_{2l}} \cos r_{20} a \sin r_{2l}(l-a) \Bigg] = 0,$$

where

$$p = 6\pi f(s)\gamma^2 h_0.$$

4.5. Numerical results

Numerical analyses for simply supported shells are carried out in the case of the shell with l=0,2m; R=0,2m; h=R/20; ρ=7850kg/m^3; ν=0,3; E=2,1×10^{11}N/m^2.

Table 4.1 shows natural frequencies for this case. Present methods 1 and 2 are based on equations (4.4.2) and (4.4.3), respectively. The quantity p is number of semiwaves in the circumferential direction. It is seen from Table 4.1 that the natural frequencies corresponding to the current analytical methods are in good agreement with the natural frequencies obtained by F. Pellicano [56].

In Table 4.2 are presented frequency parameters Ω of simply supported long shells obtained from 3D solutions by Markus [48], and Zhang [71] and by the present method (equations (4.1.15) and (4.4.1)).

We observe that the present exact solutions based on Donnell shell theory are in close agreement with the exact 3D solutions [48] and with Zhang solutions [71]. The value of p in Table 4.2 is the number of half-waves of vibration mode in the circumferential direction.

Numerical analyses for simply supported shells with stepped thickness and crack are carried out in the case described below: h_1=0,009m; l=1,2m; R=0,12m; a/l=0,5; γ=h_1/h_0 ; ν=0,3. In calculations the number of steps n=1. The results are presented in Table 4.3.

Table 4.3 presents frequency parameters Ω of the first 8 modes for circular cylindrical shells with one thickness variation. The ratio of the shell length to radius l/R is set to be 1,5 and 10, the thickness to radius ratio h_0/R is fixed at 0,01, the thickness ratio h_1/ h_0 is taken to be 0,5, and the location of the thickness variation is at the center of the shell.

The value of p indicates circumferential half-wave numbers and m denotes the mode sequence number for a given p value. In this case is m=1. An increase in the length to radius ratio l/R from 1 to 10 will lead to a decrease in the frequency parameters.

In this case is m=1. It was shown that when l/R increases then the frequency parameter decreases.

The influence of the crack c/h on the fundamental frequency parameters of simply supported circular cylindrical shells with one thickness variation is depicted in Figs. 4.6 and 4.7.

Fig. 4.6 corresponds to the case when the number of semiwaves in the circumferential direction equals to unity whereas. Fig. 4.7 is associated with the case of two semiwaves. It can be see from Fig. 4,6; 4.7 that the case of lower

number of waves corresponds to lower values of the parameter Ω. On the other hand, the frequency parameter Ω is higher for a stepped shell in comparison to that of the appropriate shell of constant thickness.

Table 4.1: Comparison of natural frequencies for a simply supported shell.

Mode	Natural frequencies (Hz)			
m/p	Present method 1	Present method 2	Exact by F.Pellicano	Diff. %
1/5	739,25	737,89	722,10	2,14%
1/6	564,15	561,65	553,30	1,49%
1/7	493,70	489,87	484,60	1,08%
1/8	498,54	493,65	489,60	0,82%
1/9	555,29	549,78	546,20	0,65%
1/10	645,97	640,17	636,80	0,53%
1/11	759,85	753,91	750,70	0,43%
1/12	891,41	885,42	882,20	0,36%
2/10	977,77	973,59	968,10	0,56%
2/11	992,84	987,94	983,40	0,46%

Table 4.2: Comparison of frequency parameters Ω for a simply supported cylindrical shell (v=0,3; l/R=20; m=1).

p	*h/R*=0,05				*h/R*=0,002			
	Markus	Zhang	Present	Diff.%	Markus	Zhang	Present	Diff.%
1	0,0161063	0,0161065	0,022	27%	0,0161011	0,0161011	0,020000	19%
2	0,0392332	0,0393038	0,058	32%	0,00545243	0,0054533	0,006120	11%
3	0,1094770	0,1098530	0,131	16%	0,00503724	0,0050419	0,005847	14%
4	0,2090080	0,2103450	0,233	10%	0,00853409	0,0085341	0,009422	9%

Table 4.3: Frequency parameters Ω for simply supported shells with a unique step (h_0/R=0,01; h_1/h_0=0,5; a/l=0,5)

l/R	*p*	1	2	3	4	5	6	7	8
1	Present	0,8150	0,5770	0,3820	0,2420	0,1460	0,1080	0,2530	0,2500
	Zhang and Xiang	0,5493	0,6224	0,4613	0,3428	0,2649	0,2204	0,2037	0,2087
5	Present	0,1210	0,0690	0,0480	0,0550	0,0720	0,1050	0,1430	0,1860
	Zhang and Xiang	0,1766	0,0730	0,0411	0,0415	0,0538	0,0643	0,0779	0,0964
10	Present	0,0680	0,0310	0,0270	0,0470	0,0720	0,1040	0,1420	0,1850
	Zhang and Xiang	0,0565	0,0207	0,0205	0,0291	0,0382	0,0520	0,0699	0,0912

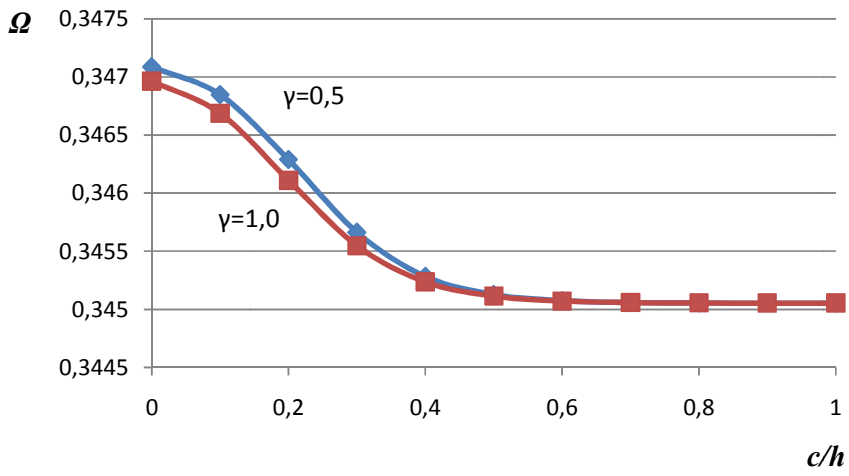

Fig 4.6: Frequency parameters Ω for simply supported shells with one-step thickness variation and crack, the case p=4; m=1.

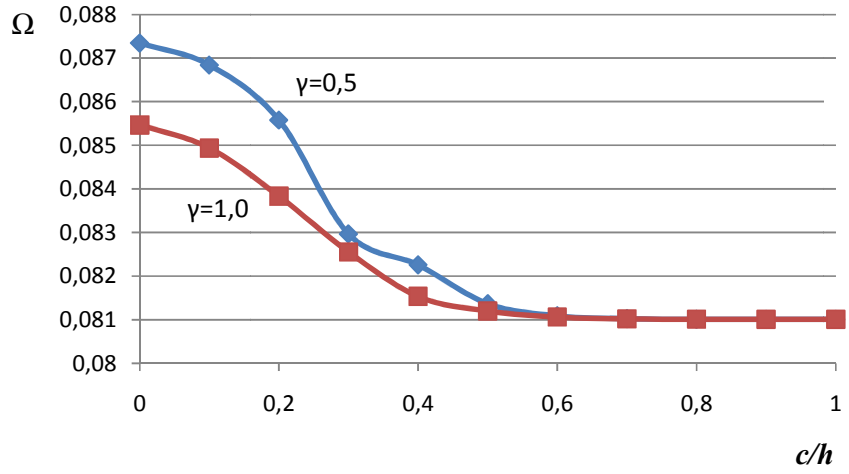

Fig 4.7: Frequency parameters Ω for simply supported shells with one-step thickness variation and crack, the case p=2; m=1.

SUMMARY

The current study consists of the introduction and four chapters.

In the first chapter free vibrations of simply supported circular cylindrical shells are considered. First of all, the governing equations for analysis of axisymmetric deformations of cylindrical shells are presented. Resorting to the concept of separation of variables a solution technique is suggested. According to this concept the solution of partial differential equations is transformed into a problem with ordinary equations.

In the next section the model of the crack is discussed. The idea of an equivalent spring and local compliance is used herein in order to quantify the relationship between loading and stress concentration around the crack tip. As regards the stress concentration it is measured by stress intensity coefficients known from the linear elastic fracture mechanics. Accounting for the local compliance one can solve the problem up to the end. The results of calculations are compared with those obtained by other methods.

In the second chapter vibrations of circular cylindrical shells with various boundary conditions are studied. The cases of shells clamped at both ends, also cantilever shells, e.g. shells clamped at the left end and absolutely free at the right hand end are treated in greater detail.

It was assumed that the stress strain state of the tube remains axisymmetric during deformation. The shells of piece wise constant thickness are treated under the condition that at re-entrant corners of steps circular cracks of constant length are located. Cracks are considered to be stationary surface cracks, problems related to re-distribution of stresses and strains due to the extension of crack are not treated herein. The influence of cracks on the behaviour of the shell is prescribed via local compliances of the shell coupled with stress intensity factors.

Calculations showed that the cracks have essential influence on vibration characteristics. It was established that if the crack location is fixed then the maximal value of the characteristic number k is achieved if the crack length is equal to zero. On the other hand, for fixed crack length and variable ratio of thicknesses maximum of the number k is achieved when $h_0=h_1$ thus for the shell of constant thickness. When ratio of thicknesses is fixed whereas $h_1<h_0$ then the minimum of k is achieved when the step and crack location tends to the free end.

The third chapter is devoted to layered and composite cylindrical shells. It is assumed here that the stress-strain state of a circular cylindrical shell remains axisymmetric during deformations. The natural frequency of vibrations is determined for various non-homogeneous materials.

In the fourth chapter non-axisymmetric vibrations of circular cylindrical shells are studied. The simplified system of equilibrium equations presented by Donnell is used. Numerical results are obtained for cylindrical shells of stepped thickness containing cracks at re-entrant corners of steps.

REFERENCES

1. R.D. Adams, P. Cawley, C. J. Pye, B. J. Stone, A vibration technique for non-destructively assessing the integrity of structures, *Journal of Mechanical Engineering Science*, 1978, 20, 93–100.
2. T. L. Anderson, *Fracture Mechanics*, Taylor and Francis, Boca Raton, 2005.
3. H. Aron, *Das Gleichgewicht und die Bewegung einer unendlich dünnen, beliebig gekrümmten elastischen Schale*, Math. Ann., 1874, 78, 136–174.
4. G. Bamnios, A. Trochides, Dynamic behaviour of a cracked cantilever beam, *Applied Acoustics*, 1995, 45, 97–112.
5. M. Behzad, A. Meghdari, A. Ebrahimi, A new approach for vibration analysis of a cracked beam, *International Journal of Engineering,* 2005, 18 (4), 319–330.
6. B. Binici, Vibration of beams with multiple open cracks subjected to axial force, *Journal of Sound and Vibration*, 2005, 287, 277–295.
7. K. B. Broberg, *Cracks and Fracture,* Academic Press, New York, 1999.
8. D. Broek, *Elementary engineering fracture mechanics*, 1974.
9. William F., Jr. Brown, John E. Srawley, Plane strain crack toughness testing of high strength metallic materials, *ASTM special technical publication*, #410, 1967.
10. P. Cawley, R. D. Adams, The location of defects in structures from measurements of natural frequencies, *Journal of Strain Analysis*, 1979, 14, 49–57.
11. Chang-Tsan Sun, J. M. Whitney, Axisymmetric vibrations of laminated composite cylindrical shells, *J. Acoust. Soc. Am.,* Vol. 55, 6, 1974.
12. T.D. Chaudhari, S.K. Maiti, A study of vibration of geometrically segmented beams with and without crack, *Int. J. Solids Struct.*, 2000, 37, #5, 761–779.
13. T.G. Chondros, A.D. Dimarogonas, Identification of cracks in welded joints of complex structures, *Journal of Sound and Vibration*, 1980, 69, #4, 531–538.
14. T.G. Chondros, A.D. Dimarogonas, Vibration of a cracked cantilever beam, *Trans. ASME, J. Vibr. Acoust.*, 1998, 120, 742–746.
15. T.G. Chondros, A.D. Dimarogonas, Yao J., Vibration of a beam with a breathing crack , *Journal of Sound and Vibration* , 2001, 239, # 1, 57–67.
16. T.G. Chondros, The continuous crack flexibility model for crack identification, *Fatigue Fract. Eng. Mater. Struct.,* 2001, 24, 643–650.
17. M.A. De Rosa, Free vibration of stepped beams with flexible ends in the presence of follower forces at the step, *Journal of Sound and Vibration,* 1996, 194, 631–635.
18. A.D. Dimarogonas, S.A. Paipetis, Analytical Methods in Rotor Dynamics, *Elsevier*, London, 1983.
19. A.D. Dimarogonas, S.A. Paipetis, *Rotar Dynamics*, Elsevier, London, 1983.
20. A.D. Dimarogonas, *Vibration Engineering*, St.Paul, West Publishers, 1976.
21. A.D. Dimarogonas, Vibration of cracked structures: a state of the art review, *Eng. Fracture Mech.*, 1996, 55, 831–857.
22. S. B. Dong, Free Vibration of Laminated Orthotropic Cylindrical Shell, *The Journal of the Acoustical Society of America*, 1968, v. 44, n.6, 1628–1635.
23. W. H. Duan, C. G. Koh, Axisymmetric transverse vibration of circular cylindrical shells with variable thickness, *Journal of Sound and Vibration*, 2008, 317, 1035–1041.
24. J. Fernandez-Saez, C. Novarro, Fundamental frequency of cracked beams in bending vibrations; an analytical approach, *Journal of Sound and Vibration,* 2002, 256(1), 17–31.

25. L. B. Freund, G. Hermann, Dynamic fracture of a beam or plate in plane bending, *Trans. ASME*, 1976, 76, 112–116.
26. G. Gounaris, A. Dimarogonas, Finite element of a cracked prismatic beam for structural analysis, *Computers & Structures*, 1988, 28 (3), 309–313.
27. P. Gudmundson, Eigenfrequency changes of structures due to cracks, notches or other geometrical changes, *J. Mech. Phys. Solids*, 1982, 30, # 5, 339–353.
28. J. Hu, R.Y. Liang, An integrated approach to detection of cracks using vibration characteristics, *J. Franklin Inst*., 1993, 330, # 5, 841–853.
29. G. R. Irwin, Fracture mechanics, In: Goodier J.N., Hoff N. J., *Structural Mechanics*, Pergamon Press, Oxford, 1960.
30. M.L. Kikidis, C.A. Papadopoulos, Slenderness ratio effect on cracked beam, *Journal of Sound and Vibration,* 1992, 155, # 1, 1–11.
31. M. Kisa, J. Brandon, M. Topcu, Free vibration analysis of cracked beams by a combination of finite elements and component mode synthesis methods, *Computers and Structures,* 1998, 67, 215–223.
32. A. S. Kobayashi, A. F. Emery, N. Polvanich, W. J. Love, Inner and outer surface cracks in internally pressurized cylinders, *Trans. ASME Journal of Pressure Vessel Technology*, 1977, 99, 83–89.
33. S. Kukla, Free vibration and stability of stepped colums with cracks, *Journal of Sound and Vibration*, 2009, 319, 1301–1311.
34. Lei Xuanyang, Guicai Zhang, Song Xigeng, Jin Chen, Guangming Dong, Simulation on the motion of crankshaft in crankpin-web fillet region, *Journal of Sound and Vibration,* 2006, 295, 890–905.
35. A. Leissa, Vibration of shells, *Acoustical Society of America*, 1973.
36. J. Lellep, P. Nestler and W. Schmidt, Optimization of elastic cylindrical shells, *Proceedings of the Twenty Second Nordic Seminar on Computational Mechanics*, 2009, 169–172.
37. J. Lellep, E. Puman, L. Roots, E. Tungel, Optimization of rotationally symmetric shells, *Proc. 14th WSEAS Conf. Applied Mathematics*, WSEAS Press, 2009, 233–238.
38. J. Lellep J., E. Puman, L. Roots, E. Tungel, Optimization of stepped shells, *WSEAS Transactions on Mathematics*, 2010, 9(2), 130–139.
39. J. Lellep, L. Roots, Vibration of stepped cylindrical shells with cracks, *3rd WSEAS International Conference on Engineering Mechanics, Structures, Engineering Geology (WORLDGEO'10),* WSEAS Press, 2010, 116–121.
40. J. Lellep, L. Roots, Vibrations of cylindrical shell with circumferential cracks, *WSEAS Transactions on Mathematics*, 2010, 9, 689–699.
41. J. Lellep, Sakkov E., Buckling of stepped composite columns, *Mech. Comp. Mater*., 2006, 42, # 1, 63–72.
42. Q.S. Li, Vibratory characteristics of multi-step beams with an arbitrary number of cracks and concentrated masses, *Applied Acoustics*, 2001, 62, # 6, 691–706.
43. R.Y. Liang, F.K. Choy, J. Hu, Detection of cracks in beam structures using measurements of natural frequencies, *J. Franklin Inst.*, 1991, 328, # 4, 505–518.
44. R.Y. Liang, J. Hu, F. Choy, Theoretical study of crack-induced eigenfrequency changes on beam structures , *J. Eng. Mech.,* 1992, 118, # 2, 384–395.
45. H.P. Lin, S.C. Chang, J. D. Wu, Beam vibrations with an arbitrary number of cracks, *Journal of Sound and Vibration*, 2002, 258, 987–999.
46. A. E. H. Love, A Treatise on the Mathematical Theory of Elasticity, First ed., Cambridge Univ. Press, 1892, fourth ed., Dover Pub., Inc. (New York), 1944.

47. A. E. H. Love, The Small Free Vibrations and Deformations of a Thin Elastic Shell, *Phil. Trans. Roy. Soc.* (London), ser. A, 179, 1888, 491- 549.
48. S. Markus, *The Mechanics of Vibrations of Cylindrical Shells*, Elsevier, Amsterdam, 1988.
49. S. Masoud, M.A. Jarrah, M. Al-Maamori, Effect of crack depth on the natural frequency of a prestressed fixed-fixed beam, *Journal of Sound and Vibration*, 1999, 214, 201–212.
50. S. Naguleswaran, Transverse vibration and stability of an Euler-Bernoulli beam with step change in cross-section and in axial force, *Journal of Sound and Vibration*, 2004, 270, 1045–1055.
51. B.P. Nandwana, S.K. Maiti, Detection of the location and size of a crack in stepped cantilever beams based on measurements of natural frequencies, *Journal of Sound and Vibration,* 1997, 203, # 3, 435–446.
52. Y. Narkis, E. Elmanah, Crack identification in a cantilever beam under uncertain end conditions, *Int. J. Mech. Sci.,* 1996, 38, # 5, 499–507.
53. Y. Narkis, Identification of crack location in vibrating simply supported beams, *Journal of Sound and Vibration,* 1994, 172, 549–558.
54. K. Nikpour, Diagnosis of axisymmetric cracks in orthotropic cylindrical shells by vibration measurement, *Compos. Science and Technol.,* 1990, 39, 45- 61.
55. W. Ostachowicz, M. Krawczuk, Analysis of the effect of cracks on the natural frequencies of a cantilever beam, *Journal of Sound and Vibration,* 1991, 150, # 2, 191–201.
56. N. Papaeconomou, A. Dimarogonas, Vibration of cracked beams, *Computational Mechanics,* 1989, 5, 88–94.
57. Pellicano Francesco, Vibrations of circular cylindrical shells: Theory and experiments, *Journal of Sound and Vibration,* 2007, 303, 154–170.
58. H. J. Petroski, The response of cracked cylindrical shell, *Trans. ASME Journal Appl. Mech.,* 1980, 47, 444–446.
59. I. S. Raju, J. C. Newman, Stress intensity factors for internal and external surface cracks in cylindrical vessels, *Trans. ASME Journal of Pressure Vessel Technology,* 1982, 104, 293–298.
60. J.W.S. Rayleigh, *The theory of sound*, London, Macmillan Co., v., 1877, v.2.
61. J.N. Reddy, *Theory and Analysis of Elastic Plates and Shells*, CRC Press, 2007.
62. J.R. Rice, N. Levy, The part-through surface crack in an elastic plate, *Journal of Applied Mechanics*, 1972, 3, 185–194.
63. P.F. Rizos, N. Aspragathos, A.D. Dimarogonas, Identification of crack location and magnitude in a cantilever beam from the vibration modes, *Journal of Sound and Vibration,* 1990, 138, # 3, 381–388.
64. W.Soedel, Simplified equations and solutions for the vibration of orthotropic cylindrical shell, *Journal of Sound and Vibration,* 1983, 87 (4), 555–566.
65. W. Soedel, *Vibrations of Shells and Plates*, *Third Edition, Revised and Expanded,* Marsel Dekker, N.Y., 2004.
66. H. Tada, P.C. Paris, G.R. Irwin, Stress Analysis of Cracks Handbook, ASME, N.Y., 2000.
67. I.Takahashi, Vibration and stability of non-uniform cracked Timoshenko beam subjected to follower force, *Computers and Structures*, 1999, 71, 585–591.
68. E. Ventsel, Th. Krauthammer, *Thin Plates and Shells. Theory, Analysis, and Applications,* Marcel Dekker, New York, 2001.
69. J. Yang, Y. Chen, Free vibrations and buckling analyses of functionally graded beams with edge cracks, *Composite Structures*, 2008, 83, 48–60.

70. T. Yokoyama, M.-C. Chen, Vibration analysis of edge-cracked beams using a line-spring model, *Eng. Fracture Mech.*, 1998, 59, # 3, 403–409.
71. L. Zhang, Y. Xiang, Exact solutions for vibration of steped circular cylindrical shells, *Journal of Sound and Vibration,*2007, 299, 948–964.
72. D.Y. Zheng, S.C. Fan, Vibration and stability of cracked hollow-sectional beams, *Journal of Sound and Vibration*, 2003, 267, 933–954.
73. X. Zhu, T.Y. Li, Y. Zhao, J. Yan, Vibration power flow analysis of thin cylindrical shell with circumferential surface crack, *Journal of Sound and Vibration*, 2007, 302, 332–349.
74. В. Л. Бажанов, И.И. Гольденблат, В.А. Копнов, А.Д. Поспелов, А.М. Синюков, *Пластинки и оболочки из стеклопластиков*, Издательство «Высшая школа», М., 1970.
75. А. Л. Гольденвейзер, *Теория упругих тонких оболочек* , М. Наука, 1976.
76. Л.Г. Доннелл, *Балки, пластины и оболочки*, Издательство «Наука», Москва, 1982.
77. А. И. Лурье, *Статика тонкостенных упругих оболочек*, М., Л.: Гостехиздат, 1947.
78. В.В. Новожилов, О физическом смысле инвариантов напряжения, используемых в теории пластичности, *Прикладная математика и механика*, 1952, Т.16, Вып. 5, 617- 619.
79. В.В. Новожилов, Р. М. Финкельштейн, О погрешности гипотезы Кирхофа в теории оболочек , *Прикладная математика и механика*, 1943, Т.7, Вып. 5, 331–340.
80. С.П. Тимошенко, С. Войновский-Кригер, *Пластинки и оболочки*, Издательство «Наука», Москва, 1966.

ACKNOWLEDGEMENTS

I am very grateful to supervisor, professor Jaan Lellep, for his advices and continuous support during my doctoral studies.

This work is devoted to my father – Denisyuk Anatoli Fedorovich.

I would like to thank my son who have helped me in translating this thesis into English.

The partial support from Estonian Reseach Foundation through grant ETF 7461 “Optimization of Elastic and Inelastic Shells” and from the Target-financed project SF0180081s08 “Models of Applied Mathematics and Mechanics” are acknowledged.

SUMMARY IN ESTONIAN

Pragudega silindriliste koorikute vabavõnkumised

Käesolev väitekiri koosneb sissejuhatusest, neljast peatükist, kirjanduse loetelust ja kokkuvõttest.

Väitekiri on pühendatud tükiti konstantse paksusega silindriliste koorikute võnkumiste uurimisele juhul, kui koorikus on praod. Praod eeldatakse olevat stabiilsed konstantse sügavusega ringikujulised praod, mis asuvad nendes ristlõigetes, kus kooriku paksus muutub hüppeliselt.

Sissejuhatuses on esitatud ajalooline ülevaade plaatide ja koorikute uurimisele pühendatud töödest. Põhitähelepanu on siin pööratud töödele, kus uuritakse konstruktsiooni elementide võnkumisi ja stabiilsust juhul, kui konstruktsioonis on praod.

Töö esimeses peatükis käsitletakse otstest vabalt toetatud ringsilindriliste koorikute vabavõnkumisi. Eeldatakse, et kooriku paksus on tükiti konstantne ja et paksuse hüppekohtades asuvad praod. Esitatakse probleemi uurimiseks vajalikud põhivõrrandid. Need koosnevad tasakaaluvõrranditest, geomeetrilistest seostest ja Hooke'i seadusest. Prao mõju kooriku käitumisele arvestatakse lokaalse järeleandlikkuse koefitsiendi abil, mis seotakse purunemismehaanikast tuntud pinge intensiivsuse koefitsiendiga.

Põhivõrrandite süsteem lahendatakse Fourier meetodil. Rahuldades seejärel rajatingimused ja vastavad pidevuse ning katkevuse tingimused ristlõigetes, kus asuvad praod, jõutakse algebraliste võrrandite süsteemini. Leides vastava maatriksi omaväärtused saadakse kooriku omavõnkesagedused.

Väitekirja teises peatükis uuritakse astmeliste koorikute võnkumisi mitmessuguste kinnitustingimuste korral arvestades paksuse astme kohtades asuvate pragudega. Detailsemalt analüüsitakse juhte, kui kooriku mõlemad otsad on jäigalt kinnitatud ning kui üks ots on jäigalt kinnitatud, aga teine vaba. Tulemuste võrdlemisel kirjandusest teada olevate lahenditega on näidatud, et konstantse paksusega kooriku korral on tulemused heas kooskõlas teiste autorite töödega.

Töö kolmandas peatükis vaadeldakse komposiitmaterjalist valmistatud ning kihiliste koorikute võnkumisi tükiti konstantse paksuse korral. On lahendatud konkreetne näide klaasplastikust silindrilise kooriku võnkumise kohta.

Väitekirja neljandas peatükis käsitletakse ringsilindriliste koorikute mittetelgsümmeetrilisi võnkumisi. On töötatud välja ligikaudne meetod omavõnkesageduste määramiseks kasutades Donnelli poolt esitatud põhivõrrandite süsteemi approksimatsiooni. Ka siin arvestatakse prao mõjuga koorikute dünaamilisele käitumisele pinge intensiivsuse koefitsiendi abil.

CURRICULUM VITAE

Larissa Roots

Born: Aprill 8, 1960, Korosten, Ukraina
Citizenship: Estonian Republic
Marital status: Married, 1 child
Address: Liivi 2, 50409 Tartu, Estonia
Phone.: +372 5566 3484
e-mail: a42119@ut.ee

Education

1967–1977 Secondary School # 7 (Korosten)
1977–1983 St. Petersburg State Polytechnical Institute, Dep. of Phys.-mech.,
2004–2010 PhD student , University of Tartu, Estonia

Scientific work

1983–1992 VNIIG Vedeneyev's name, research fellow
2004– 2010 Extraordinary researcher at Institute of Applied Mathematics, University of Tartu

Conferences and seminars

1. J. Lellep, L. Roots, Free vibrations of stepped cylindrical shells containing flaws, *NSCM – 23:Proceeding of the 23rd Nordic Seminar on Computational Mechanics*, Stockholm, 2010, 251–254.
2. J. Lellep, T. Kraav, L. Roots, Analysis and optimization of structural elements with cracks, *Mechanics of Composite Materials- XVI International Conference*, May 24–28, 2010, Riga, Latvia.
3. L. Dmitrijeva (Roots), Dependence of the dynamic properties of the icesoil's material from the icy-coefficient on samples-cores, *NSCM- 17: Proceeding of the 17th Nordic Seminar on Computational Mechanics*, Stockholm, 2004, 74–77.

LIST OF PUBLICATIONS

1. J. Lellep, L. Roots, Free vibrations of stepped cylindrical shells containing flaws, *NSCM- 23: Proceeding of the 23rd Nordic Seminar on Computational Mechanics*, Stockholm, 2010, 251–254.

2. J. Lellep, L. Roots, Vibrations of cylindrical shells with circumferential cracks, *WSEAS Transactions on Mathematics*, 2010, 9, 689–699.
3. J. Lellep, E. Puman, L. Roots, E. Tungel, Optimization of stepped shells, *WSEAS Transactions on Mathematics*, 2010, 9(2), 130–139.
4. J. Lellep, T. Kraav, L. Roots, Analysis and optimization of structural elements with cracks, Mechanics of Composite Materials – XVI International Conference, May 24–28,2010, Riga, Latvia.
5. J. Lellep, L. Roots, Vibration of stepped cylindrical shells with cracks, *3rd WSEAS International Conference on Engineering Mechanics, Structures, Engineering Geology (WORLDGEO'10),* WSEAS Press, 2010, 116–121.
6. J. Lellep, E. Puman, L. Roots, E. Tungel, Optimization of rotationally symmetric shells, *Proc. 14th WSEAS Conf. Applied Mathematics*, WSEAS Press, 2009, 233–238.
7. L. Dmitrijeva (Roots), Dependence of the dynamic properties of the icesoil's material from the icy-coefficient on samples-cores, *NSCM- 17: Proceeding of the 17th Nordic Seminar on Computational Mechanics*, Stockholm, 2004, 74–77.

ELULOOKIRJELDUS

Larissa Roots

Sünniaeg ja koht:	8. Aprill 1960, Korosten, Ukraina
Kodakondsus:	Eesti Vabariik
Aadress:	Kaunase pst., 80–33, 50807, Tartu, Eesti
Telefon:	+372 55663484
e-mail:	a42119@ut.ee, larisadm78@yahoo.co.uk

Haridus

1967–1977	Korosteni 7. Keskkool (Ukraina), keskharidus
1977–1983	Kalinini nim. LPI Füüs-mehh.teaduskond, kõrgharidus
2004–2010	Tartu Ülikool, Matemaatika-informaatikateaduskond, doktoriõpe

Keelteoskus: ukraina, vene – emakeel, inglise, eesti – keskmine tase

Teenistuskäik

1983–1992	Vedenejevi nim. Hüdrotehnika Teadusliku Uurimise Instituut (Leningrad), teadur
1992–1994	Firma“Ime”, insener-programmeerija
1994–1996	Narva Kergetööstuskool, programmeerija-raamatupidaja
1996–2004	Narva Linna Haridusosakond, pearaamatupidaja
2010–	TÜ matemaatika instituudi spetsialist

Teaduslik tegevus: On uuritud elastsete koorikute dünaamikat ja defektidega koorikute võnkumisi [1–6]. Töös [7] on uuritud pinnase dünaamikat.

DISSERTATIONES MATHEMATICAE UNIVERSITATIS TARTUENSIS

1. **Mati Heinloo.** The design of nonhomogeneous spherical vessels, cylindrical tubes and circular discs. Tartu, 1991, 23 p.
2. **Boris Komrakov.** Primitive actions and the Sophus Lie problem. Tartu, 1991, 14 p.
3. **Jaak Heinloo.** Phenomenological (continuum) theory of turbulence. Tartu, 1992, 47 p.
4. **Ants Tauts.** Infinite formulae in intuitionistic logic of higher order. Tartu, 1992, 15 p.
5. **Tarmo Soomere.** Kinetic theory of Rossby waves. Tartu, 1992, 32 p.
6. **Jüri Majak.** Optimization of plastic axisymmetric plates and shells in the case of Von Mises yield condition. Tartu, 1992, 32 p.
7. **Ants Aasma.** Matrix transformations of summability and absolute summability fields of matrix methods. Tartu, 1993, 32 p.
8. **Helle Hein.** Optimization of plastic axisymmetric plates and shells with piece-wise constant thickness. Tartu, 1993, 28 p.
9. **Toomas Kiho.** Study of optimality of iterated Lavrentiev method and its generalizations. Tartu, 1994, 23 p.
10. **Arne Kokk.** Joint spectral theory and extension of non-trivial multiplicative linear functionals. Tartu, 1995, 165 p.
11. **Toomas Lepikult.** Automated calculation of dynamically loaded rigid-plastic structures. Tartu, 1995, 93 p, (in Russian).
12. **Sander Hannus.** Parametrical optimization of the plastic cylindrical shells by taking into account geometrical and physical nonlinearities. Tartu, 1995, 74 p, (in Russian).
13. **Sergei Tupailo.** Hilbert's epsilon-symbol in predicative subsystems of analysis. Tartu, 1996, 134 p.
14. **Enno Saks.** Analysis and optimization of elastic-plastic shafts in torsion. Tartu, 1996, 96 p.
15. **Valdis Laan.** Pullbacks and flatness properties of acts. Tartu, 1999, 90 p.
16. **Märt Põldvere.** Subspaces of Banach spaces having Phelps' uniqueness property. Tartu, 1999, 74 p.
17. **Jelena Ausekle.** Compactness of operators in Lorentz and Orlicz sequence spaces. Tartu, 1999, 72 p.
18. **Krista Fischer.** Structural mean models for analyzing the effect of compliance in clinical trials. Tartu, 1999, 124 p.
19. **Helger Lipmaa.** Secure and efficient time-stamping systems. Tartu, 1999, 56 p.
20. **Jüri Lember.** Consistency of empirical k-centres. Tartu, 1999, 148 p.
21. **Ella Puman.** Optimization of plastic conical shells. Tartu, 2000, 102 p.
22. **Kaili Müürisep.** Eesti keele arvutigrammatika: süntaks. Tartu, 2000, 107 lk.
23. **Varmo Vene.** Categorical programming with inductive and coinductive types. Tartu, 2000, 116 p.

24. **Olga Sokratova.** Ω-rings, their flat and projective acts with some applications. Tartu, 2000, 120 p.
25. **Maria Zeltser.** Investigation of double sequence spaces by soft and hard analitical methods. Tartu, 2001, 154 p.
26. **Ernst Tungel.** Optimization of plastic spherical shells. Tartu, 2001, 90 p.
27. **Tiina Puolakainen.** Eesti keele arvutigrammatika: morfoloogiline ühestamine. Tartu, 2001, 138 p.
28. **Rainis Haller.** *M(r,s)*-inequalities. Tartu, 2002, 78 p.
29. **Jan Villemson.** Size-efficient interval time stamps. Tartu, 2002, 82 p.
30. **Eno Tõnisson.** Solving of expession manipulation exercises in computer algebra systems. Tartu, 2002, 92 p.
31. **Mart Abel.** Structure of Gelfand-Mazur algebras. Tartu, 2003. 94 p.
32. **Vladimir Kuchmei.** Affine completeness of some ockham algebras. Tartu, 2003. 100 p.
33. **Olga Dunajeva.** Asymptotic matrix methods in statistical inference problems. Tartu 2003. 78 p.
34. **Mare Tarang.** Stability of the spline collocation method for volterra integro-differential equations. Tartu 2004. 90 p.
35. **Tatjana Nahtman.** Permutation invariance and reparameterizations in linear models. Tartu 2004. 91 p.
36. **Märt Möls.** Linear mixed models with equivalent predictors. Tartu 2004. 70 p.
37. **Kristiina Hakk.** Approximation methods for weakly singular integral equations with discontinuous coefficients. Tartu 2004, 137 p.
38. **Meelis Käärik.** Fitting sets to probability distributions. Tartu 2005, 90 p.
39. **Inga Parts.** Piecewise polynomial collocation methods for solving weakly singular integro-differential equations. Tartu 2005, 140 p.
40. **Natalia Saealle.** Convergence and summability with speed of functional series. Tartu 2005, 91 p.
41. **Tanel Kaart.** The reliability of linear mixed models in genetic studies. Tartu 2006, 124 p.
42. **Kadre Torn.** Shear and bending response of inelastic structures to dynamic load. Tartu 2006, 142 p.
43. **Kristel Mikkor.** Uniform factorisation for compact subsets of Banach spaces of operators. Tartu 2006, 72 p.
44. **Darja Saveljeva.** Quadratic and cubic spline collocation for Volterra integral equations. Tartu 2006, 117 p.
45. **Kristo Heero.** Path planning and learning strategies for mobile robots in dynamic partially unknown environments. Tartu 2006, 123 p.
46. **Annely Mürk.** Optimization of inelastic plates with cracks. Tartu 2006. 137 p.
47. **Annemai Raidjõe.** Sequence spaces defined by modulus functions and superposition operators. Tartu 2006, 97 p.
48. **Olga Panova.** Real Gelfand-Mazur algebras. Tartu 2006, 82 p.

49. **Härmel Nestra.** Iteratively defined transfinite trace semantics and program slicing with respect to them. Tartu 2006, 116 p.
50. **Margus Pihlak.** Approximation of multivariate distribution functions. Tartu 2007, 82 p.
51. **Ene Käärik.** Handling dropouts in repeated measurements using copulas. Tartu 2007, 99 p.
52. **Artur Sepp.** Affine models in mathematical finance: an analytical approach. Tartu 2007, 147 p.
53. **Marina Issakova.** Solving of linear equations, linear inequalities and systems of linear equations in interactive learning environment. Tartu 2007, 170 p.
54. **Kaja Sõstra.** Restriction estimator for domains. Tartu 2007, 104 p.
55. **Kaarel Kaljurand.** Attempto controlled English as a Semantic Web language. Tartu 2007, 162 p.
56. **Mart Anton.** Mechanical modeling of IPMC actuators at large deformations. Tartu 2008, 123 p.
57. **Evely Leetma.** Solution of smoothing problems with obstacles. Tartu 2009, 81 p.
58. **Ants Kaasik.** Estimating ruin probabilities in the Cramér-Lundberg model with heavy-tailed claims. Tartu 2009, 139 p.
59. **Reimo Palm.** Numerical Comparison of Regularization Algorithms for Solving Ill-Posed Problems. Tartu 2010, 105 p.
60. **Indrek Zolk.** The commuting bounded approximation property of Banach spaces. Tartu 2010, 107 p.
61. **Jüri Reimand.** Functional analysis of gene lists, networks and regulatory systems. Tartu 2010, 153 p.
62. **Ahti Peder.** Superpositional Graphs and Finding the Description of Structure by Counting Method. Tartu 2010, 87 p.
63. **Marek Kolk.** Piecewise Polynomial Collocation for Volterra Integral Equations with Singularities. Tartu 2010, 134 p.
64. **Vesal Vojdani.** Static Data Race Analysis of Heap-Manipulating C Programs. Tartu 2010, 137 p.